IQ imbalance in OFDM wireless LAN systems

Schoonen, A.M.J.M.

Award date:
2009

Eindhoven University of Technology
Department of Electrical Engineering
Signal Processing Systems

TU/e

IQ imbalance in OFDM Wireless LAN systems

Admar Schoonen

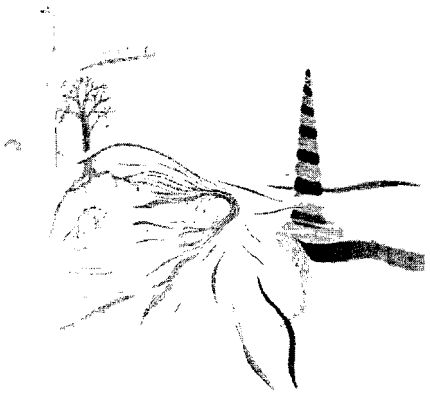

Master of Science Thesis

Project period: February 2005 - January 2006
Report Number: 20-06

Commissioned by: Prof. dr. ir. J. W. Bergmans

Supervisors:
Dr. ir. F. M. J. Willems (TU/e)
Dr. ir. J. Oostveen (Philips Research)

Abstract

In today's competitive wireless communication markets such as the wireless local area network (LAN) market, it is very advantageous to develop low cost transceivers. One way to create low cost transceivers is to develop transceivers which can be integrated very well on a chip without requiring external IF components like SAW filters. Zero-IF (or direct baseband) modulators and demodulators have the potential to fulfill that promise, once all negative aspects of such designs are overcome. One of those negative aspects is IQ imbalance, which is the topic of this report.

Almost any modern transceiver contains two branches, an in-phase and a quadrature-phase branch. A typical problem for zero-IF transceivers is that the branches are not exactly identical. The mismatch between those two branches is called IQ imbalance, and it leads to interference of the image band signal on the desired signal.

In this report, the modeling of IQ imbalance in both transmitter and receiver is discussed, as well as the impact of IQ imbalance on the performance of an IEEE 802.11a wireless LAN OFDM system. This report shows that IQ imbalance in zero-IF transceivers can have a severe influence on the bit error rate (BER) for orthogonal frequency division multiplexing (OFDM) systems at higher order signal constellations (eg 64 QAM).

Furthermore, this report proposes a digital baseband algorithm to compensate for the influence of IQ imbalance and several algorithms to estimate the IQ imbalance parameters. The algorithms are developed specifically for systems based on the IEEE 802.11a standard and can be used to compensate IQ imbalance in the receiver, in the transmitter or in both the receiver and transmitter. It is shown that even for very large values of IQ imbalance, the bit error rate and packet error rate performance of a system with IQ imbalance applying one of the compensation algorithms is comparable to the performance of a system without any IQ imbalance.

This could eventually give designers of wireless communication systems more freedom and provide more opportunities for low cost, high data rate communication devices.

Contents

Chapter 1

Introduction

The upcoming digital convergence, where computers, mobile communication devices and consumer electronics will seamlessly operate together, will enable new applications and services which can make life both easier and more fun. Those applications and services can range from seamlessly handing over a mobile phone call to a cheaper fixed line or voice over IP (VoIP) once the user is in the proximity of a wireless access point, to streaming audio and video to the nearest display, or to refrigerators which automatically notifies the owner which products are passed their expiration date by scanning RFID tags or even other applications that no-one has ever thought of before.

This prospect requires the availability of cheap wireless local area network (LAN) chips which support high data rates. The current IEEE 802.11a [1] and 802.11g [2] wireless LAN standards supports data rates up to 54 Mbps. However, this is not fast enough for streaming multi-media applications and therefore, a faster standard (IEEE 802.11n) is currently in consideration.

The IEEE 802.11n standard will achieve a higher throughput by using multiple transmit and receive chains, to exploit the benefits of multi input, multi output (MIMO). technology. This can significantly increase the data rate of a system, as is shown by Paulraj [3] and others. However, the use of multiple transmit and receive chains will increase the costs of a wireless LAN chip.

In order to reduce the costs of wireless LAN chips and specifically of wireless LAN chips for MIMO systems, it is interesting to investigate in simple and low cost transceiver architectures.

One of such architectures is a zero-IF transceiver, which directly converts a baseband signal to an RF signal and directly converts an RF signal to a baseband signal, as is explained in more detail in Chapter 3 of this report.

However, one of the main drawbacks of a zero-IF architecture compared to a more advanced architecture, is that a zero-IF transceiver is much more sensitive to IQ imbalance.

In this report, we will therefore discuss the effect of IQ imbalance in both a zero-IF transmitter and a zero-IF receiver and the impact of IQ imbalance on the bit error rate (BER) performance of such a system. Furthermore, we will propose several methods to compensate for these effects and show the performance of a zero-IF system with IQ imbalance in both transmitter and receiver with and without the estimation and compensation algorithms.

The algorithms presented in this report are developed specifically for the IEEE 802.11a standard, but with some minor modifications, they should be applicable to the IEEE 802.11g and the future IEEE 802.11n standards as well.

1.1 Framework and objectives

The topic of this thesis is IQ imbalance in zero-IF transmitters and receivers. The project was part of the Master of Science program for electrical engineering at the University of Technology, Eindhoven. It was carried out at Philips Research, Eindhoven, previously known as Natuurkundig Laboratorium (NatLab).

The objectives were to use simulations to evaluate the influence of IQ imbalance in zero IF transmitters and receivers in an IEEE 802.11a based system and to find estimation and compensation methods which can compensate for the effects of IQ imbalance. The methods should preferably be software based only, and should require as little extra hardware as possible.

1.2 Organization of this thesis

Chapter 2 of this thesis explains the structure of an IEEE 802.11a packet. The focus in this chapter is on pilot symbols in the long training field, in the SIGNAL and DATA fields and on the SIGNAL field itself.

In Chapter 3, real and complex mixing will be discussed, followed by a discussion of zero-IF transmitters and receivers.

Modelling of IQ imbalance is the topic of Chapter 4, where we will introduce IQ imbalance into the models of the zero-IF transmitter and receiver. In this chapter, we will furthermore evaluate the effects of IQ imbalance on the received signal and on the channel estimate. At the end of Chapter 4, we will use simulations to show the effect of IQ imbalance on the bit error rate (BER) performance of an IEEE 802.11a system.

Chapter 5 will propose several algorithms to estimate and compensate IQ imbalance in both transmitter and receiver. In this chapter, we will present several solutions which find the exact value of the IQ imbalance parameters in one step in case either only the transmitter or only the receiver experiences IQ imbalance and when there is no noise. Furthermore, we will also present two iterative solutions which estimate the IQ imbalance parameters of both transmitter and receiver.

Performance evaluation of the proposed algorithms is carried out in Chapter 6, where we will evaluate the influence of noise on the estimates and where we will use BER simulations to evaluate the performance of systems applying these algorithms.

Finally, in Chapter 7, conclusions are drawn and recommendations are given.

Chapter 2

IEEE 802.11a Wireless LAN packet structure

This chapter will shortly summarize the packet structure of IEEE 802.11a Wireless LAN packets, as standardized in [1]. The focus will be on the pilot symbols in the long training field, in the SIGNAL field and in the DATA fields and on the contents of the SIGNAL field itself, since, as we shall see in later chapters, those symbols can help in estimating IQ imbalance.

2.1 IEEE 802.11a packet structure

An IEEE 802.11a packet consists of a short training sequence, a long training sequence, a SIGNAL field and one or more DATA fields. This is depicted in Figure 2.1. The short training sequence contains 10 short training symbols of $0.8\mu s$ each, and is primarily meant to aid the receiver in detecting a signal and adjusting the automatic gain control (AGC). It is also meant to allow the receiver to do diversity selection, coarse frequency offset estimation and timing synchronization.

The long training sequence consists of long guard interval of $1.6\mu s$ and two long training sequences of $1.6\mu s$ each. The purpose of the long training sequence is to aid the receiver in channel estimation and fine frequency offset estimation. The long guard interval in this symbol is to avoid inter symbol interference (ISI) from the previous symbol due to multi-path propagation.

The guard interval in the long training sequence is $1.6\mu s$ long, and contains a copy of the last $1.6\mu s$ of the contents of T2. Similarly, the guard interval in the SIGNAL and DATA fields contain a copy of the last $0.8\mu s$ of the contents of SIGNAL and DATA respectively. This copy reduces the inter-carrier interference (ICI) which would be present if the guard interval would be left empty. Note that the guard interval is just 20% of the total length of a symbol. Therefore, the maximum excess delay as defined by Rappaport in [4] is $0.8\mu s$. A more detailed description of guard intervals can be found in, for example, Harno [5], Van Nee [6] or Proakis [7].

The SIGNAL field consists of a copy of the last $0.8\mu s$ of the SIGNAL symbol to reduce ISI and ICI. The contents of the SIGNAL field is created from 24 bits which are BPSK rate 1/2 coded. The resulting 48 coded symbols are modulated on 48 subcarriers according to the scheme in the IEEE 802.11a standard. Of the remaining 16 subcarriers, 4 are used for BPSK pilot tones to aid the receiver in frequency offset estimation and phase noise estimation. The other 12 are left empty since they are at DC or at the outer edges of the spectrum.

The 24 bits in the SIGNAL field contain 4 bits which specify the rate in the following DATA symbols and 12 bits which specify the total number of bytes in the DATA symbols. The remaining 8 bits are reserved,

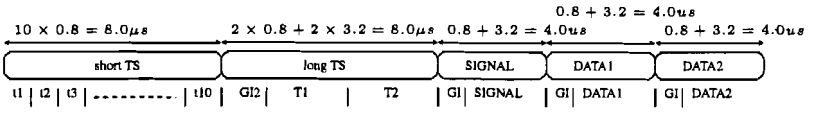

Figure 2.1: IEEE 802.11a packet structure

parity and tailing bits.

2.2 IEEE 802.11a pilot symbols

The pilot symbols in the long training field are 52 BPSK symbols at subcarriers -26 to -1 and 1 to 26. The remaining 12 subcarriers are left empty since they are at DC or at the outer edges of the spectrum.

The pilot symbols in the SIGNAL field and in the DATA field are 4 BPSK symbols at subcarriers -21, -7, 7 and 21.

This is illustrated in Figure 2.2. Note that the short training symbol is not shown in this illustration. Furthermore, the long training symbol is depicted as a block of equal length (in time) as the SIGNAL field, while in reality, it lasts twice as long.

We can conclude that there are 52 BPSK pilot symbols in the long training field and 4 BPSK pilot symbols in the SIGNAL and DATA symbols. Note further, that the data in the SIGNAL field is BPSK rate 1/2 coded, and can therefore be decoded very reliably. Once the SIGNAL field is decoded, it could be an option to encode it again and use the encoded symbols as pilot symbols. This would add another 48 BPSK pilot symbols, although one has to keep in mind that those are less reliable than the official pilot tones.

If we use the symbols in the SIGNAL field as pilot symbols, we can form pairs of pilot symbols. One pair of pilot symbols is (P_{-k}, P_k), i.e., the pilot symbols from the long training sequence on subcarriers $-k$ and k. Another pair of symbols is (X_{-k}, X_k). As we shall see in Chapter 5, orthogonal combinations of pairs (P_{-k}, P_k) and (X_{-k}, X_k) can aid in estimating IQ imbalance.

Appendix B shows the combination of SIGNAL field parameters for which the IEEE 802.11a specification results in the minimum respectively maximum number of orthogonal pairs. As we can see from that appendix, there are always at least 4 orthogonal pairs in an IEEE 802.11a packet, and at most 20.

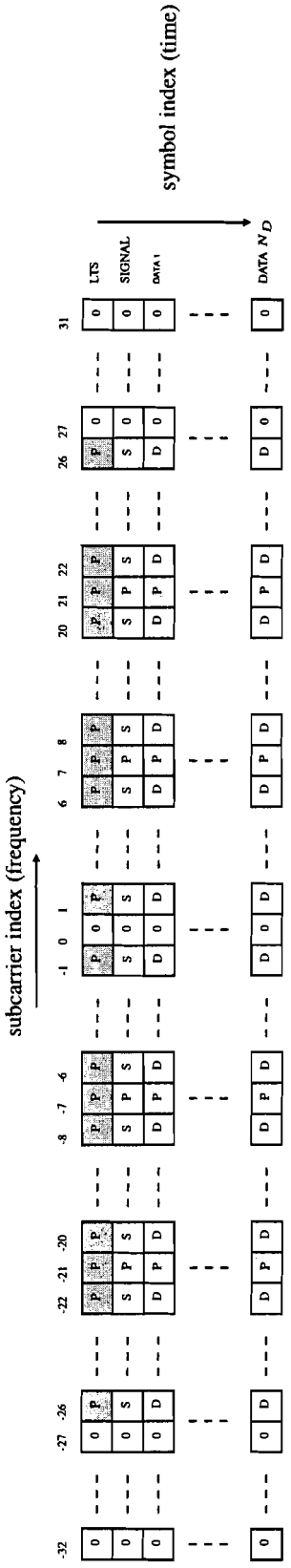

Figure 2.2: Pilot symbols in an IEEE 802.11a packet; pilot symbols used for channel estimation are colored dark grey, pilot symbols used for frequency offset estimation are colored light grey

Chapter 3

Zero-IF transceivers

In most digital communication system, there is a digital to analogue converter (DAC), which converts the digital signal into an analogue baseband representation. The analogue baseband signal is then converted into a passband signal by the mixer. After amplification, this signal is ready to be sent through the communication path. At the receiver this signal is amplified by the low noise amplifier (LNA). After amplification, the mixer converts the received passband signal back to an analog baseband signal and then into a digital signal by an analogue to digital converter (ADC).

In this chapter, we will first discuss the basic operation of a mixer. Later on, we will describe a simple receiver architecture and we will describe how a baseband signal in the transmitter will be up converted by a perfect transmitter, passed through a channel and down converted by a perfect receiver.

3.1 Real and complex mixing

The received signal at the antenna output is a real valued signal. Therefore, the spectral components at negative frequencies are the complex conjugate of the spectral components at the positive frequencies. In other words, if the signal is centered around frequency ω_{LO}, there is also a copy of that signal centered around frequency $-\omega_{LO}$.

If we try to convert the real bandpass signal $r(t)$ to a baseband signal by mixing it with $\cos(\omega_{LO}t)$, we essentially multiply it with

$$\frac{e^{j\omega_{LO}t} + e^{-j\omega_{LO}t}}{2}. \tag{3.1}$$

Multiplication in time domain is equivalent to convolution in frequency domain. The Fourier transform of $e^{-j\omega_{LO}t}$ is $\delta(\omega+\omega_{LO})$, and therefore, the multiplication is equivalent to convolving $R(\omega)$ with $\delta(\omega+\omega LO)$ and with $\delta(\omega - \omega_{LO})$:

$$\mathcal{F}\{r(t) \cdot \cos(\omega_{LO}t)\} = \frac{1}{2}R(\omega) \star (\delta(\omega + \omega_{LO}) + \delta(\omega - \omega_{LO}))\,, \tag{3.2}$$

where $\mathcal{F}\{x(t)\}$ denotes the Fourier transform of $x(t)$ and $R(\omega)$ is the Fourier transform of $r(t)$. Furthermore, $x(t) \star y(t)$ denotes the convolution of signals $x(t)$ and $y(t)$.

Convolving a signal $r(t)$ in frequency domain with delta pulse $\delta(-\omega_{LO})$, essentially shifts the spectrum of $r(t)$ ω_{LO} to the left. Thus, multiplying $r(t)$ with $\cos(\omega_{LO}t)$ is equivalent to adding a left-shifted version of $R(\omega)$ with a right-shifted version of $R(\omega)$. This is illustrated in case 1 in Figure 3.1. Note that in this figure, the frequency components at $-2\omega_{LO}$ and $2\omega_{LO}$ are not shown.

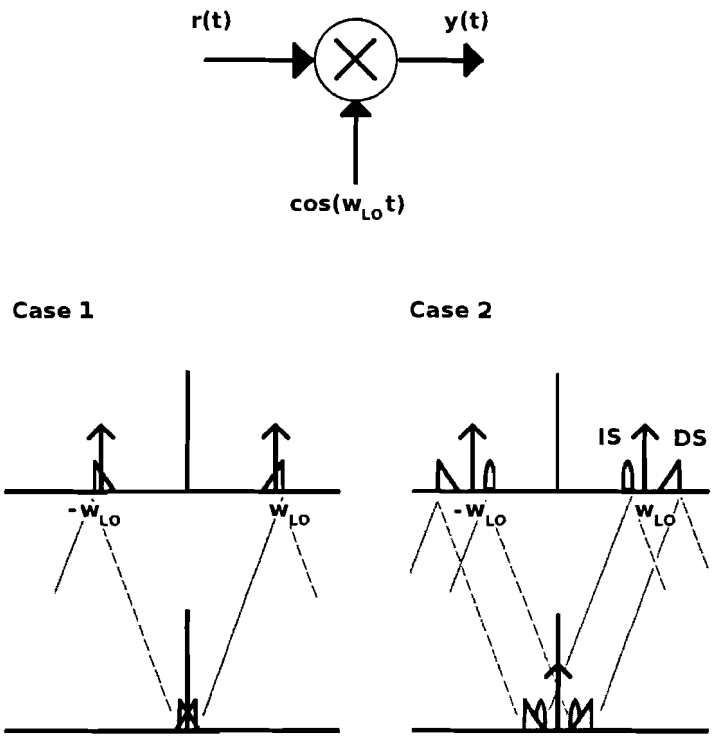

Figure 3.1: Mixing a real signal with a cosine. In case 1, the frequency ω_{LO} is equal to the center frequency of the desired signal, and in case 2, ω_{LO} is not equal to the center frequency of the desired signal.

Case 1 in Figure 3.1 clearly shows that mixing a real signal with a cosine results in interference of the desired signal with a copy of that signal, but mirrored in frequency. Due to this effect, the original signal cannot be reconstructed.

To overcome this problem, one could try to mix the signal with $\cos(\omega_{LO}t)$ where we chose ω_{LO} just outside the frequency band. This is illustrated in case 2 in Figure 3.1, where ω_{LO} is just below the frequency band of the desired signal (DS). However, as we can see in this picture, this will lead to problems if there is another signal (image signal, IS) just below ω_{LO}. In that case, the image signal will interfere with the desired baseband signal.

To eliminate this interference, one could use very sharp bandpass filters. However, those filters should operate at the carrier frequency (RF) and have very strict requirements. Such filters are expensive, and difficult to integrate on a chip.

Another approach to reliably convert the signal to a baseband signal is by using complex mixing, i.e., by multiplying $r(t)$ with $e^{-j\omega_{LO}t}$. Since this will only shift the spectrum of $r(t)$ to the left, and no components will be shifted to the right, there will be no interference at all.

Multiplication by $e^{-j\omega_{LO}t}$ can be realized by multiplying the signal with $\cos(\omega_{LO}t)$ and with $-j\sin(\omega_{LO}t)$ and adding the result. This is illustrated in Figure 3.2. The signal $y_i(t)$ is obtained by mixing $r(t)$ with $\cos(\omega_{LO}t)$ and the signal $jy_q(t)$ is obtained by mixing $r(t)$ with $-j\sin(\omega_{LO}t)$. Adding $y_i(t)$ and $jy_q(t)$ results in $y(t)$, which is the baseband equivalent of $r(t)$.

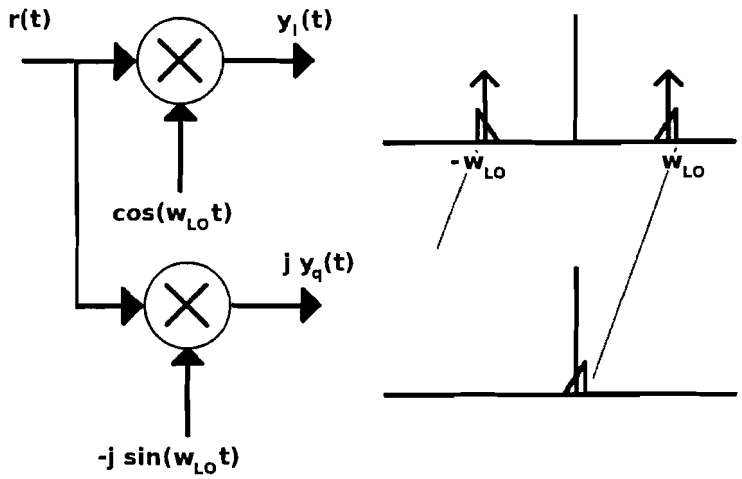

Figure 3.2: Mixing a real signal with a cosine and a sine; left: the operation in time domain, right: the effect on the spectrum of the received signal $r(t)$.

In practice, an ideal analogue front-end multiplies the signal with $\cos(\omega LOt)$ and $-\sin(\omega_{LO}t)$ and after the resulting signals are filtered and sampled, the digital signal processor can create $y(t) = y_i(t) + jy_q(t)$.

3.2 Zero-IF receiver

In the previous section, we have shown that we can reliably convert a passband into a baseband signal by complex mixing. An intuitive approach to complex mixing is to directly convert the passband signal into a baseband signal by choosing ω_{LO} equal to the center of the frequency band. Such a receiver is shown in Figure 3.3.

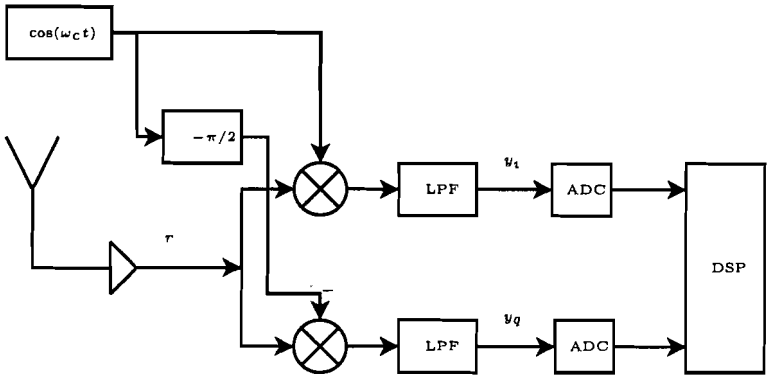

Figure 3.3: Zero-IF receiver

The receiver in this figure is called a zero-IF receiver or a homodyne receiver. However, according to Couch [8], Razavi [9] and Mirabbasi [10], there are a couple drawbacks to this approach:

- DC-offsets due to self-mixing of the LO signal and/or the received signal;
- LO leakage can be caused by leakage of the LO signal to the antenna and radiation from there can cause interference for systems operating in the same frequency band;
- IQ mismatch (or IQ imbalance) is the effect when the in-phase (cosine) branch is not exactly identical to the quadrature-phase (sine) branch and will lead to interference of desired signal with a copy of this signal but mirrored in frequency;
- poor noise figure since the front end usually is not a high-gain, low-noise stage;
- Even-Order distortion caused by non-linearities in the LNA can result in two high-frequency interferers generating a low-frequency signal which corrupts the desired baseband signal.

A traditional solution to those drawbacks is to do the down conversion in several stages. In the first stage, the bandpass signal at RF frequency is converted to a bandpass signal at an intermediate frequency (IF), by mixing it with a frequency much lower than the center frequency of the desired signal. The IF signal is then filtered before it is converted to a baseband signal by a complex mixer. Such receivers are called heterodyne receivers.

Note that if the intermediate frequency is chosen properly, complex mixing in the IF stage is not required, since the interfering signals are at frequencies far away from the desired signal, and can be filtered out in advance. However, according to Mirabbasi [10], such filters usually require off-chip components, and therefore, such receivers are difficult to integrate on a single chip.

In this report, we will focus on zero-IF receivers. A more detailed description of heterodyne receivers can be found for example in Mirabbasi [10], Couch [8] or Razavi [9].

3.3 Zero-IF transmitter and receiver

According to Couch [8], up conversion in the transmitter can be done by an AM-PM generation technique, or by using complex mixing. The complex mixing technique is very similar to complex mixing in receivers. A zero-IF transmitter uses complex mixing and is therefore conceptually very similar to a zero-IF receiver.

In the remainder of this report, we will solely focus on IQ imbalance in zero-IF receivers and transmitters.

In this section, we will describe the signals in a communication system where both transmitter and receiver are based on the zero-IF architecture. In the following chapter, we will discuss the effect of IQ imbalance on these signals.

Figure 3.4 shows a zero-IF transmitter and a zero-IF receiver. The transmitted baseband signal is $x(t) = x_i(t) + jx_q(t)$. The pass band signal $s(t)$ that is transmitted is:

$$\begin{aligned} s(t) &= x_i(t)\cos(\omega_c t) - x_q(t)\sin(\omega_c t) \\ &= \frac{1}{2}\left(e^{j\omega_c t}x(t) + e^{-j\omega_c t}x^*(t)\right) \\ &= \Re\{x(t)e^{j\omega_c t}\} \end{aligned} \tag{3.3}$$

At the receiver, this signal has passed through a channel with impulse response $h_{RF}(t)$. Amplification by the LNA adds noise to the signal, and thus, the received signal after the LNA is

$$r(t) = (s \star h_{RF})(t) + n_{RF}(t), \tag{3.4}$$

where $(s \star h_{RF})(t)$ denotes the convolution of $s(t)$ and $h_{RF}(t)$ and $n_{RF}(t)$ is the radio frequency (RF) noise.

This signal is mixed with $\cos(\omega_c t)$ and low pass filtered in the in-phase branch. After the low pass filter, this signal equals

$$\begin{aligned} y_i(t) &= \cos(\omega_c t)r(t) \\ &= \frac{1}{2}((x_r \star h_r)(t) - (x_i \star h_i)(t)) + n_r(t), \end{aligned} \tag{3.5}$$

where

$$h(t) = h_{RF}(t)e^{-j\omega_c t} \tag{3.6}$$

is the baseband equivalents of $h_{RF}(t)$ and

$$n_r(t) = n_{RF}(t)\cos(\omega_c t) \tag{3.7}$$

is the real part of the baseband equivalent of $n_{RF}(t)$.

The corresponding signal in the quadrature-phase branch equals

$$\begin{aligned} y_q(t) &= -\sin(\omega_c t)r(t) \\ &= \frac{1}{2}((x_i \star h_r)(t) + (x_r \star h_i)(t)) + n_i(t), \end{aligned} \tag{3.8}$$

with

$$n_i(t) = -n_{RF}(t)\sin(\omega_c t) \tag{3.9}$$

being the imaginary part of the baseband equivalent of $n_{RF}(t)$.

From equations (3.5) and (3.8), we can conclude that the nett effect of up conversion, channel and down conversion for ideal transmitters and receivers can be described by filtering the baseband representation of the transmit signal and adding noise.

The DSP can create signal $y(t) = 2(y_i(t) + jy_q(t))$, where the factor 2 is added for notational convenience.

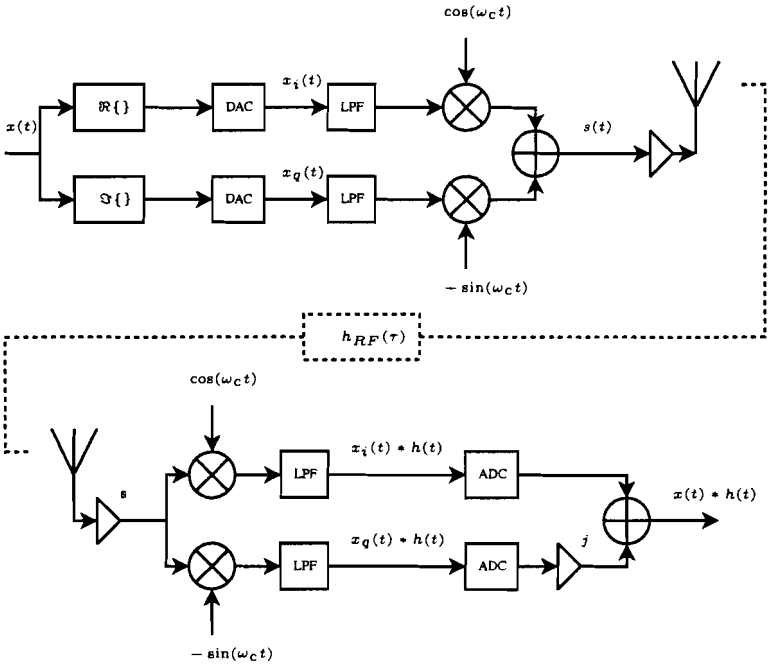

Figure 3.4: Transmitter - receiver chain

Chapter 4

IQ imbalance modeling

Chapter 3 discussed several ways to convert a digital baseband signal into an analog signal suitable for transmission, as well as to convert a received radio frequency (RF) analog signal into a digital baseband signal. All those methods assume that the quadrature-phase path is exactly identical to the in-phase path. However, in reality, not two paths will be exactly the same, as those paths consist of analog components. These differences can be caused by differences between two realizations of the same analog component and/or different environments around each path causing different parasitic effects.

It is important to note that these differences are fairly constant over time. They can change over time due to heating aging. However, the duration of an IEEE 802.11a packet is less than 6 ms for a BPSK modulated rate 1/2 coded packet with 4096 bytes payload. This is the maximum duration of an IEEE 802.11a packet, and in practice, it will usually even be less than 2.1 ms, since the payload is often 1560 bytes or less. Therefore, it is valid to assume that IQ imbalance is time invariant for the duration of at least one packet.

This chapter will discuss the effect of small differences between both paths, called in-phase / quadrature-phase imbalance (IQ imbalance). Section 4.1 discusses IQ imbalance in the receiver, followed by Section 4.2 which discusses IQ imbalance in the transmitter. Section 4.3 will treat the combination of receiver and transmitter caused imbalance. In Section 4.4, the effects of IQ imbalance on a received OFDM signal will be shown, where Section 4.5 will show the effects on channel and symbol estimation in OFDM systems. Finally, Section 4.6 will show the influence of IQ imbalance on the bit error rate and packet error rate performance of a wireless LAN system based on IEEE 802.11a applying 64 QAM modulation and rate 3/4 convolutional coding.

4.1 IQ imbalance in receiver

There are two ways to model IQ imbalance in the receiver: the symmetric model and the asymmetric model. The difference is in the way the models define the reference gain and phase: in the symmetric model, the reference gain is the average of the gain in both branches whereas in the asymmetric model, the reference gain is the gain in the in-phase branch. Similar for the phase, the reference phase in the symmetric model is the average of the phase error in both branches and in the asymmetric model, the reference phase is the phase in the in-phase branch. Both models will be discussed shortly for receiver caused imbalance, followed by a comparison of both models.

The phase imbalance can be caused by many components in the frond end. However, we will model it as an effect in the 90 degrees phase shifter. Also the difference in gain can be caused by many components in the frond and, but we will model it as if it is caused by the mixers in the in-phase and quadrature-phase branches. We will model both effects as if they are constant over the bandwidth of interest, i.e., frequency independent.

However, frequency dependent IQ imbalance can occur if there is a difference in the low pass filters of both branches. Therefore, at the end of this section, the asymmetric model is extended to an asymmetric frequency dependent model, to cover for mismatch between the low pass filters as well.

4.1.1 Frequency independent symmetric model

For frequency independent IQ imbalance, the differences between the in-phase (I) branch and the quadrature-phase (Q) branch are constant over the whole signal bandwidth. For a zero-IF receiver, this usually means that the IQ imbalance is caused in the mixer or in the 90 degrees phase shifter.

The symmetric model spreads out those differences evenly between the "I" and "Q" branches, as illustrated in figure 4.1.

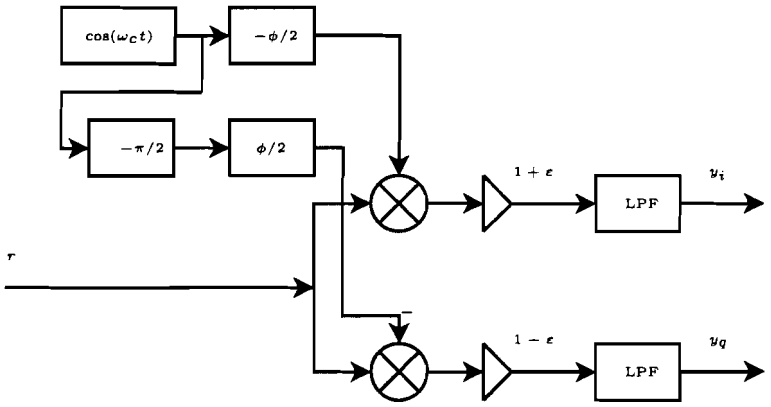

Figure 4.1: Symmetrical model for frequency independent receiver-caused IQ imbalance

As can be seen in this figure, there is a difference of ϕ rad between the cosine and the sine, modeled as the cosine having a phase offset of $-\phi/2$ rad and the sine having a phase offset of $\phi/2$ rad. The gain mismatch between both paths is modeled as $1+\varepsilon$ for the in-phase path and $1-\varepsilon$ for the quadrature-phase path.

The signals y_i and y_q are the signals right after the Low Pass Filter (LPF) operation. They can be written as a function of the received RF signal $r(t)$ by

$$y_i(t) = \mathrm{LPF}\{(1+\varepsilon)\cos(\omega_c t - \phi/2)\, r(t)\} \tag{4.1}$$

$$y_q(t) = -\mathrm{LPF}\{(1-\varepsilon)\sin(\omega_c t + \phi/2)\, r(t)\}, \tag{4.2}$$

where $\mathrm{LPF}\{\cdot\}$ denotes the low pass filtering operation, ω_c is the carrier frequency in rad/s and $r(t)$ can be expressed by

$$\begin{aligned} r(t) &= (x_i(t)\cos(\omega_c t) - x_q(t)\sin(\omega_c t)) \star h_{RF}(t) \\ &= \frac{1}{2}\left(x(t)e^{j\omega_c t} + x^*(t)e^{-j\omega_c t}\right) \star h_{RF}(t) \\ &= \Re\left\{x(t)e^{j\omega_c t}\right\} \star h_{RF}(t). \end{aligned} \tag{4.3}$$

$x_i(t)$ and $x_q(t)$ are the original transmitted baseband signals with $x(t) = x_i(t) + jx_q(t)$ and $h_{RF}(t)$ is the RF channel impulse response. ω_c denotes the carrier frequency and $x(t)$ denotes the transmitted baseband signal.

Assuming the low pass filters completely suppress the higher order modulation terms, $y_i(t)$ and $y_q(t)$ can

be written as

$$y_i(t) = \frac{1+\varepsilon}{2}(\cos(\phi/2)\,\Re\{(x \star h)(t)\} - \sin(\phi/2)\,\Im\{(x \star h)(t)\}) \tag{4.4}$$

$$y_q(t) = \frac{1-\varepsilon}{2}(-\sin(\phi/2)\,\Re\{(x \star h)(t)\} + \cos(\phi/2)\,\Im\{(x \star h)(t)\}), \tag{4.5}$$

where $h(t)$ is the baseband equivalent of $h_{RF}(t)$ (according to equation (3.6)) and $\Re\{(x \star h)(t)\} = (x_i \star h_r)(t) - (x_q \star h_i)(t)$ and $\Im\{(x \star h)(t)\} = (x_q \star h_r)(t) + (x_i \star h_i)(t)$. After the ADC, the signal processing is purely digital and $y_i(t)$ and $y_q(t)$ can be combined into the complex signal $y(t) = 2(y_i(t) + iy_q(t))$, where the factor 2 was added for notational convenience. This signal can be written as

$$y(t) = ax(t) \star h(t) + b(x(t) \star h(t))^*, \tag{4.6}$$

with $a = \cos(\phi/2) + j\varepsilon \sin(\phi/2)$ and $b = \varepsilon \cos(\phi/2) - j \sin(\phi/2)$.

For small values of IQ imbalance, i.e., $\phi \approx 0$ and $\varepsilon \approx 0$, the values of a and b are approximately $a \approx 1$ and $b \approx 0$. In that case, equations (4.4) and (4.5) reduce to equations (3.5) and (3.8) and the system is equal to the ideal zero-IF transmitter and receiver that we analyzed in Section 3.3.

The Fourier transform of $y(t)$ is given by

$$Y(\omega) = aX(\omega)H(\omega) + bX^*(-\omega)H^*(-\omega). \tag{4.7}$$

In equation (4.7) we can see that in case of IQ imbalance, the received signal on frequency ω consists not only of the transmitted symbol on frequency ω, but also of an interference term of the transmitted symbol on frequency $-\omega$. For an OFDM system, Proakis shows in [7] that equation (4.7) can be written as

$$Y_k = aX_kH_k + bX^*_{-k}H^*_{-k}, \tag{4.8}$$

where

- Y_k is a short notation for $Y(\omega_k)$ with $\omega_k = \frac{k}{N_s}W$ and where k is the subcarrier index,
- N_s is the number of subcarriers,
- W is the signal bandwidth.

This is illustrated in figure 4.2. In part (a) of this figure, the spectrum of the transmitted baseband signal is shown. In this example, we assume that the transmitted signal power is equal for all subcarriers. In part (b), the positive side of the spectrum of the received RF signal is shown. Here, we see that some subcarriers experienced a stronger attenuation than others due to the frequency selective channel. In part (c), the spectrum of the received baseband signal is shown. In this figure, we explicitly plot the desired signal (light grey) and the interfering signal (dark grey). The interfering signal is a scaled version of the desired signal, but mirrored in frequency. The received baseband signal is the superposition of both signals.

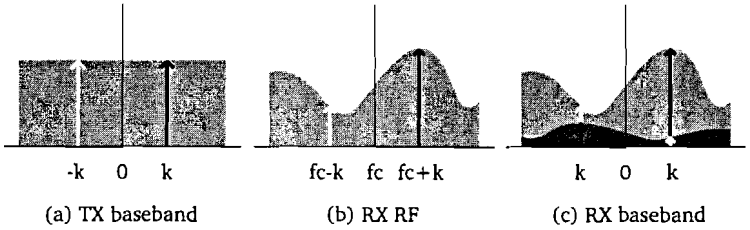

Figure 4.2: Influence of receiver caused IQ imbalance on received OFDM signal spectrum

Note that ε and ϕ can be derived from a and b by

$$\phi = 2\tan^{-1}\left(\frac{\Im\{a+b^*\}}{\Re\{a+b^*\}}\right) \tag{4.9}$$

$$\varepsilon = 2|a+b^*| - 1. \tag{4.10}$$

This model is used by e.g. Buchholz [11] and Tubbax [12] and in a slightly modified form for transmitter-caused IQ imbalance by Brötje [13].

4.1.2 Frequency independent asymmetric model

In contrast to the symmetric model, the asymmetric model assumes a perfect in-phase branch and moves all differences between the in-phase and quadrature-phase branches into the quadrature branch, as illustrated in figure 4.3.

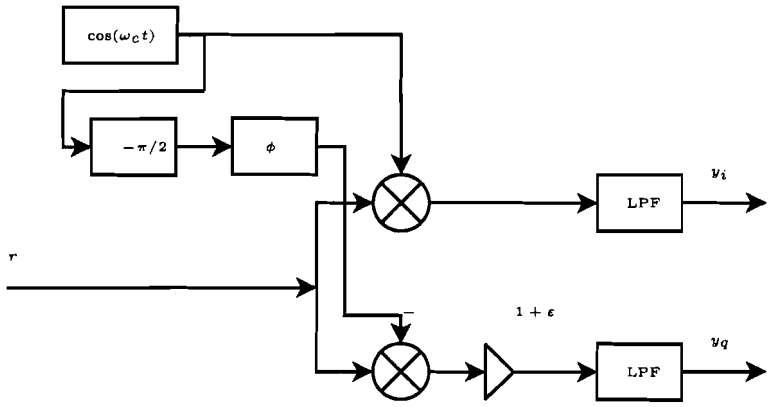

Figure 4.3: Asymmetrical model for frequency independent receiver-caused IQ imbalance

According to this model, the received signal after the LPF is $y(t) = y_i(t) + iy_q(t)$, where

$$y_i(t) = \text{LPF}\{\cos(\omega_c t)r(t)\} \tag{4.11}$$

$$y_q(t) = -\text{LPF}\{(1+\varepsilon)\sin(\omega_c t + \phi)r(t)\}. \tag{4.12}$$

Substituting equation (4.3) in (4.12) yields

$$y_i(t) = \frac{1}{2}\Re\{(x \star h)(t)\} \tag{4.13}$$

$$y_q(t) = \frac{1}{2}(1+\varepsilon)\left(-\sin(\phi)\Re\{(x \star h)(t)\} + \cos(\phi)\Im\{(x \star h)(t)\}\right). \tag{4.14}$$

where again $\Re\{(x \star h)(t)\} = (x_i \star h_r)(t) - (x_q \star h_i)(t)$ and $\Im\{(x \star h)(t)\} = (x_q \star h_r)(t) + (x_i \star h_i)(t)$.

After the ADC, the complex signal $y(t)$ can be formed, which can be written as

$$y(t) = ax(t) \star h(t) + b(x(t) \star h(t))^*, \tag{4.15}$$

with

$$a = \left(1 + (1+\varepsilon)e^{-j\phi}\right)/2 \tag{4.16}$$

and

$$b = \left(1 - (1+\varepsilon)e^{j\phi}\right)/2. \tag{4.17}$$

Again, for small values of IQ imbalance, i.e., $\phi \approx 0$ and $\varepsilon \approx 0$, we have $a \approx 1$ and $b \approx 0$. In that case, equations (4.13) and (4.14) reduce to equations (3.5) and (3.8) and the system is equal to the ideal zero-IF transmitter and receiver that we analyzed in Section 3.3.

The Fourier transform of $y(t)$ in equation (4.15) is then found by

$$Y(\omega) = aX(\omega)H(\omega) + bX^*(-\omega)H^*(-\omega). \tag{4.18}$$

When we rewrite $Y(\omega_k)$ as Y_k with $\omega_k = \frac{k}{N_s}W$, the signal that is received by the DSP in an OFDM system can be written as

$$Y_k = aH_kX_k + bH^*_{-k}X^*_{-k}. \tag{4.19}$$

Note that ε and ϕ can be calculated from a and b using

$$\phi = \tan^{-1}\left(\frac{1-(a+b)}{j(a-b)}\right) \tag{4.20}$$

$$\varepsilon = \frac{a-b}{\cos(\phi)} - 1. \tag{4.21}$$

This model and a slightly modified model for transmitter caused IQ imbalance is used in Schenk [14] and Valkama [15].

4.1.3 Comparison of symmetric and asymmetric model

In the previous section, we have presented two models for frequency independent IQ imbalance in the receiver. In this section, we will compare both models. We will show that they are functionally equivalent and discuss a nice advantage of the asymmetric model.

To compare the symmetric model with the asymmetric model, we write the imbalance parameters ε, ϕ and a and b for the symmetric model as ε_s, ϕ_s and a_s and b_s. The corresponding parameters for the asymmetric model are then denoted by ε_a, ϕ_a and a_a and b_a.

Let $y(t)$ be the received signal in the symmetric model with coefficients ε_s and ϕ_s. We can now define a new signal $y'(t) = gy(t)$ and we will show that this new signal can be written as the received signal in the asymmetric model, with coefficients ε_a and ϕ_a.

If the input signal $r(t)$, i.e., the signal right after the Low Noise Amplifier (LNA) is multiplied with constant $g = \frac{1}{1+\varepsilon_s}e^{-j\phi_s/2}$, the received signal of equation (4.6) can be written as

$$\begin{aligned} y(t)' &= gy(t) \\ &= a_s\, g\, x(t) \star h(t) + b_s(g\, x(t) \star h(t))^* && (4.22) \\ &= \frac{1}{2}\left(1 + \frac{1-\varepsilon_s}{1+\varepsilon_s}e^{-j\phi_s}\right) x(t) \star h(t) + \frac{1}{2}\left(1 - \frac{1-\varepsilon_s}{1+\varepsilon_s}e^{j\phi_s}\right)(x(t) \star h(t))^*. && (4.23) \end{aligned}$$

If we now choose ϕ_s equal to ϕ_a and ε_s equal to $\frac{-\varepsilon_a}{2+\varepsilon_a}$, equation (4.23) yields

$$y'(t) = \frac{1}{2}\left(1 + (1+\varepsilon_a)e^{-j\phi_a}\right) x(t) \star h(t) + \frac{1}{2}\left(1 - (1+\varepsilon_a)e^{j\phi_a}\right)(x(t) \star h(t))^*, \tag{4.24}$$

which equals equation 4.15, i.e., the expression from the asymmetric model.

Thus, by multiplying the received signal $r(t)$ with g and choosing the proper values for ε_a and ϕ_a, we can rewrite the symmetric model into the asymmetric model.

Note that this factor g can be moved into the channel impulse response, since it is present in both the in-phase and quadrature-phase branch. Let us therefore rewrite equation (4.22) as

$$\begin{aligned} y'(t) &= a_s\, x(t) \star (g\, h(t)) + b_s (x(t) \star (g\, h(t)))^* \\ &= a_s\, x(t) \star h'(t) + b_s (x(t) \star h'(t))^*. \end{aligned}$$

Now, the input signals to both models are equal, but the factor g is included in the channel impulse response.

Thus, the main difference between both models is that the effective channel impulse response in the asymmetric model differs from the effective channel impulse response in the symmetric model by a factor g. Otherwise, there is no difference and the two models are functionally equivalent. Note that this factor g is applied after the LNA, and is thus also applied to the noise which is added by the LNA. Therefore, the signal to noise ratio is not affected by g.

Advantage of the asymmetric model

Although the expressions for the signal $y(t)$ in both the symmetric and asymmetric model are equivalent, there exists an important difference for properties of the coefficients a and b. Looking back at equations (4.16) and (4.17), we can conclude that for the asymmetric model, they have the nice property

$$a_a + b_a^* = 1. \tag{4.25}$$

However, for symmetric model, the relationship between a_s and b_s is not so straightforward.

Since there is such a simple relationship between a_a and b_a, it is easier to work with the asymmetric model. When designing an algorithm to estimate the IQ imbalance, this model allows one to estimate just one complex variable (either a or b), and to obtain the other with a simple computation using equation (4.25). Hence, in the remainder of this document, we will only use the asymmetric model.

4.1.4 Frequency dependent asymmetric model

In the previous sections, we discussed frequency independent IQ imbalance. While it is valid to model the mismatch in RF components such as mixers and oscillators as a frequency independent mismatch, it is not valid to do so for baseband components like low pass filters. Therefore, in this section, we will discuss a model for frequency dependent IQ imbalance.

To model frequency dependent IQ imbalance, equation (4.14) must be changed to

$$y_i(t) = \frac{1}{2}\left[x_i \star h' \star g'_{RX,i}\right](t) \tag{4.26}$$

$$y_q(t) = \frac{1}{2}(1+\varepsilon)\left(-\sin(\phi)[x_i \star h' \star g'_{RX,q}](t) + \cos(\phi)[x_q \star h' \star g'_{RX,q}](t)\right), \tag{4.27}$$

where $[f_1 \star f_2](t)$ denotes the convolution of $f_1(t)$ with $f_2(t)$, $g'_{RX,i}(t)$ is the impulse response of the baseband filter in the in-phase branch of the receiver and $g'_{RX,q}(t)$ the impulse response of the corresponding filter in the quadrature-branch.

When signal $y(t) = y_i(t) + jy_q(t)$ is written as

$$y(t) = \left[a' \star x \star h'\right](t) + \left[b' \star (x \star h')^*\right](t), \tag{4.28}$$

the coefficients $a'(\tau)$ and $b'(\tau)$ can be written as

$$a'(\tau) = \left(g'_{RX,i}(\tau) + (1+\varepsilon) g'_{RX,q}(\tau) e^{-j\phi}\right)/2 \tag{4.29}$$

$$b'(\tau) = \left(g'_{RX,i}(\tau) - (1+\varepsilon) g'_{RX,q}(\tau) e^{j\phi}\right)/2. \tag{4.30}$$

In a practical system, $g'_{RX,i}(\tau)$ and $g'_{RX,q}(\tau)$ are real filters, and therefore

$$a'(\tau) + b'^{*}(\tau) = g'_{RX,i}(\tau). \tag{4.31}$$

When the impulse response of the filter in the quadrature branch is modeled as

$$g'_{RX,q}(\tau) = \left[g'_{RX,i} \star \Delta g_{RX}\right](\tau),$$

$g'_{RX,i}(\tau)$ is present in both paths and can be accounted for in the effective channel impulse response:

$$h(t) = h'(t) \star g'_{RX,i}(\tau). \tag{4.32}$$

Now we can define the IQ imbalance parameters $a(\tau)$ and $b(\tau)$ by:

$$a'(\tau) = a(t) \star g'_{RX,i}(\tau) \tag{4.33}$$

$$b'(\tau) = b(t) \star g'_{RX,i}(\tau). \tag{4.34}$$

As a result, signal $y(t)$ can be written as

$$y(t) = a(\tau) \star x(t) \star h(t) + b(\tau) \star (x(t) \star h(t))^{*}. \tag{4.35}$$

Moreover, equation (4.31) can be rewritten as

$$a(t) + b^{*}(t) = \delta(t). \tag{4.36}$$

In frequency domain, this yields

$$A_k + B^{*}_{-k} = 1. \tag{4.37}$$

Taking the Fourier transform of equation (4.35), we obtain the following representation of the received signal Y_k:

$$Y_k = \qquad\qquad = A_k X_k H_k + B_k X^{*}_{-k} H^{*}_{-k}. \tag{4.38}$$

It is to be expected that IQ imbalance for subcarriers close to the outer edges ($-N/2$ and $N/2$) is more severe than for subcarriers around 0, considering the outer edges are usually close to the cut off frequency of the low pass filters.

Note that the algorithms in the remainder of this report are developed for frequency independent IQ imbalance only.

4.2 IQ imbalance in transmitter

Section 4.1 discussed the modeling of IQ imbalance in receivers. However, IQ imbalance can also occur in transmitters. Therefore, in this section, we will derive a model for frequency independent IQ imbalance in transmitters, similar to the asymmetric model for frequency independent IQ imbalance in receivers from Section 4.1.2.

Note though, that most standards for wireless communications do not specify the amount of IQ imbalance that is allowed in the transmitter or receiver. However, they usually do specify that the error in the transmitted signal is within certain ranges. Therefore, this in principle limits the amount of IQ imbalance that is allowed in the transmitter, while IQ mismatch in the receiver can be arbitrarily large.

In case of transmitter caused IQ imbalance, the distorted transmitted signal can be modeled as

$$\begin{aligned} s(t) &= x_i(t)\cos(\omega_c t) - x_q(t)(1+\varepsilon)\sin(\omega_c t + \phi) \\ &= \frac{1}{2}\left(e^{j\omega_c t}(x_i(t) + jx_q(t)(1+\varepsilon)e^{j\phi}) + e^{-j\omega_c t}(x_i(t) + jx_q(t)(1+\varepsilon)e^{j\phi})^*\right) \\ &= \Re\left\{e^{j\omega_c t}\left(x_i(t) + jx_q(t)(1+\varepsilon)e^{j\phi}\right)\right\}. \end{aligned} \tag{4.39}$$

In a perfect receiver, i.e. one without any IQ imbalance at all, the signals after the low pass filters are then

$$y_i(t) = \frac{1}{2}\left(x_i(t) - (1+\varepsilon)\sin(\phi)x_q(t)\right) \star h(t) \tag{4.40}$$

$$y_q(t) = \frac{1}{2}x_q(t)(1+\varepsilon)\cos(\phi) \star h(t). \tag{4.41}$$

The DSP could combine $y_i(t)$ and $y_q(t)$ to form $y(t) = 2\left(y_i(t) + jy_q(t)\right)$: (adding a factor 2 for notational convenience)

$$\begin{aligned} y(t) &= \left(x_i(t) - (1+\varepsilon)\sin(\phi)x_q(t) + jx_q(t)(1+\varepsilon)\cos(\phi)\right) \star h(t) \\ &= \left(x_i(t) + j(1+\varepsilon)e^{j\phi}x_q(t)\right) \star h(t) \\ &= \left(ax(t) + b^*x^*(t)\right) \star h(t), \end{aligned} \tag{4.42}$$

with

$$\begin{aligned} a &= \left(1 + (1+\varepsilon)e^{j\phi}\right)/2 \\ b &= \left(1 - (1+\varepsilon)e^{-j\phi}\right)/2. \end{aligned} \tag{4.43}$$

Note that again $a = 1 - b^*$.

Taking the Fourier transform of equation (4.42) yields for the received signal Y_k:

$$\begin{aligned} Y_k &= S_k H_k \\ &= (aX_k + b^*X^*_{-k})H_k. \end{aligned} \tag{4.44}$$

We see here that the effect of transmitter caused IQ imbalance on the received signal is similar to receiver caused IQ imbalance and the property of $a = 1 - b^*$ that we found for receiver caused imbalance is also applicable for transmitter caused imbalance.

Note that ε and ϕ can be calculated from a and b with

$$\phi = \tan^{-1}\left(\frac{a+b-1}{j(a-b)}\right) \tag{4.45}$$

$$\varepsilon = \frac{a-b}{\cos(\phi)} - 1. \tag{4.46}$$

4.3 IQ imbalance in both transmitter and receiver

If both the transmitter and the receiver have IQ mismatch, the models in the previous sections can be combined to describe the received baseband signal on the k-th carrier:

$$\begin{aligned} Y_k &= a_{RX}S_kH_k + b_{RX}S^*_{-k}H^*_{-k} \\ &= a_{RX}(a_{TX}X_k + b^*_{TX}X^*_{-k})H_k + b_{RX}(a_{TX}X_{-k} + b^*_{TX}X^*_k)^*H^*_{-k} \\ &= (a_{RX}a_{TX}H_k + b_{RX}b_{TX}H^*_{-k})X_k + (a_{RX}b^*_{TX}H_k + b_{RX}a^*_{TX}H^*_{-k})X^*_{-k}, \end{aligned} \tag{4.47}$$

where a_{TX} and b_{TX} are the IQ imbalance parameters of the transmitter and a_{RX} and b_{RX} are the corresponding parameters of the receiver.

In case there is also additive white Gaussian noise experienced in the receiver of the system, equation (4.47) becomes

$$Y_k = (a_{RX}a_{TX}H_k + b_{RX}b_{TX}H^*_{-k})X_k + (a_{RX}b^*_{TX}H_k + b_{RX}a^*_{TX}H^*_{-k})X^*_{-k} + a_{RX}N_k + b_{RX}N^*_{-k}, \tag{4.48}$$

where N_k represents the noise on subcarrier k.

From equation (4.48) we see that the noise is only affected by IQ imbalance in the receiver. Furthermore, there will be some very small noise coloring due to correlation between noise on the mirror subcarriers.

4.4 Effect on received OFDM signals

Figure 4.4 shows the effect of transmitter IQ imbalance and receiver IQ imbalance on the constellation diagram observed at one subcarrier which is modulated with a QPSK signal. The received signal Y_k at this subcarrier is divided by H_k, so what we plot in this figure is the signal

$$Y_k/H_k = ((a_{RX}a_{TX} + b_{RX}b_{TX}H^*_{-k}/H_k)X_k + (a_{RX}b^*_{TX} + b_{RX}a^*_{TX}H^*_{-k}/H_k)X^*_{-k}). \tag{4.49}$$

As can be seen from the upper right and the lower left graphs, IQ imbalance in the transmitter and receiver both cause a superposition, i.e. interference, of the complex scaled constellation diagram of the opposite subcarrier $-k$ on the observed subcarrier k.

It can be observed from the above equation that the amplitude of the interference term does not depend on the channel realization in the case of only transmitter IQ imbalance. For receiver IQ imbalance however, also the combination of channel realizations of the desired subcarrier, H_k and the interfering subcarrier, H_{-k} determine the amount of interference.

The effect of this is that in case of receiver based IQ imbalance, the interference term can be very strong if the channel coefficient at subcarrier k is small compared to the channel coefficient at $-k$ (in other words: if k is in a deep fade and $-k$ is not). For transmitter imbalance however, the channel realization has no effect on the strength of the interference. This is illustrated in Figure 4.4, where the superimposed constellation in case of receiver imbalance contains more energy than the superimposed constellation in case of transmitter imbalance.

Although not immediately clear from the figures, the original constellation is scaled by a factor $a_{RX}a_{TX}$, as can be seen from equation (4.49).

We can conclude from Figure 4.4 that IQ imbalance degrades the received signal. For low order constellation types like BPSK and QPSK, IQ imbalance is not a serious problem, since the amount of interference is relatively small compared to the spacing between the constellation points. However, for larger constellation sizes such as 16 QAM or 64 QAM, IQ imbalance can seriously affect the performance of the system.

4.5 Effect on channel and symbol estimation in OFDM systems

In an OFDM system, there are usually pilot tones which can help the receiver in estimating the transmission channel. Suppose an OFDM system uses the first OFDM symbol of a packet to transmit pilot tones. A very basic method to do channel estimation for such a system, is then to divide each subcarrier of the received training field by the pilot tone.

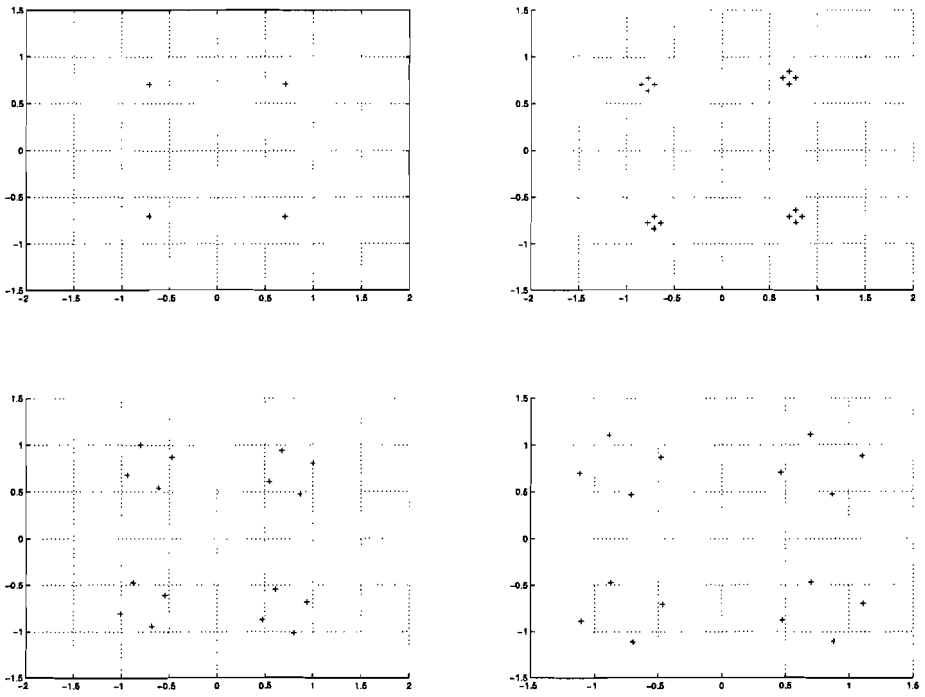

Figure 4.4: Effect of IQ imbalance in transmitter and receiver on observed QPSK constellation; upper left: no IQ imbalance; upper right: TX imbalance 10%, 5°, lower left: RX imbalance 10%, 5°, lower right: both TX and RX imbalance 10%, 5°

The resulting estimated channel coefficient for subcarrier k is

$$\begin{aligned}\hat{H}_k &= Y_{P,k}/P_k \\ &= (a_{RX}a_{TX} + a_{RX}b^*_{TX}P^*_{-k}/P_k)H_k + (b_{RX}a^*_{TX}P^*_{-k}/P_k + b_{RX}b_{TX})H^*_{-k},\end{aligned} \tag{4.50}$$

where P_k is the pilot symbol on subcarrier k and $Y_{P,k}$ is the received signal in the pilot field on subcarrier k. This shows that the estimated channel coefficient will be scaled by $(a_{RX}a_{TX} + a_{RX}b^*_{TX}P^*_{-k}/P_k)$ and, in addition, there will be interference from the mirror subcarrier coefficient H_{-k}.

In case $P^*_{-k}/P_k = 1$, equation (4.50) reduces to $\hat{H}_k = a_{RX}H_k + b_{RX}H^*_{-k}$. Thus, for the subcarriers where $P^*_{-k}/P_k = 1$, transmitter imbalance will not degrade the channel estimate.

Using the channel estimate from equation (4.50) for zero forcing equalization, the estimated transmitted symbol before de-mapping will be

$$\begin{aligned}\hat{X}_k &= Y_k/\hat{H}_k \\ &= \frac{a_{RX}a_{TX}H_k + b_{RX}b_{TX}H^*_{-k} + (a_{RX}b^*_{TX}H_k + b_{RX}a^*_{TX}H^*_{-k})X^*_{-k}/X_k}{a_{RX}a_{TX}H_k + b_{RX}b_{TX}H^*_{-k} + (a_{RX}b^*_{TX}H_k + b_{RX}a^*_{TX}H^*_{-k})P^*_{-k}/P_k}X_k.\end{aligned} \tag{4.51}$$

In the special case that $X^*_{-k}/X_k = P^*_{-k}/P_k$, this reduces to $\hat{X}_k = X_k$. This means, that for some combinations of pilot tones and data symbols, zero forcing equalization will cancel out the effects of both transmitter and receiver IQ imbalance on subcarriers k and $-k$.

4.6 Effect on error rates in 802.11a systems

Sections 4.4 and 4.5 showed the effect of IQ imbalance on the received signal and on the channel and symbol estimates. They showed that it can be a serious problem for systems which use large constellation sizes. Therefore, it is interesting to see how IQ imbalance will actually effect the average bit error rate (BER) and average packet error rate (PER) of a system which does not compensate for IQ imbalance.

The simulation results presented in this section were done for a wireless LAN system based on IEEE 802.11a applying 64 QAM modulation and rate 3/4 convolutional coding.

The channel model used for the simulations in this section is a Rayleigh fading channel with an exponentially decaying power delay profile. The channel impulse response had an rms delay spread of 50 ns, which, according to Rappaport [4] and Van Nee [16], is a typical value for a wireless channel in small-office and home-office environments. The total impulse response had a fixed length of 500 ns. At 20 MHz sample rate, this corresponds to 11 samples.

Furthermore, channel equalization was done using a zero forcing approach. While it is generally known that zero forcing can cause noise enhancement, as shown by Bergmans [17], it does give a lot of insight and has low computational complexity.

In Figure 4.5, the line marked with '*' symbols, shows the bit error rate for a 64 QAM rate 3/4 system without IQ imbalance. As we can see, the error rate decreases if the signal to noise ratio (SNR) increases.

The line marked with triangles pointing upwards shows a system where the transmitter has an IQ imbalance of 10% and 5°. As we can see from this figure, such a system shows a bit error rates which are not as low as the bit error rates for a perfect system at the same SNR, but the curve is still acceptable.

As we can see, the curve marked with triangles pointing downwards, a system where the receiver has an IQ imbalance of 10% and 5° performs much worse. There appears to be a floor at about $5 \cdot 10^{-2}$ and the bit error rate cannot become any lower than that by just increasing the signal to noise ratio.

Finally, the curve marked with dots shows the bit error rate performance of a system where both the transmitter and the receiver have an IQ imbalance of 10% and 5°. As could be expected, this system performs even worse than the previous system, and has an error floor at about $1 \cdot 10^{-1}$.

Figure 4.6 shows the corresponding packet error rates. As we can see from that plot, in a perfect system, the packet error rate at an SNR of 48 dB is a little more than $2 \cdot 10^{-2}$, while the corresponding PER for a system with only transmitter imbalance is about 0.33. For a system where the receiver has IQ imbalance, or both the transmitter and receiver have IQ imbalance, the packet error rate is almost 1. This means, that there are hardly any packets for which all bits can be decoded correctly by the receiver.

Those figures clearly demonstrate that IQ imbalance in the receiver has a stronger effect on bit error rate than IQ imbalance in the transmitter, due to the fact that the interference for receiver caused imbalance can be very strong at subcarrier k, if subcarrier k is in a deep fade, as was shown in Section 4.4.

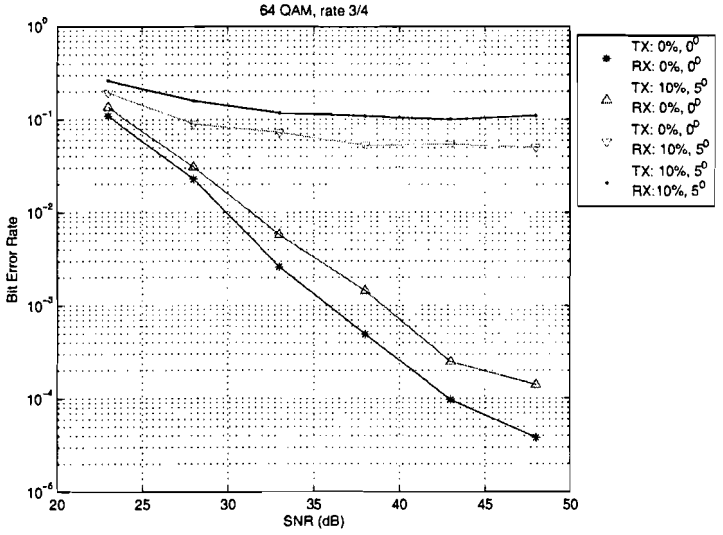

Figure 4.5: Bit Error Rates for systems with and without IQ imbalance

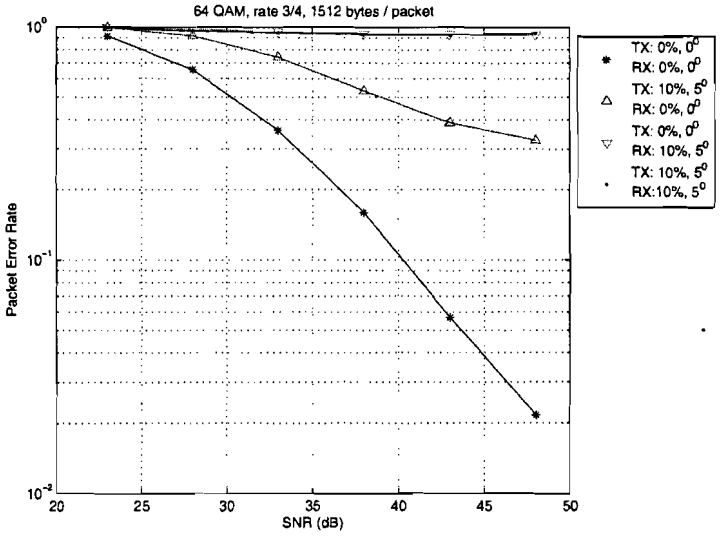

Figure 4.6: Packet Error Rates for systems with and without IQ imbalance

Chapter 5

Estimation and compensation algorithms

The previous chapter introduced models for IQ imbalance in both transmitter and receiver. It showed the influence of IQ imbalance on the received signal, on the estimated channel and on the equalized signal. Furthermore, it showed that IQ imbalance can limit the bit error rate and packet error rate performance of a system when higher order constellations are used.

This chapter will start by proposing a simple solution to compensate the received signal and the channel estimate for IQ imbalance in both transmitter and receiver in Section 5.1. Section 5.2 will give a short overview of current solutions for IQ imbalance estimation. Sections 5.3 and 5.4 will present some novel solutions for receiver respectively transmitter caused IQ imbalance. In Section 5.5, we will propose a solution for the case when there is IQ imbalance in both receiver and transmitter. A different approach to this problem is proposed in Section 5.6. At the end of this chapter, Section 5.7 will give a short summary of the proposed solutions.

Note that all of the proposed solutions in sections 5.3 - 5.6 are developed for frequency independent IQ imbalance only, for the sake of simplicity.

5.1 Compensation algorithm

5.1.1 Removing IQ imbalance from received signal

In the previous chapter, we described the joined influence of transmitter imbalance, a frequency selective fading channel and receiver imbalance on the received signal by equation (4.47). This equation can be rewritten as

$$\begin{pmatrix} Y_{-k}^* \\ Y_k \end{pmatrix} = \begin{pmatrix} a_{RX}^* & b_{RX}^* \\ b_{RX} & a_{RX} \end{pmatrix} \begin{pmatrix} H_{-k}^* & 0 \\ 0 & H_k \end{pmatrix} \begin{pmatrix} a_{TX}^* & b_{TX} \\ b_{TX}^* & a_{TX} \end{pmatrix} \begin{pmatrix} X_{-k}^* \\ X_k \end{pmatrix}. \tag{5.1}$$

The receiver can estimate the transmitted symbol X_k by inverting all three matrices. In doing so, the receiver would estimate the baseband equivalent of the received RF signal with

$$\begin{pmatrix} \hat{R}_{-k}^* \\ \hat{R}_k \end{pmatrix} = \begin{pmatrix} \hat{a}_{RX}^* & \hat{b}_{RX}^* \\ \hat{b}_{RX} & \hat{a}_{RX} \end{pmatrix}^{-1} \begin{pmatrix} Y_{-k}^* \\ Y_k \end{pmatrix}. \tag{5.2}$$

Once $\hat{R}_k$ is known, the receiver can to estimate the baseband equivalent of the transmitted RF signal by

$$\begin{pmatrix} \hat{S}^*_{-k} \\ \hat{S}_k \end{pmatrix} = \begin{pmatrix} 1/\hat{H}^*_{-k} & 0 \\ 0 & 1/\hat{H}_k \end{pmatrix} \begin{pmatrix} \hat{R}^*_{-k} \\ \hat{R}_k \end{pmatrix}. \tag{5.3}$$

Finally, the receiver can estimate the transmitted symbols by inverting the transmitter imbalance matrix by

$$\begin{pmatrix} \hat{X}^*_{-k} \\ \hat{X}_k \end{pmatrix} = \begin{pmatrix} \hat{a}^*_{TX} & \hat{b}_{TX} \\ \hat{b}^*_{TX} & \hat{a}_{TX} \end{pmatrix}^{-1} \begin{pmatrix} \hat{S}^*_{-k} \\ \hat{S}_k \end{pmatrix}. \tag{5.4}$$

These equations show that, if the receiver would have correct estimates of the channel and of the IQ imbalance parameters in both transmitter and receiver, it could completely compensate for all imbalance and fading effects.

However, in practice, the receiver initially does not have any estimates at all. Therefore, we need to develop a method for estimating the imbalance parameters.

5.1.2 Removing IQ imbalance from channel estimate

In equation (4.50) we showed the influence of TX and RX IQ imbalance on the channel estimate. Using that equation, it is possible to calculate a new estimate $\hat{H}_{c,k}$ of the channel, assuming that the estimates for transmitter and receiver imbalance are correct:

$$\begin{pmatrix} \hat{H}^*_{c,-k} \\ \hat{H}_{c,k} \end{pmatrix} = \begin{pmatrix} (\hat{a}_{RX}(\hat{a}_{TX} + \hat{b}^*_{TX}P^*_{-k}/P_k))^* & (\hat{b}_{RX}(\hat{a}^*_{TX}P^*_{-k}/P_k + \hat{b}_{TX}))^* \\ \hat{b}_{RX}(\hat{a}^*_{TX}P^*_{-k}/P_k + \hat{b}_{TX}) & \hat{a}_{RX}(\hat{a}_{TX} + \hat{b}^*_{TX}P^*_{-k}/P_k) \end{pmatrix}^{-1} \begin{pmatrix} \hat{H}^*_{-k} \\ \hat{H}_k \end{pmatrix}. \tag{5.5}$$

If there is only an estimate for receiver imbalance and no estimate for the imbalance in the transmitter, then we can temporarily assume the absence of transmitter IQ imbalance. The resulting correction for the raw channel estimate then becomes

$$\begin{pmatrix} \hat{H}^*_{c,-k} \\ \hat{H}_{c,k} \end{pmatrix} = \begin{pmatrix} 1/P^*_{-k} & 0 \\ 0 & 1/P_k \end{pmatrix} \begin{pmatrix} a^*_{RX} & b^*_{RX} \\ b_{RX} & a_{RX} \end{pmatrix}^{-1} \begin{pmatrix} P^*_{-k} & 0 \\ 0 & P_k \end{pmatrix} \begin{pmatrix} \hat{H}^*_{-k} \\ \hat{H}_k \end{pmatrix}. \tag{5.6}$$

The challenging task is now to find accurate estimates for b_{RX} and b_{TX}. Once these parameters are known, we can use the properties

$$a_{RX} = 1 - b^*_{RX} \tag{5.7}$$

$$a_{TX} = 1 - b^*_{TX} \tag{5.8}$$

to compute the estimates for a_{RX} and a_{TX}.

5.2 Existing estimation algorithms

Much research on estimation algorithms for IQ imbalance has already been done, and many solutions are already presented. Some of those algorithms, such as proposed by Fettweis [18], Windisch [19] and Shafiee [20], operate independently of the standard by measuring the correlation between subcarrier k and $-k$, or in time domain, as proposed by Valkama [15]. However, such methods usually require many samples to converge to the correct value. Much faster convergence can be achieved by exploiting the properties specific to one communication system. Therefore, in this section, we will give a short overview of the already existing solutions for estimators for an OFDM communication system.

Tubbax [12] proposes a solution for frequency flat IQ imbalance in the receiver in an 802.11a system by exploiting the fact that the channel estimate in frequency domain contains 64 taps, while in time domain, there are only 16 taps ($8.0\mu s$) allowed. Therefore, the channel estimate in frequency domain is oversampled and there should be a strong correlation between adjacent subcarriers. Due to the interference and the sign of the pilot symbols, this correlation is reduced. This method exploits the reduction in correlation to estimate the IQ imbalance parameters. This method does not obtain the exact value of IQ imbalance in one step. Therefore, the author proposes an iterative solution in which the estimation algorithm is stopped after one and a half iterations, as, according to the author, the accuracy of the estimate does not improve with further iterations.

Lin and Tsui [21], [22] offer a solution for IQ imbalance in 802.11a receivers. This solution exploits the difference in sign between the pilot symbol on subcarrier k and the mirrored subcarrier $-k$ in the long training field. It is in fact, an extension to the solution proposed by Tubbax, by using the long training field to do normal channel estimation and using the SIGNAL field to estimate IQ imbalance. This method typically needs 20 to 30 iterations on the SIGNAL field to converge to the exact value. In this paper, they also extend the method for frequency selective IQ imbalance.

Brötje [13] proposes a solution for frequency flat IQ imbalance in the receiver in an 802.11a system by exploiting orthogonality between pilot symbols in the long training field and in the DATA fields on subcarrier pairs -21 and 21 and -7 and 7. However, in this paper, the symmetric model for IQ imbalance is used and with that, the relationship between the IQ imbalance parameters is not exploited. In this proposed solution, the exact value of IQ imbalance is not immediately obtained. Furthermore, since the estimates are only based on 4 subcarriers, this solution does not perform very well. Therefore, a modified preamble is proposed, such that there are more subcarrier pairs with orthogonal symbols. However, this violates the 802.11a specification and the proposed solution still does not give an exact estimate for the IQ imbalance parameters after the first iteration.

Note that none of the solutions above deal with the combination of transmitter imbalance, receiver imbalance and a fading channel.

In [14], Schenk et al. propose a modified preamble to estimate both receiver and transmitter imbalance in an OFDM MIMO system. They propose a solution which finds the exact value for receiver imbalance if there is no transmitter imbalance and no noise, and they propose a solution which finds the exact value for transmitter imbalance if there is no receiver imbalance and no noise. When both methods are used in combination and if there is IQ imbalance in both receiver and transmitter the exact values cannot be found in one iteration. Therefore, they propose an iterative algorithm. In this iterative solution, the imbalance in the receiver and in the transmitter are estimated once for every received packet. The estimated values of the current packet are used as initial estimates for the next packet. This method requires many packets to converge to the exact value of transmitter and receiver imbalance. Note also, that this method only works if all received packets are from the same transmitter. In a multi user environment, a received packet can be originated at any time from a different transmitter which has a different transmitter imbalance. Therefore, this solution is not suited for multi-user environments.

In the next sections, we will present some novel methods to estimate frequency independent IQ imbalance in transmitter and receiver, which eliminate some of the drawbacks of the existing solutions.

5.3 Estimation algorithm for receiver caused IQ imbalance

As a first attempt, the problem of estimating the IQ imbalance parameters is simplified by considering only IQ imbalance in the receiver and assuming BPSK data symbols. These data symbols could for example be the BPSK rate $1/2$ coded SIGNAL field in an IEEE 802.11a WLAN system, as described in Chapter 2.

5.3.1 Model for receiver-caused IQ imbalance

For the case of receiver-caused IQ imbalance, the received signal and estimated channel on subcarrier k (equations (4.47) and (4.50)) can be simplified to

$$Y_k = a_{RX} H_k X_k + b_{RX} H^*_{-k} X^*_{-k} \tag{5.9}$$

and

$$\hat{H}_k = a_{RX} H_k + b_{RX} H^*_{-k} \frac{P^*_{-k}}{P_k} \tag{5.10}$$

respectively.

Note that for an 802.11a system, $P_k = \pm 1$, and therefore

$$P_k = P^*_k \tag{5.11}$$

and

$$\frac{P_k}{P_{-k}} = \frac{P_{-k}}{P_k}. \tag{5.12}$$

In the following analysis, equations (5.11) and (5.12) are used often and therefore this analysis is not applicable to arbitrary types of pilot tones.

5.3.2 Dependent estimation

In the previous chapter, we found the relation $a_{RX} = 1 - b^*_{RX}$ (equation (4.25)) between the imbalance parameters. When we substitute this relation into equation (5.9), we obtain a model for the received signal which does not depend on a_{RX}. However, in order to maintain a linear equation in the components of b_{RX}, we have to explicitly split up the received signal into real and imaginary parts:

$$\begin{aligned} Y_{k,r} =& H_{k,r}X_{k,r} - H_{k,i}X_{k,i} \\ &+ b_{RX,r}(-H_{k,r}X_{k,r} + H_{k,i}X_{k,i} + H_{-k,r}X_{-k,r} - H_{-k,i}X_{-k,i}) \\ &+ b_{RX,i}(-H_{k,r}X_{k,i} - H_{k,i}X_{k,r} + H_{-k,r}X_{-k,i} + H_{-k,i}X_{-k,r}) \end{aligned} \tag{5.13}$$

$$\begin{aligned} Y_{k,i} =& H_{k,r}X_{k,i} + H_{k,i}X_{k,r} \\ &- b_{RX,r}(H_{k,r}X_{k,i} + H_{k,i}X_{k,r} + H_{-k,r}X_{-k,i} + H_{-k,i}X_{-k,r}) \\ &+ b_{RX,i}(H_{k,r}X_{k,r} - H_{k,i}X_{k,i} + H_{-k,r}X_{-k,r} - H_{-k,i}X_{-k,i}) \end{aligned} \tag{5.14}$$

where the subscripts "r" and "i" denote the real and imaginary part respectively.

Equations (5.13) and (5.14) can be combined in matrix notation as

$$\begin{aligned} \begin{pmatrix} Y_{k,r} \\ Y_{k,i} \end{pmatrix} &= \begin{pmatrix} A_1 & A_2 \\ A_3 & A_4 \end{pmatrix} \begin{pmatrix} b_{RX,r} \\ b_{RX,i} \end{pmatrix} + \begin{pmatrix} A_5 \\ A_6 \end{pmatrix} \\ &= \mathbf{R_{1,k}} \begin{pmatrix} b_{RX,r} \\ b_{RX,i} \end{pmatrix} + \mathbf{R_{2,k}}, \end{aligned} \tag{5.15}$$

where

$$A_1 = -\Re\{H_k X_k\} + \Re\{H_{-k} X_{-k}\} \tag{5.16}$$

$$A_2 = -\Im\{H_k X_k\} + \Im\{H_{-k} X_{-k}\} \tag{5.17}$$

$$A_3 = -\Im\{H_k X_k\} - \Im\{H_{-k} X_{-k}\} \tag{5.18}$$

$$A_4 = \Re\{H_k X_k\} + \Re\{H_{-k} X_{-k}\} \tag{5.19}$$

$$A_5 = \Re\{H_k X_k\} \tag{5.20}$$

$$A_6 = \Im\{H_k X_k\} \tag{5.21}$$

and where $\Re\{x\}$ and $\Im\{x\}$ denote the real and imaginary parts of x, respectively.

The imbalance parameters $b_{RX,r}$ and $b_{RX,i}$ can now be obtained by

$$\begin{pmatrix} b_{RX,r} \\ b_{RX,i} \end{pmatrix} = \mathbf{R_{1,k}}^{-1} \left(\begin{pmatrix} Y_{k,r} \\ Y_{k,i} \end{pmatrix} - \mathbf{R_{2,k}} \right), \tag{5.22}$$

provided that the system has perfect knowledge of H and X and there is no noise.

However, $\mathbf{R_{1,k}}$ and $\mathbf{R_{2,k}}$ depend on the channel coefficients H_k and H_{-k}, and on the transmitted symbols X_k and X_{-k}. In reality, the receiver only has an estimate of those parameters. Therefore, the receiver can only obtain an estimate of $b_{RX,r}$ and $b_{RX,i}$. Such an estimate can for example be based on subcarrier k and $-k$ by

$$\begin{pmatrix} \hat{b}_{RX,k,r} \\ \hat{b}_{RX,k,i} \end{pmatrix} = \hat{\mathbf{R}}_{\mathbf{1,k}}^{-1} \left(\begin{pmatrix} Y_{k,r} \\ Y_{k,i} \end{pmatrix} - \hat{\mathbf{R}}_{\mathbf{2,k}} \right), \tag{5.23}$$

where $\hat{x}$ denotes the estimate of variable x.

The actual estimate of b_{RX} can then be found by combining the real and imaginary parts, and averaging over all subcarriers. With estimate $\hat{b}_{RX}$, the receiver can compute the estimate for a_{RX} using $\hat{a}_{RX} = 1 - \hat{b}^*_{RX}$. As the estimator exploits the dependency between a_{RX} and b_{RX}, we call this the dependent estimator. Later on, in Section 5.6.1, we will also consider an independent estimator, which treats a_{RX} and b_{RX} as two independent parameters.

A first attempt at estimating receiver IQ imbalance: zero forcing

A first attempt to estimate receiver IQ imbalance could be to assume that the channel estimate is perfect and that there are no decoding errors, i.e., the channel estimate is not affected by noise and IQ imbalance, and the estimated data symbols are correct. In case the data symbols X are BPSK modulated and rate $1/2$ convolutional coding is applied, decoding is very reliable, even if there is IQ imbalance present in the received signal and in the channel estimate. Thus, the estimated symbols $\hat{X}$ are very reliable and the assumption that there are no decoding errors is valid for most cases. BPSK rate $1/2$ coded symbols can be found in the SIGNAL field of an 802.11a packet.

In this section, we will shortly derive a simple expression for the determinant of $\hat{\mathbf{R}}_{\mathbf{1,k}}$. After that, we can analyze the value of $\hat{b}_{RX,k,r}$ as given by equation (5.23), if the estimator assumes that the channel estimate is perfect, when in reality, the channel estimate is corrupted by IQ imbalance, as expressed in equation (5.10). The analysis for the value $\hat{b}_{RX,k,i}$ will follow later on.

For the determinant of $\hat{\mathbf{R}}_{\mathbf{1,k}}$, we can write

$$\det(\hat{\mathbf{R}}_{\mathbf{1,k}}) = \hat{A}_1 \hat{A}_4 - \hat{A}_2 \hat{A}_3. \tag{5.24}$$

After substituting equations (5.16)-(5.19) and under the assumption of correct decoding, i.e. $\hat{X} = X$, this can be simplified for BPSK symbols to

$$\det(\hat{\mathbf{R}}_{\mathbf{1,k}}) = (1 - 2b_{RX,r}) \left(|H_{-k}|^2 - |H_k|^2 \right). \tag{5.25}$$

Note that $\det(\hat{\mathbf{R}}_{\mathbf{1,k}}) = -\det(\hat{\mathbf{R}}_{\mathbf{1,-k}})$. Note also that the determinant in equation (5.25) equals zero if the channel frequency response is symmetric, i.e., $H_k = H_{-k}$ for all k. An example of a symmetric channel is an AWGN channel, where $H_k = 1$ for all k. In case the channel frequency response is symmetric, it is not possible to calculate $\hat{b}_{RX,r}$ and $\hat{b}_{RX,i}$ by using equation (5.23). However, in a typical indoor wireless LAN scenario, the channel frequency response is usually not symmetric. Therefore, in the remainder of this section, we will assume that the determinant is non-zero.

For the real part of the estimate of b_{RX} based on carrier k, we can write

$$\det(\hat{\mathbf{R}}_{\mathbf{1},\mathbf{k}}) \cdot \hat{b}_{RX,k,r} = \hat{A}_4(Y_{k,r} - \hat{A}_5) - \hat{A}_2(Y_{k,i} - \hat{A}_6) \tag{5.26}$$

$$= (\Re\{\hat{H}_k\hat{X}_k\} + \Re\{\hat{H}_{-k}\hat{X}_{-k}\})(Y_{k,r} - \Re\{\hat{H}_k\hat{X}_k\}) - (-\Im\{\hat{H}_k\hat{X}_k\} + \Im\{\hat{H}_{-k}\hat{X}_{-k}\})(Y_{k,i} - \Im\{\hat{H}_k\hat{X}_k\}). \tag{5.27}$$

If X is a BPSK symbol, and assuming correct decoding (i.e. $\hat{X} = X$), substituting equations (5.10), (5.13) and (5.14) into equation (5.27) yields

$$\begin{aligned}
&\det(\hat{\mathbf{R}}_{\mathbf{1},\mathbf{k}}) \cdot \hat{b}_{RX,k,r} = \\
&b_{RX,r}(1 - s_k)(H_{-k,r}^2 + H_{-k,i}^2 - \frac{P_k}{P_{-k}^*}(H_{-k,r}H_{k,r} - H_{-k,i}H_{k,i})) \\
&+ b_{RX,i}\frac{P_k}{P_{-k}^*}(s_k - 1)(H_{-k,i}H_{k,r} + H_{-k,r}H_{k,i}) \\
&- 4b_{RX,r}b_{RX,i}\frac{P_k}{P_{-k}^*}(s_k - 1)(H_{-k,i}H_{k,r} + H_{-k,r}H_{k,i}) \\
&+ 2b_{RX,r}^2(s_k - 1)(H_{-k,r}^2 + H_{-k,i}^2 - \frac{P_k}{P_{-k}^*}(H_{-k,r}H_{k,r} - H_{-k,i}H_{k,i})) \\
&+ 2b_{RX,i}^2(s_k - 1)(H_{-k,r}^2 + H_{-k,i}^2 + \frac{P_k}{P_{-k}^*}(H_{-k,r}H_{k,r} - H_{-k,i}H_{k,i})),
\end{aligned} \tag{5.28}$$

with

$$s_k = X_{-k,r}X_{k,r}P_kP_{-k}. \tag{5.29}$$

Note that $s_kP_kP_{-k} = X_{-k,r}X_{k,r}$.

For all subcarriers k satisfying $X_k/X_{-k}^* = P_k/P_{-k}^*$, i.e., $s_k = 1$, the above equation simplifies to

$$\det(\hat{\mathbf{R}}_{\mathbf{1},\mathbf{k}})\hat{b}_{RX,k,r} = 0 \tag{5.30}$$

and thus $\hat{b}_{RX,k,r} = 0$. The case where $s_k = 1$ corresponds to the case when there is no orthogonality between the pairs (P_{-k}, P_k) and (X_{-k}, X_k). This means that, for those subcarriers where $s_k = 1$, the estimate for the real part of b_{RX} yields 0. This is not very surprising, as in that case, $X_k/X_{-k}^* = P_k/P_{-k}^*$ and thus the signal at those subcarriers is identical to the signal in the preamble[1], which was used to create the channel estimate. Thus, the received signal will not provide any new information, and an estimate for $b_{RX,r}$ cannot be made in this way.

If we define the error of the estimate $\hat{b}_{RX,k,r}$ as $\varepsilon_{\hat{b}_{RX,k,r}} = \hat{b}_{RX,k,r} - b_{RX,r}$, then

$$\varepsilon_{\hat{b}_{RX,k,r}} = -b_{RX.r} \tag{5.31}$$

for those subcarriers satisfying $s_k = 1$.

All other subcarriers satisfy $X_k/X_{-k}^* = -P_k/P_{-k}^*$, i.e. $s_k = -1$, and in that case, equation (5.28) can be

[1] The only possible difference is a factor -1

written as

$$\begin{aligned}
&\det(\hat{\mathbf{R}}_{\mathbf{1},\mathbf{k}}) \cdot \hat{b}_{RX,k,r} = \\
&\quad 2b_{RX,r}(H_{-k,r}^2 + H_{-k,i}^2) \\
&\quad - 2b_{RX,r}\frac{P_k}{P_{-k}^*}(H_{-k,r}H_{k,r} - H_{-k,i}H_{k,i}) \\
&\quad - 2b_{RX,i}\frac{P_k}{P_{-k}^*}(H_{-k,r}H_{k,i} - H_{-k,i}H_{k,r}) \\
&\quad + 8b_{RX,r}b_{RX,i}\frac{P_k}{P_{-k}^*}(H_{-k,i}H_{k,r} + H_{-k,r}H_{k,i}) \\
&\quad - 4b_{RX,r}^2(H_{-k,r}^2 + H_{-k,i}^2 - \frac{P_k}{P_{-k}^*}(H_{-k,r}H_{k,r} - H_{-k,i}H_{k,i})) \\
&\quad - 4b_{RX,i}^2(H_{-k,r}^2 + H_{-k,i}^2 + \frac{P_k}{P_{-k}^*}(H_{-k,r}H_{k,r} - H_{-k,i}H_{k,i})).
\end{aligned} \tag{5.32}$$

For the case where $s_k = -1$, the pairs (P_{-k}, P_k) and (X_{-k}, X_k) are orthogonal.

For those subcarriers where $s_k = -1$, calculating the error term for the estimate of $b_{RX,r}$ based on subcarrier k yields

$$\begin{aligned}
\varepsilon_{\hat{b}_{RX,k,r}} = &\Big[b_{RX,r}(|H_k|^2 + |H_{-k}|^2) \\
&+ 2b_{RX,r}\frac{P_k}{P_{-k}^*}(H_{-k,i}H_{k,i} - H_{-k,r}H_{k,r}) \\
&+ 2b_{RX,i}\frac{P_k}{P_{-k}^*}(H_{-k,i}H_{k,r} - H_{-k,r}H_{k,i}) \\
&+ 8b_{RX,r}b_{RX,i}\frac{P_k}{P_{-k}^*}(H_{-k,i}H_{k,r} + H_{-k,r}H_{k,i}) \\
&+ 2b_{RX,r}^2\left(2\frac{P_k}{P_{-k}^*}(H_{-k,r}H_{k,r} - H_{-k,i}H_{k,i}) - |H_k|^2 - |H_{-k}|^2\right) \\
&+ 4b_{RX,i}^2\left(\frac{P_k}{P_{-k}^*}(H_{-k,i}H_{k,i} - H_{-k,r}H_{k,r}) - |H_{-k}|^2\right)\Big] / \det(\hat{\mathbf{R}}_{\mathbf{1},\mathbf{k}}).
\end{aligned} \tag{5.33}$$

We can conclude from equations (5.31) and (5.33) that the error term depends on the value of s_k. This error term is either equal to $-b_{RX,r}$, i.e., the actual estimate $\hat{b}_{RX,k,r}$ equals 0, if $s_k = 1$, or the expression for this error term is very long, and is hard to deal with if $s_k = -1$. We can overcome these problems if we slightly modify our estimator.

Modified zero forcing based estimator

In the previous section, we tried to analyze the performance of a zero forcing estimator which computes an estimate for $b_{RX,r}$ based on subcarrier k. The estimator assumed that the channel estimate was exact, when in practice it was corrupted by IQ imbalance. We found that the expression for the error term depends on s_k, as defined by equation (5.29). The error term was either $-b_{RX,r}$ if $s_k = 1$, or it was a very long expression described by equation (5.33) if $s_k = -1$. In this section, we will introduce a slightly modified estimator, and analyze the estimated value for that estimator.

In the previous section, the estimate of $b_{RX,r}$ was equal to 0, for the subcarriers which satisfy $s_k = 1$. Therefore, the received signal on these subcarriers did not provide any useful information. The modified zero forcing based estimator should thus only regard subcarriers which do provide useful information, i.e.,

subcarriers which satisfy $s_k = -1$. For those subcarriers, the combination of pilot symbol P_k and data symbol X_k are orthogonal to P_{-k} and X_{-k}.

For the subcarriers where $s_k = -1$, the error term for the estimated value of $b_{RX,r}$ on subcarrier k was a very long expression, as given by equation (5.33). However, if we also consider the estimated value on the mirrored subcarrier $-k$, and if we use the property $\det(\hat{\mathbf{R}}_{\mathbf{1},\mathbf{k}}) = -\det(\hat{\mathbf{R}}_{\mathbf{1},-\mathbf{k}})$, we can write for the error of $\hat{b}_{RX,-k,r}$:

$$\begin{aligned}
\varepsilon_{\hat{b}_{RX,-k,r}} = -\Big[& b_{RX,r}(|H_k|^2 + |H_{-k}|^2) \\
& + 2b_{RX,r}\frac{P_k}{P_{-k}^*}(H_{-k,i}H_{k,i} - H_{-k,r}H_{k,r}) \\
& + 2b_{RX,i}\frac{P_k}{P_{-k}^*}(H_{k,i}H_{-k,r} - H_{k,r}H_{-k,i}) \\
& + 8b_{RX,r}b_{RX,i}\frac{P_k}{P_{-k}^*}(H_{k,i}H_{-k,r} + H_{k,r}H_{-k,i}) \\
& + 2b_{RX,r}^2\left(2\frac{P_k}{P_{-k}^*}(H_{-k,r}H_{k,r} - H_{-k,i}H_{k,i}) - |H_k|^2 - |H_{-k}|^2\right) \\
& + 4b_{RX,i}^2\left(\frac{P_k}{P_{-k}^*}(H_{-k,i}H_{k,i} - H_{-k,r}H_{k,r}) - |H_k|^2\right)\Big] / \det(\hat{\mathbf{R}}_{\mathbf{1},\mathbf{k}}).
\end{aligned} \tag{5.34}$$

If we compare this expression with equation (5.33), we notice that a large part of the error term is anti-symmetric in k. Therefore, by averaging the estimates $\hat{b}_{RX,k,r}$ and $\hat{b}_{RX,-k,r}$, the expression reduces to a much more compact form.

The new estimation algorithm then becomes:

$$\hat{b}'_{RX,r} = \frac{\hat{b}_{RX,k,r} + \hat{b}_{RX,-k,r}}{2}, \tag{5.35}$$

for those subcarriers where $s_k = -1$. On subcarriers where $s_k = 1$, no estimate should be made. Note that $\hat{b}_{RX,k,r}$ (and implicitly also $\hat{b}_{RX,-k,r}$) are still defined by equation (5.23).

After substitution of equation (5.32), the equivalent of (5.32) for subcarrier $-k$, and equation (5.25) into equation (5.35) and after simplification, the expression for $\hat{b}'_{RX,r}$ can be written as

$$\hat{b}'_{RX,r} = \frac{b_{RX,r} - 2(b_{RX,r}^2 + b_{RX,i}^2)}{1 - 2b_{RX,r}} \tag{5.36}$$

$$= b_{RX,r} - \frac{2b_{RX,i}^2}{1 - 2b_{RX,r}}. \tag{5.37}$$

The error in $\hat{b}'_{RX,r}$ is then

$$\begin{aligned}
\varepsilon_{b'_{RX,r}} &= \hat{b}'_{RX,r} - b_{RX,r} \\
&= -\frac{2b_{RX,i}^2}{1 - 2b_{RX,r}}.
\end{aligned} \tag{5.38}$$

We can conclude from this that the real part of the estimated value has an error term which is approximately quadratic in $b_{RX,i}$ for small values of b_{RX}. This means that with the new algorithm, the real part of the estimate will still be biased. This bias is caused by the fact that the algorithm assumes that the channel estimate is perfect, while in reality it is corrupted by IQ imbalance.

Analysis of imaginary part of estimated value

In the previous part, we have analyzed the error term in the real part of estimated value of a simple zero forcing based estimator and of a slightly modified estimator. We have seen that the expression for the former estimator is very long and complicated, while for the latter, it is quadratic in $b_{RX,i}$.

A very similar derivation can be made for the imaginary part of the estimator. In this case, the equivalent of equation (5.28) is

$$\begin{aligned}
&\det(\hat{\mathbf{R}}_{\mathbf{1},\mathbf{k}})\hat{b}_{RX,k,i} = \\
&\quad b_{RX,r}(s_k - 1)\frac{P_k}{P^*_{-k}}(H_{-k,r}H_{k,i} + H_{-k,i}H_{k,r}) + \\
&\quad b_{RX,i}(s_k - 1)\left(\frac{P_k}{P^*_{-k}}(H_{-k,i}H_{k,i} - H_{-k,r}H_{k,r}) - (H^2_{-k,i} + H^2_{-k,r})\right).
\end{aligned} \tag{5.39}$$

For those subcarriers which satisfy $X_k/X^*_{-k} = P_k/P^*_{-k}$, i.e. $s_k = 1$, the expression above can be reduced to

$$\det(\hat{\mathbf{R}}_{\mathbf{1},\mathbf{k}})\hat{b}_{RX,k,i} = 0. \tag{5.40}$$

The explanation for this is again that in this case, the signal does not provide any new information, since there is no orthogonality between the pilot symbols P_k and P_{-k} and the data symbols X_k and X_{-k}.

All other subcarriers satisfy $X_k/X^*_{-k} = -P_k/P^*_{-k}$, i.e. $s_k = -1$. For those subcarriers, equation (5.39) can be written as

$$\begin{aligned}
&\det(\hat{\mathbf{R}}_{\mathbf{1},\mathbf{k}})\hat{b}_{RX,k,i} = \\
&\quad - 2b_{RX,r}\frac{P_k}{P^*_{-k}}(H_{-k,r}H_{k,i} + H_{-k,i}H_{k,r}) + \\
&\quad - 2b_{RX,i}\left(\frac{P_k}{P^*_{-k}}(H_{-k,i}H_{k,i} - H_{-k,r}H_{k,r}) - (H^2_{-k,i} + H^2_{-k,r})\right).
\end{aligned} \tag{5.41}$$

Just as in the case of $b_{RX,r}$, a large part of the error expression for $\hat{b}_{RX,k,i}$ gets canceled by averaging the estimate of $b_{RX,i}$ over subcarriers k and $-k$.

We should therefore use a modified estimator, which averages the estimated values for subcarrier k and $-k$ in case $s_k = -1$, and which ignores the estimated values for subcarriers which satisfy $s_k = 1$, just like we did for the modified zero forcing based estimator. The new estimated value for $b_{RX,i}$ therefore becomes

$$\hat{b}'_{RX,i} = \frac{\hat{b}_{RX,k,i} + \hat{b}_{RX,-k,i}}{2} \tag{5.42}$$

for those subcarriers where $s_k = -1$.

After substituting equation (5.41), the equivalent of (5.41) for subcarrier $-k$ and equation (5.25) into equation (5.42) and after simplification, $\hat{b}'_{RX,i}$ becomes

$$\hat{b}'_{RX,i} = \frac{b_{RX,i}}{1 - 2b_{RX,r}} \tag{5.43}$$

$$= b_{RX,i} + \frac{2b_{RX,r}b_{RX,i}}{1 - 2b_{RX,r}}. \tag{5.44}$$

The error of $\hat{b}'_{RX,i}$ therefore is

$$\begin{aligned}
\varepsilon_{b'_{RX,i}} &= \hat{b}'_{RX,i} - b_{RX,i} \\
&= \frac{2b_{RX,r}b_{RX,i}}{1 - 2b_{RX,r}}.
\end{aligned} \tag{5.45}$$

By combining error expressions of equations (5.38) and (5.45), we can write for the total error in $\hat{b}'_{RX}$:

$$\begin{aligned}\varepsilon_{b'_{RX}} &= \varepsilon_{b'_{RX,r}} + j\varepsilon_{b'_{RX,i}} \\ &= \frac{2jb_{RX,i}(b_{RX,r} + jb_{RX,i})}{1 - 2b_{RX,r}} \\ &= \frac{2jb_{RX,i}}{1 - 2b_{RX,r}} b_{RX}. \end{aligned} \tag{5.46}$$

We have now analyzed a zero forcing based estimator which only regards subcarriers that satisfy $s_k = -1$ and which averages the estimated values on subcarrier k and $-k$. This estimator wrongly assumes that the channel estimate is not affected by IQ imbalance, and therefore, the estimated value for b_{RX} will have an error as described by equation (5.46).

Note that since $\hat{a}'_{RX}$ is calculated using equation (4.25), the error in the estimate of a_{RX} is equal to $\varepsilon^*_{\hat{b}'_{RX}}$.

5.3.3 Elimination of error term ("1 step" method)

In the previous section, we derived equations (5.37) and (5.44) which express the relation between the actual value and the estimated value of the IQ imbalance parameters. There, we considered the quadratic part of the expressions as an error term. Instead, we can exactly solve these quadratic equations to obtain an exact expression for the IQ imbalance as a function of the estimated values in the previous section.

To solve the quadratic equations, equations (5.36) and (5.43) can be combined to form the following two equations:

$$b_{RX,r} = \frac{1}{2}\left(1 - \frac{b_{RX,i}}{\hat{b}'_{RX,i}}\right) \tag{5.47}$$

and

$$b_{RX,i}^2\left(-\frac{1}{2} - 2\hat{b}'^2_{RX,i}\right) + b_{RX,i}\left(-\hat{b}'_{RX,i}\hat{b}'_{RX,r} + \frac{1}{2}\hat{b}'_{RX,i}\right) = 0. \tag{5.48}$$

Solving equation (5.48) gives either $b_{RX,i} = 0$ or

$$b_{RX,i} = -\frac{2\hat{b}'_{RX,r} - 1}{1 + 4\hat{b}'^2_{RX,i}}\hat{b}'_{RX,i}. \tag{5.49}$$

The former solution should always be discarded, as $b_{RX,i}$ is definitely not always 0. Furthermore, equation (5.43) shows that if $b_{RX,i}$ indeed is 0, then $\hat{b}'_{RX,i} = 0$. Substituting that into the latter solution shows then that this solution will also yield $b_{RX,i} = 0$. We can conclude that the first solution can be safely discarded, since equation (5.49) will always give the exact value for $b_{RX,i}$, whether it is 0 or not.

Substituting equation (5.49) into equation (5.47) yields

$$b_{RX,r} = \frac{2\hat{b}'^2_{RX,i} + \hat{b}'_{RX,r}}{1 + 4\hat{b}'^2_{RX,i}}. \tag{5.50}$$

With those equations and with the estimates from equations (5.35) and (5.42), it is possible for the dependent estimator to calculate the exact value of IQ imbalance in the receiver in one step, provided that the system is free of noise and free of IQ imbalance in the transmitter.

5.4 Estimation algorithm for transmitter caused IQ imbalance

In this section, we will consider the estimation problem for transmitter IQ imbalance. We will assume a fading channel and a perfect receiver, i.e., one without any IQ imbalance. Again, we will assume BPSK symbols, which can for example be found in the SIGNAL field of a 802.11a packet.

5.4.1 Model for transmitter-caused IQ imbalance

If there is only transmitter caused IQ imbalance in the system, the received signal is defined by equation (4.44) and given by

$$Y_k = (a_{TX} X_k + b_{TX}^* X_{-k}^*) H_k. \tag{5.51}$$

In this case, the estimated channel coefficient for subcarrier k, which is given by equation (4.50), can be simplified to

$$\hat{H}_k = (a_{TX} - b_{TX}^*) H_k \qquad \text{if } P_k = -P_{-k}^* \tag{5.52}$$

$$\hat{H}_k = H_k \qquad \text{if } P_k = P_{-k}^*. \tag{5.53}$$

In case $P_k = P_{-k}^*$, the estimate of the channel coefficient for subcarrier k is correct and the receiver will estimate the transmitted signal as

$$\begin{aligned} \hat{S}_k &= Y_k / \hat{H}_k \\ &= a_{TX} X_k + b_{TX}^* X_{-k}^*. \end{aligned} \tag{5.54}$$

In case $P_k = -P_{-k}^*$, the receiver will estimate the transmitted signal as

$$\begin{aligned} \hat{S}_k &= Y_k / \hat{H}_k \\ &= \frac{a_{TX} X_k + b_{TX}^* X_{-k}^*}{a_{TX} - b_{TX}^*}. \end{aligned} \tag{5.55}$$

5.4.2 "1 Step" method

If the transmitted symbols are BPSK symbols, equation (5.54) becomes

$$\hat{S}_k = X_k \qquad \text{if } X_k = X_{-k} \text{ and } P_k = P_{-k}^* \tag{5.56}$$

$$\hat{S}_k = X_k (a_{TX} - b_{TX}^*) \qquad \text{if } X_k = -X_{-k}^* \text{ and } P_k = P_{-k}^*. \tag{5.57}$$

Therefore, if $P_k = P_{-k}^*$ and $X_k = -X_{-k}^*$

$$\begin{aligned} \frac{\hat{S}_k}{X_k} &= a_{TX} - b_{TX}^* \\ &= 1 - 2b_{TX}^* \end{aligned} \tag{5.58}$$

and thus the receiver can estimate b_{TX} on subcarriers where $P_k = P_{-k}$ and $X_k = -X_{-k}^*$ with

$$\begin{aligned} \hat{b}_{TX} &= \frac{1}{2} \left(1 - \frac{\hat{S}_k}{\hat{X}_k} \right)^* \\ &= \frac{1}{2} \left(1 - \frac{\hat{Y}_k}{\hat{H}_k \hat{X}_k} \right)^*. \end{aligned} \tag{5.59}$$

If the receiver did not make any decoding errors and if the system is free of noise, $\hat{b}_{TX} = b_{TX}$.

A very similar derivation can be made for the case when $P_k = -P^*_{-k}$ and $X_k = X_{-k}$. In that case, if the transmitted symbols are BPSK symbols, equation (5.55) yields

$$\hat{S}_k = \frac{X_k}{a_{TX} - b^*_{TX}} \qquad \text{if } X_k = X^*_{-k} \text{ and } P_k = -P^*_{-k} \tag{5.60}$$

$$\hat{S}_k = X_k \qquad \text{if } X_k = -X^*_{-k} \text{ and } P_k = -P^*_{-k}. \tag{5.61}$$

Thus, if $P_k = -P^*_{-k}$ and $X_k = X^*_{-k}$:

$$\begin{aligned} \frac{X_k}{\hat{S}_k} &= a_{TX} - b^*_{TX} \\ &= 1 - 2b^*_{TX} \end{aligned} \tag{5.62}$$

and the receiver can estimate b_{TX} on subcarriers where $P_k = -P^*_{-k}$ and $X_k = X_{-k}$ with

$$\begin{aligned} \hat{b}_{TX} &= \frac{1}{2}\left(1 - \frac{\hat{X}_k}{\hat{S}_k}\right)^* \\ &= \frac{2}{2}\left(1 - \frac{\hat{H}_k \hat{X}_k}{\hat{Y}_k}\right)^*. \end{aligned} \tag{5.63}$$

Similar to the case for receiver caused imbalance, it is possible for a receiver to estimate transmitter caused imbalance in one step using equations (5.59) and (5.63), provided that there is no receiver imbalance and no noise.

5.5 Combining "1 step" methods for receiver and transmitter

In the previous two sections, we have derived two estimators which can find the exact value for receiver respectively transmitter imbalance. However, if the system has both transmitter and receiver caused IQ imbalance, neither of the "1 step" methods will give an exact solution. For this case, an iterative algorithm is developed. This iterative algorithm consists of two estimators, one for receiver imbalance and one for transmitter imbalance. In the iterations, we correct the channel estimate using the latest IQ imbalance parameter estimations according to equations (5.5) and (5.6).

5.5.1 Combining estimators

This iterative algorithm operates on one data symbol. Initially, it starts by assuming that transmitter and receiver imbalance is absent and decodes the data symbol using the uncorrected channel estimate.

In the second step, it estimates the receiver imbalance based on the received signal by assuming that the transmitter does not have any IQ imbalance.

In the second step, it corrects the received signal, after which the channel estimate can be corrected for the estimated receiver imbalance in step three.

In the fourth step, transmitter imbalance is estimated and in the fifth step, the received signal and the channel are corrected for both transmitter and receiver imbalance.

With these new estimates of receiver and transmitter imbalance and with the improved channel estimate, the algorithm can start all over again by decoding the data symbol again. After decoding the data symbol, a new estimate for receiver imbalance is made using the new estimates for data, channel and transmitter imbalance etc. Using this approach, the estimates for data, channel and receiver and transmitter imbalance (hopefully) improve with every iteration.

5.5.2 Receiver imbalance estimation

Since the "1 step" algorithm for receiver imbalance always returns the same estimate, independent of the estimate for transmitter imbalance, a different algorithm has to be used.

The estimator for IQ imbalance in the receiver first estimates the signal S_k that was the direct input the channel, by using the current estimates for transmitter imbalance and for the data symbols:

$$\begin{pmatrix} \hat{S}^*_{-k} \\ \hat{S}_k \end{pmatrix} = \begin{pmatrix} \hat{a}^*_{TX} & \hat{b}_{TX} \\ \hat{b}^*_{TX} & \hat{a}_{TX} \end{pmatrix} \begin{pmatrix} \hat{X}^*_{-k} \\ \hat{X}_k \end{pmatrix}. \tag{5.64}$$

Then, using the channel estimate, the receiver can estimate the direct output of the channel by

$$\begin{pmatrix} \hat{R}^*_{-k} \\ \hat{R}_k \end{pmatrix} = \begin{pmatrix} \hat{H}^*_{-k} & 0 \\ 0 & \hat{H}_k \end{pmatrix} \begin{pmatrix} \hat{S}^*_{-k} \\ \hat{S}_k \end{pmatrix}. \tag{5.65}$$

It then creates an estimate of b_{RX} for those subcarriers k where $P_k P_{-k} X_k X_{-k} = -1$ by using a modified version of equation (5.22):

$$\begin{pmatrix} \hat{b}_{RX,k,r} \\ \hat{b}_{RX,k,i} \end{pmatrix} = \begin{pmatrix} -\hat{R}_{k,r} + \hat{R}_{-k,r} & -\hat{R}_{k,i} + \hat{R}_{-k,i} \\ -\hat{R}_{k,i} - \hat{R}_{-k,i} & \hat{R}_{k,r} + \hat{R}_{-k,r} \end{pmatrix}^{-1} \begin{pmatrix} Y_{k,r} - \hat{R}_{k,r} \\ Y_{k,i} - \hat{R}_{k,i} \end{pmatrix}. \tag{5.66}$$

The estimate for b_{RX} is finally found by averaging over all $\hat{b}_{RX,k}$ (with $\hat{b}_{RX,k} = \hat{b}_{RX,k,r} + i\hat{b}_{RX,k,i}$).

Note that this estimator does not find the exact value of receiver imbalance in one step, not even if there is no noise and no IQ imbalance in the transmitter. At best, this solution converges to the exact value and has approximated that value well enough after a few iterations.

5.5.3 Transmitter imbalance estimation

The "1 step estimator" for transmitter caused IQ imbalance in Section 5.4.2 relies on the properties

$$\hat{H}_k = (a_{TX} - b^*_{TX}) H_k \tag{5.67}$$

in case $P_k = -P^*_{-k}$ and

$$\hat{H}_k = H_k \tag{5.68}$$

in case $P_k = P^*_{-k}$.

However, in the second iteration, we have already removed the receiver and transmitter imbalance from $\hat{H}_k$ using previous estimates of those imbalances. Therefore, the property in equation (5.67) does not hold any more after the first iteration. The property in equation (5.68) is still valid, since for those subcarriers where $P_k = P^*_{-k}$, we have only removed receiver imbalance.

Thus, the transmitter imbalance estimator can only use equations (5.59) and (5.63) in the first iteration. In the second and further iterations, only equation (5.59) can be used to estimate transmitter imbalance.

5.5.4 Total estimation algorithm

In the previous two subsections, we have derived two estimators which can be used in the iterative estimator to estimate both receiver and transmitter imbalance. In this section, we will give an overview of this iterative algorithm and summarize the estimators which are used.

A schematic overview of this iterative combined estimation algorithm is given in figure 5.1.

Let's call the initial channel estimate $\hat{H}_{raw}$, which is obtained by dividing the received pilot field with the pilot symbols: $\hat{H}_{raw,k} = Y_{p,k}/P_k$.

In the first iteration of the estimation algorithm, the estimator performs the following steps:

1. assume there is no receiver and no transmitter imbalance, i.e. $\hat{b}_{RX,0} = 0$ and $\hat{b}_{TX,0} = 0$ and use $\hat{H}_{raw}$ to decode the BPSK data symbol. Encode it again to create the estimate $\hat{X}_1$ of the transmitted symbols. (Note that the subscripts "0" and "1" here indicate the initial respectively the first estimate. Those subscripts should not be confused with the previous subscript k which was used as subcarrier index.)

2. assume there is no transmitter imbalance, i.e. $\hat{b}_{TX,0} = 0$ and use $\hat{H}_{raw}$ and $\hat{X}_1$ to create a first estimate of the receiver imbalance ($\hat{b}_{RX,1}$), using equation (5.66)

3. use $\hat{b}_{RX,1}$ to remove receiver imbalance from $\hat{H}_{raw}$ to create channel estimate $\hat{H}'_{raw}$ by using equation (5.6)

4. use $\hat{H}'_{raw}$ and $\hat{b}_{RX,1}$ to create an estimate of the transmitter imbalance ($\hat{b}_{TX,1}$) using equations (5.59) and (5.63)

5. use both $\hat{b}_{RX,1}$ and $\hat{b}_{TX,1}$ to remove IQ imbalance from $\hat{H}_{raw}$ using equation (5.5), thereby creating $\hat{H}_1$

At this point, the algorithm has it's first estimates for the data, the receiver and transmitter imbalance and for the corrected channel. Those estimates can be improved by going through the previous steps again for a couple of times with a few small modifications. For the n^{th} iteration ($n \geq 2$), those steps are:

1. use $\hat{b}_{RX,n-1}$, $\hat{b}_{TX,n-1}$ and $\hat{H}_{n-1}$ for equalization and to remove transmitter and receiver imbalance from the received signal, by using equations (5.2) - (5.4). Use the resulting signal to decode the BPSK data symbol. Encode it again to create the estimate $\hat{X}_n$ of the transmitted symbols

2. use $\hat{b}_{TX,n-1}$, $\hat{H}_{raw}$ and $\hat{X}_n$ to create a new estimate of the receiver imbalance ($\hat{b}_{RX,n}$), using equation (5.66)

3. use $\hat{b}_{RX,n}$ and $\hat{b}_{TX,n}$ to remove receiver and transmitter imbalance from $\hat{H}_{raw}$ to create channel estimate $\hat{H}'_{raw}$ by using equation (5.5)

4. use $\hat{H}'_{raw}$ and $\hat{b}_{RX,n}$ to create an estimate of the transmitter imbalance ($\hat{b}_{TX,n}$) using equation (5.63)

5. use both $\hat{b}_{RX,n}$ and $\hat{b}_{TX,n}$ to remove IQ imbalance from $\hat{H}_{raw}$ using equation (5.5), thereby creating $\hat{H}_n$

After this step, the receiver can start again at step 1 to create the estimates for iteration $n + 1$.

Note that the receiver does not always have to do full decoding and re-encoding in the first step. It has to do this for the first iteration, but if the receiver uses hard decisioning, it only has to map the (for IQ imbalance and channel corrected) received signal to the nearest constellation point. If the result of this mapping in iteration n is the same as in $n - 1$, the receiver can use the decoding and re-encoding results from step $n - 1$ and thereby bypass the Viterbi decoder and re-encoding process.

It can even occur that if the result of the de-mapper in step n is different than in step $n - 1$ (in which case the receiver cannot bypass the Viterbi decoder), it is still possible that the result of the Viterbi decoder in step n is the same as in step $n - 1$, and thus it is possible to bypass the encoding step.

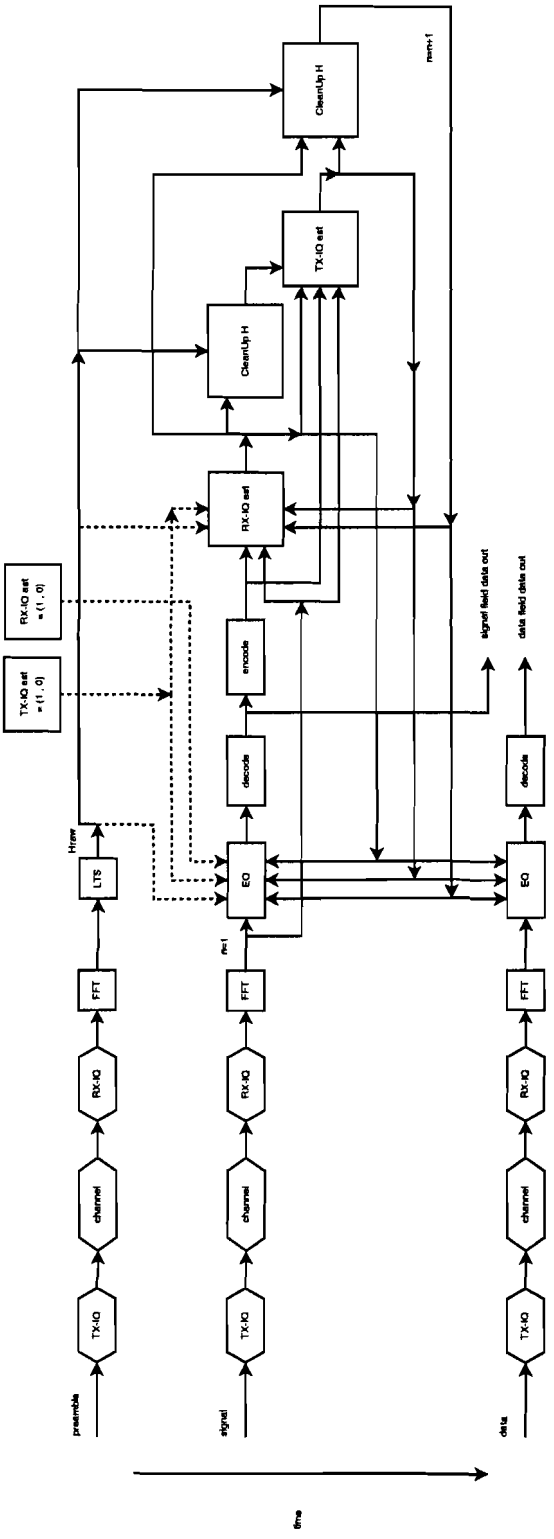

Figure 5.1: Schematic overview of iterative RX and TX imbalance estimator
Dashed lines represent initial values which are only used in the first iteration.

5.5.5 Convergence

In sections 5.5.2 and 5.5.3, we have proposed two estimators for receiver and transmitter imbalance respectively. Those estimators can be used in the iterative algorithm of Section 5.5.4. In this section, we will try to analyze the performance of those estimators.

First, we will analyze the receiver imbalance estimator for the case when there is no noise and no transmitter imbalance, to see if it indeed converges to the correct value. After that, we will analyze the transmitter imbalance estimator assuming there is no noise and no receiver imbalance. Finally, we will try to see if convergence can be guaranteed for the combination of both estimators as proposed in Section 5.5.4 when there is IQ imbalance in both transmitter and receiver.

Convergence of receiver imbalance estimation

In case there is no imbalance in the transmitter, the algorithm can skip steps 4 and 5 and move directly back to step 1 after it has finished step 3.

In this case, assume that the n-th estimate of b_{RX} has the error $\varepsilon_{RX,n}$, i.e.

$$\hat{b}_{RX,n} = b_{RX} + \varepsilon_{RX,n}. \tag{5.69}$$

Then, for subcarriers satisfying $P_k P_{-k} X_k X_{-k} = 1$, the $n+1$-st estimate of b_{RX} on subcarrier k equals

$$\begin{aligned} \hat{b}_{RX,n+1,k} &= b_{RX} + \varepsilon_{RX,n} \\ &= \hat{b}_{RX,n}, \end{aligned} \tag{5.70}$$

since, for this subcarrier, there is no orthogonality between the pair of pilot symbols (P_k, P_{-k}) and the pair of data symbols (X_k, X_{-k}).

Thus, if we use equation (5.66) on subcarriers where $P_k P_{-k} X_k X_{-k} = 1$, the $n+1$-st estimate will be exactly equal to the n-th estimate.

For subcarriers where $P_k P_{-k} X_k X_{-k} = -1$, the $n+1$-st estimate can be shown to equal

$$\begin{aligned} \hat{b}_{RX,n+1,k} &= b_{RX} + \frac{2ib_{RX,i}}{-1 + 2b_{RX,r}} \varepsilon_{RX,n} \\ &= b_{RX} + c_{RX}\, \varepsilon_{RX,n} \qquad (5.71) \\ &= b_{RX} + \varepsilon_{RX,n+1}. \qquad (5.72) \end{aligned}$$

Therefore, if we use this equation on subcarriers which satisfy $P_k P_{-k} X_k X_{-k} = -1$, the error in the $n+1$-st estimate is equal to the error in the n-th estimate, but multiplied with a factor c_{RX}.

If we only use the estimates on subcarriers where $P_k P_{-k} X_k X_{-k} = -1$, as proposed in Section 5.5.2, the absolute squared error in the $n+1$-st estimate equals

$$|\varepsilon_{RX,n+1}|^2 = |c_{RX}|^2 |\varepsilon_{RX,n}|^2. \tag{5.73}$$

A sufficient condition for convergence is that $|c_{RX}|^2 < 1$, i.e.

$$\frac{4b_{RX,i}^2}{1 - 4b_{RX,r} + 4b_{RX,r}^2} < 1. \tag{5.74}$$

Therefore, as long as

$$|b_{RX,i}| < \frac{1}{2} - b_{RX,r}, \tag{5.75}$$

this algorithm is guaranteed to converge to the correct value. For realistic values of IQ imbalance, i.e. $b_{RX,r} \approx 0$ and $b_{RX,i} \approx 0$, this condition will be met.

Note that for this algorithm, the first 3 estimates are

$$\begin{aligned}\hat{b}_{RX,1} &= b_{RX} + \varepsilon_{RX} \\ \hat{b}_{RX,2} &= b_{RX} + c_{RX}\,\varepsilon_{RX} \\ \hat{b}_{RX,3} &= b_{RX} + c_{RX}^2\,\varepsilon_{RX}.\end{aligned} \tag{5.76}$$

With those equations, b_{RX} can be derived by

$$b_{RX} = \frac{\hat{b}_{RX,2}^2 - \hat{b}_{RX,1}\,\hat{b}_{RX,3}}{-\hat{b}_{RX,3} - \hat{b}_{RX,1} + 2\hat{b}_{RX,2}}. \tag{5.77}$$

Thus, for this estimator, it is possible to obtain an exact value after just 3 iterations. Note however, that this is only the case if there is no transmitter caused imbalance, no noise and if the channel frequency response is not symmetric. Since the algorithm described in Section 5.3.3 can do the same under the same conditions, but only needs one step, the algorithm in Section 5.3.3 is to be preferred for systems where there is only receiver caused imbalance.

Convergence of transmitter imbalance estimation

If there is only transmitter caused IQ imbalance, the algorithm proposed in Section 5.5.4 can skip steps 2 and 3. Then, assuming the n-th estimate of b_{TX} has an error $\varepsilon_{TX,n}$, the n-th estimate of the channel on subcarrier k will be

$$\hat{H}_{n,k} = \frac{1}{\hat{a}_{TX,n} + \hat{b}_{TX,n}^* P_{-k}^*/P_k}\hat{H}_{raw,k} \tag{5.78}$$

where $\hat{b}_{TX,n} = b_{TX} + \varepsilon_{TX,n}$ and $\hat{a}_{TX,n} = 1 - \hat{b}_{TX,n}^*$ and $\hat{H}_{raw,k}$ is the raw channel estimate.

The transmitter imbalance estimator of Section 5.5.3 operates only on subcarriers satisfying $P_k = P_{-k}^*$ and $X_k = -X_{-k}$. Using equation (5.53) and the property $\hat{a}_{TX,n} + \hat{b}_{TX,n}^* = 1$, we can conclude that for those subcarriers, the n-th channel estimate equals H_k.

Therefore, an error in the n-th estimate of b_{TX} does not affect the n-th channel estimate for subcarriers where $P_k = P_{-k}^*$.

Since the channel estimate is only used for subcarriers satisfying $P_k = P_{-k}^*$, error $\varepsilon_{TX,n}$ will not propagate to the $n+1$-st estimate of b_{TX} and $\hat{b}_{TX,n+1}$ will not have any error: $\varepsilon_{TX,n+1} = 0$.

Note that this analysis is of course only valid if there is indeed only transmitter caused IQ imbalance and if the system is free of noise.

Convergence of combined transmitter and receiver imbalance estimation

If both estimators are combined according to Section 5.5.4, convergence cannot be guaranteed. Even more so, in Chapter 6, we will see that there are combinations of channel, IQ imbalance and data in the SIGNAL field for which this algorithm does not converge.

5.5.6 Stopping criteria

If the receiver experiences additive white Gaussian noise, it cannot get the error in the estimates of b_{RX}, b_{TX} and H arbitrarily small. The number of steps needed to reach this floor is determined by the signal to noise ratio, the actual values of b_{RX}, b_{TX} and H and the symbols in the SIGNAL field. However, simulations seem to indicate that for most cases, this error floor is reached after $\lceil \mathrm{SNR}/10 \rceil$ steps, where SNR is the signal to noise ratio expressed in dB and $\lceil x \rceil$ denotes the ceiling operation on x. Therefore, the receiver should have an idea about the signal to noise ratio.

Estimating noise is well known. In this section, we will work out how to do this in case of IQ imbalance.

Estimating noise power

If the system is subject to additive white Gaussian noise, the received signal on carrier k at time instant m, can be modeled as

$$\begin{aligned} Y_{k,m} &= a_{RX}a_{TX}H_kX_{k,m} + a_{RX}b^*_{TX}H_KX^*_{-k,m} + b_{RX}a^*_{TX}H^*_{-k}X^*_{-k,m} + b_{RX}b_{TX}H^*_{-k}X_{k,m} \\ &\quad + a_{RX}n_{k,m} + b_{RX}n^*_{-k,m} \end{aligned} \tag{5.79}$$

according to equation (4.48), where $n_{k,m}$ is the AWGN process on carrier k which is zero mean and has variance σ_n^2.

In case the system transmits the pilot sequence for channel estimation twice, which is the case for an IEEE 802.11a based system, the raw channel estimate on carrier k can be modeled as

$$\begin{aligned} \hat{H}_k &= \frac{Y_{p1,k} + Y_{p2,k}}{2P_k} \\ &= a_{RX}a_{TX}H_k + a_{RX}b^*_{TX}H_k\frac{P^*_{-k}}{P_k} + b_{RX}a^*_{TX}H^*_{-k}\frac{P^*_{-k}}{P_k} + b_{RX}b_{TX}H^*_{-k} + a_{RX}n'_k + b_{RX}n'_{-k} \end{aligned} \tag{5.80}$$

where $n'_k = \frac{n_{k,1}+n_{k,2}}{2P_k}$ and $n'_{-k} = b_{RX}\frac{n^*_{-k,1}+n^*_{-k,2}}{2P_k}$, due to averaging of both long preamble symbols. $Y_{p1,k}$ denotes the k-th subcarrier of the received signal when the first long trainging symbol was transmitted. Similarly, $Y_{p2,k}$ denotes the k-th subcarrier of the received signal when the second long trainging symbol was transmitted. Note that since P_k and P_{-k} are either $+1$ or -1, the variance of n'_k (and n'_{-k}) is $\sigma_n^2/2$.

For the carriers in the SIGNAL field where $\frac{X^*_{-k}}{X_k} = \frac{P^*_{-k}}{P_k}$, the signal constellation is not affected at all by IQ imbalance, and the noise is only affected by IQ imbalance in the receiver:

$$\begin{aligned} \nu_k &= X_k\left(\frac{Y_k}{X_k} - \hat{H}_k\right) \\ &= a_{RX}n_{k,3} + b_{RX}n^*_{-k,3} + a_{RX}n''_k + b_{RX}n''^*_{-k} \\ &= a_{RX}(n_{k,3} + n''_k) + b_{RX}(n_{-k,3} + n''_{-k})^* \\ &= a_{RX}n'''_k + b_{RX}n'''^*_{-k} \end{aligned} \tag{5.81}$$

where $n''_k = -n'_kX_k$, $n''_{-k} = -n'_{-k}X_k$, $n'''_k = n_{k,3} + n''_k$ and $n'''_{-k} = n_{-k,3} + n''_{-k}$. Note that the variance of n'''_k is $3\sigma_n^2/2$.

The estimate of the power of ν_k can then be found by averaging $|\nu_k|^2$ over all carriers k where $\frac{X^*_{-k}}{X_k} = \frac{P^*_{-k}}{P_k}$:

$$\begin{aligned} \hat{P}_\nu &= \mathbb{E}_k[\nu_k\nu^*_k] \\ &= (|a_{RX}|^2 + |b_{RX}|^2)\frac{3\sigma_n^2}{2} \end{aligned} \tag{5.82}$$

As the receiver only has estimates $\hat{R}_k$ and $\hat{X}_k$ of R_k and X_k, the receiver can only determine the estimate $\hat{\nu}_k$ instead of ν_k. The estimated power of ν_k will therefore not be $\hat{P}_\nu = \mathbb{E}_k[\nu_k \nu_k^*]$ but $\hat{P}'_\nu = \mathbb{E}_k[\hat{\nu}_k \hat{\nu}_k^*]$.

Thus, the noise power σ_n^2 can be estimated by

$$\begin{aligned} \hat{\sigma}_n^2 &= \frac{2}{3} \frac{\hat{P}'_\nu}{|\hat{a}_{RX}|^2 + |\hat{b}_{RX}|^2} \\ &= \frac{2}{3} \frac{\mathbb{E}_k[|\hat{\nu}_k|^2]}{|\hat{a}_{RX}|^2 + |\hat{b}_{RX}|^2} \end{aligned} \tag{5.83}$$

If the signal power is normalized to 1, the stopping criterion could be to stop after $\lceil -\log_{10} \hat{\sigma}_n^2 \rceil$ iterations.

Note however, that for the simulation results in this report, we have used a stop criteria of 20 iterations on SIGNAL field, just to be sure that the performance of the estimator is not limited by this stop criteria.

5.5.7 Computational complexity

The required number of computations for the individual functions of this algorithm is listed in Table 5.1. Note that those algorithms are not yet optimized for computational simplicity, and therefore those numbers are merely upper bounds to the required number of computations.

The required number of computations per iteration depend on the number of subcarrier pairs for which $X_k/X_{-k}^* = -P_k/P_{-k}^*$ holds. If this holds for all subcarrier pairs, the algorithm requires 768 complex multiplications, 384 complex additions and 168 complex divisions, as well as 192 real multiplications, 240 real additions and 26 real divisions per iteration.

Table 5.1: computational complexity of the estimation and compensation algorithms

function	**multiplications**	**additions**	**divisions**	**notes**
compensate TX and RX imbalance	16 (complex)	6 (complex)	4 (complex)	[a]
1 step RX estimator	5 (real)	4 (real)	2 (real) 1 (real)	[b] [c]
1 step TX estimator	1 (complex)	2 (complex)	2 (complex) 1 (real)	[b] [c]
iterative RX estimator	3 (complex) 8 (real)	1 (complex) 10 (real)	 1 (real) 1 (real)	[b] [b] [c]
Remove RX and TX imb from $\hat{H}$	12 (complex)	7 (complex)	1 (complex)	[a]
Remove RX imb from $\hat{H}$	8 (complex)	3 (complex)	1 (complex)	[a]
Estimate noise power	2 (complex) 5 (real)	2 (complex) 1 (real)	1 (complex) 2 (real)	[a]

Notes:

- [a]: per subcarrier pair
- [b]: per subcarrier pair for which $X_k/X_{-k}^* = -P_k/P_{-k}^*$
- [c]: only needed for averaging

5.6 Iterative estimator based on channel smoothing

In the previous sections, we have derived estimators for both transmitter and receiver imbalance by exploiting the orthogonality between the symbols in the pilot field and in a BPSK data field on subcarrier k and the corresponding symbols on the mirrored subcarrier $-k$.

A totally different approach is to estimate IQ imbalance based on the assumption that the channel estimate is exact. In order to get an estimate of the channel that is as close as possible to the exact channel realization, one can use a smoothing filter.

For 802.11a systems, the channel impulse response can have a maximum channel delay of 0.8 μs. At a sample rate of 20 MHz, the channel impulse response can be represented by 16 taps (in time domain). However, if the receiver uses per-tone channel estimation[2], the channel transfer function is represented by 64 taps (in frequency domain). This is 4 times as much as what is actually needed and this oversampling in frequency domain can lead to a channel estimate that contains a rapid variation between neighboring subcarriers. To remove these variations, a least squares based smoothing filter can be used as such proposed by Ghosh [23] or Van de Beek [24] and is explained in Appendix A.

Due to this smoothing filter, equation (4.50) is not valid any more for the initial channel estimate. Therefore, the estimators that we derived in the previous sections cannot be used, and different estimators have to be derived. Note that removing IQ imbalance from the channel estimate is still possible with equations (5.5) and (5.6), after which the new channel estimate can be smoothed with the channel smoothing filter.

5.6.1 Receiver imbalance estimation

The dependent estimator calculates an estimate for $b_{RX,r}$ and $b_{RX,i}$ on subcarrier k by

$$\begin{aligned}\begin{pmatrix} \hat{b}_{RX,k,r} \\ \hat{b}_{RX,k,i} \end{pmatrix} &= \begin{pmatrix} -\hat{R}_{k,r} + \hat{R}_{-k,r} & -\hat{R}_{k,i} + \hat{R}_{-k,i} \\ -\hat{R}_{k,i} - \hat{R}_{-k,i} & \hat{R}_{k,r} + \hat{R}_{-k,r} \end{pmatrix}^{-1} \begin{pmatrix} Y_{k,r} - \hat{R}_{k,r} \\ Y_{k,i} - \hat{R}_{k,i} \end{pmatrix} \\ &= \hat{\mathbf{R}}_{\mathbf{1,k}}^{-1} \left(\begin{pmatrix} Y_{k,r} \\ Y_{k,i} \end{pmatrix} - \hat{\mathbf{R}}_{\mathbf{2,k}} \right), \end{aligned} \tag{5.84}$$

where $\hat{\mathbf{R}}_{\mathbf{1,k}}$ and $\hat{\mathbf{R}}_{\mathbf{2,k}}$ depend on the smoothed channel estimate and the estimated symbols in the SIGNAL field. This estimator works identically to the 1 step estimator in equation (5.66), but instead now operates on all subcarriers, and not just those for which $P_k P_{-k} X_k X_{-k} = -1$.

Note that separating between subcarrier pairs where $P_k/P_{-k}^* = X_k/X_{-k}^*$ and $P_k/P_{-k}^* = -X_k/X_{-k}^*$ will not give very clear gains in this case. The estimate for b_{RX} can thus be found by averaging over all subcarriers. Once the estimate for b_{RX} is known, the estimate of a_{RX} can be computed by using the property

$$a_{RX} = 1 - b_{RX}^*. \tag{5.85}$$

Another method to estimate a_{RX} and b_{RX} is by treating them independently and estimating them at the same time. Hereto, we have to write the received signal on subcarrier k and its mirrored subcarrier $-k$ in matrix notation. The received signal on subcarrier k can be written as

$$Y_k = a_{RX} R_k + b_{RX} R_{-k}^*. \tag{5.86}$$

In matrix notation, the received signal on subcarrier k and $-k$ can be expressed as

$$\begin{pmatrix} Y_{-k} \\ Y_k \end{pmatrix} = \begin{pmatrix} \hat{R}_{-k} & \hat{R}_k^* \\ \hat{R}_k & \hat{R}_{-k}^* \end{pmatrix} \begin{pmatrix} \hat{a}_{RX} \\ \hat{b}_{RX} \end{pmatrix}. \tag{5.87}$$

[2] per-tone channel estimation can be done in frequency domain by dividing the received value on subcarrier k by the pilot symbol on subcarrier k, as expressed in equation (4.50).

We can now find the estimates for a_{RX} and b_{RX} by a simple inversion:

$$\begin{pmatrix} \hat{a}_{RX} \\ \hat{b}_{RX} \end{pmatrix} = \begin{pmatrix} \hat{R}_{-k} & \hat{R}_k^* \\ \hat{R}_k & \hat{R}_{-k}^* \end{pmatrix}^{-1} \begin{pmatrix} Y_{-k} \\ Y_k \end{pmatrix}. \tag{5.88}$$

Since this estimator does not exploit the relationship between a_{RX} and b_{RX} as expressed in equation (5.85), this estimator is called the independent estimator.

Simulations indicate that for the independent estimator, the absolute squared error of $\hat{b}_{RX}$ is usually much smaller than the absolute squared error of $\hat{a}_{RX}$. The simulations even indicate that the absolute squared error of $\hat{b}_{RX}$ is even smaller than the absolute squared error of $\hat{b}_{RX}$ from the dependent estimator. Unfortunately, there was not enough time to investigate why this is the case.

However, this indicates that the iterative estimator that uses channel smoothing should use independent estimation and ignore the estimate of a_{RX}.

5.6.2 Transmitter imbalance estimation

The signal S_k which is created by the transmitter, can be written as

$$S_k = a_{TX} X_k + b_{TX}^* X_{-k}^* \tag{5.89}$$
$$= X_k + b_{TX}^* (X_{-k}^* - X_k) \tag{5.90}$$

and estimated by equations (5.2) and (5.3).

The dependent estimator calculates the estimate for b_{TX} at subcarrier k by

$$\hat{b}_{TX,k} = \left((\hat{X}_{-k}^* - \hat{X}_k)^{-1} (\hat{S}_k - \hat{X}_k) \right)^* \tag{5.91}$$

Similar to the estimator for receiver imbalance in the previous section, we can develop an independent estimator which estimates a_{TX} and b_{TX} independently and at the same time. Therefore, we have to express signal S_k and S_{-k} as given by (5.89) in matrix notation:

$$\begin{pmatrix} \hat{S}_{-k} \\ \hat{S}_k \end{pmatrix} = \begin{pmatrix} \hat{X}_{-k} & \hat{X}_k^* \\ \hat{X}_k & \hat{X}_{-k}^* \end{pmatrix} \begin{pmatrix} \hat{a}_{TX} \\ \hat{b}_{TX}^* \end{pmatrix} \tag{5.92}$$

The estimates for a_{TX} and b_{TX} at subcarrier k can be found by

$$\begin{pmatrix} \hat{a}_{TX,k} \\ \hat{b}_{TX,k}^* \end{pmatrix} = \begin{pmatrix} \hat{X}_{-k} & \hat{X}_k^* \\ \hat{X}_k & \hat{X}_{-k}^* \end{pmatrix}^{-1} \begin{pmatrix} \hat{S}_{-k} \\ \hat{S}_k \end{pmatrix}. \tag{5.93}$$

The final estimate can be obtained by averaging over all subcarriers.

Simulations indicate that for this estimator, the absolute squared error of $\hat{b}_{TX}$ is usually much smaller than for the dependent estimator.

However, simulations also indicate that the absolute squared error of $\hat{b}_{TX}$ is even smaller if the estimator calculates the estimate by independently calculating estimates for a_{TX}, a_{TX}^*, b_{TX} and b_{TX}^*. Therefore, we have to write the received signal as expressed in equation (4.47) as

$$Y_k = a_{RX} a_{TX} H_k X_k + b_{RX} a_{TX}^* H_{-k}^* X_{-k}^* + b_{RX} b_{TX} H_{-k}^* X_k + a_{RX} b_{TX}^* H_k X_{-k}^* \tag{5.94}$$

$$= \begin{pmatrix} a_{RX} H_k X_k & b_{RX} H_{-k}^* X_{-k}^* & b_{RX} H_{-k}^* X_k & a_{RX} H_k X_{-k}^* \end{pmatrix} \begin{pmatrix} a_{TX} \\ a_{TX}^* \\ b_{TX} \\ b_{TX}^* \end{pmatrix} \tag{5.95}$$

By expanding equation (5.95) for four subcarriers, the estimates for a_{TX}, a^*_{TX}, b_{TX} and b^*_{TX} can be obtained by simple inversion:

$$\begin{pmatrix} Y_k \\ Y_{k+1} \\ Y_{k+2} \\ Y_{k+3} \end{pmatrix} = \begin{pmatrix} a_{RX}H_kX_k & b_{RX}H^*_{-k}X^*_{-k} & b_{RX}H^*_{-k}X_k & a_{RX}H_kX^*_{-k} \\ a_{RX}H_{k+1}X_{k+1} & b_{RX}H^*_{-(k+1)}X^*_{-(k+1)} & b_{RX}H^*_{-(k+1)}X_{k+1} & a_{RX}H_{k+1}X^*_{-(k+1)} \\ a_{RX}H_{k+2}X_{k+2} & b_{RX}H^*_{-(k+2)}X^*_{-(k+2)} & b_{RX}H^*_{-(k+2)}X_{k+2} & a_{RX}H_{k+2}X^*_{-(k+2)} \\ a_{RX}H_{k+3}X_{k+3} & b_{RX}H^*_{-(k+3)}X^*_{-(k+3)} & b_{RX}H^*_{-(k+3)}X_{k+3} & a_{RX}H_{k+3}X^*_{-(k+3)} \end{pmatrix} \cdot \begin{pmatrix} a_{TX} \\ a^*_{TX} \\ b_{TX} \\ b^*_{TX} \end{pmatrix} \tag{5.96}$$

and thus

$$\begin{pmatrix} a_{TX} \\ a^*_{TX} \\ b_{TX} \\ b^*_{TX} \end{pmatrix} = \begin{pmatrix} a_{RX}H_kX_k & b_{RX}H^*_{-k}X^*_{-k} & b_{RX}H^*_{-k}X_k & a_{RX}H_kX^*_{-k} \\ a_{RX}H_{k+1}X_{k+1} & b_{RX}H^*_{-(k+1)}X^*_{-(k+1)} & b_{RX}H^*_{-(k+1)}X_{k+1} & a_{RX}H_{k+1}X^*_{-(k+1)} \\ a_{RX}H_{k+2}X_{k+2} & b_{RX}H^*_{-(k+2)}X^*_{-(k+2)} & b_{RX}H^*_{-(k+2)}X_{k+2} & a_{RX}H_{k+2}X^*_{-(k+2)} \\ a_{RX}H_{k+3}X_{k+3} & b_{RX}H^*_{-(k+3)}X^*_{-(k+3)} & b_{RX}H^*_{-(k+3)}X_{k+3} & a_{RX}H_{k+3}X^*_{-(k+3)} \end{pmatrix}^{-1} \cdot \begin{pmatrix} Y_k \\ Y_{k+1} \\ Y_{k+2} \\ Y_{k+3} \end{pmatrix}. \tag{5.97}$$

Simulations indicate that the estimator should ignore all estimated values, except $\hat{b}^*_{TX}$ and use that estimate to compute $\hat{b}_{TX}$ and $\hat{a}_{TX}$. Unfortunately, there was not enough time to investigate why this is the case.

5.6.3 Pseudo inverse instead of averaging

In the previous sections we have derived several estimators to estimate receiver and transmitter imbalance by using a smoothed channel estimate. We derived those estimates based on 1, 2 or at most 4 subcarriers and suggested that the final estimate can be found by calculating the estimates for all subcarriers and average the result.

However, unlike the estimators of the non-smoothing algorithms, all of the algorithms for the smoothing estimators can be applied to any subcarrier, independent of the sign of $P_k \cdot P_{-k}$ or $X_k \cdot X_{-k}$. Therefore, instead of averaging over all subcarriers, we can also expand the previous equations to cover all $2 \cdot N_s$ OFDM subcarriers and use a pseudo inverse instead of a normal inverse.

For example, the estimate for the independent estimator for receiver imbalance can be written as

$$\begin{pmatrix} \hat{a}_{RX} \\ \hat{b}_{RX} \end{pmatrix} = \begin{pmatrix} \hat{R}_{-N} & \hat{R}^*_N \\ \vdots & \vdots \\ \hat{R}_k & \hat{R}^*_{-k} \\ \vdots & \vdots \\ \hat{R}_N & \hat{R}^*_{-N} \end{pmatrix}^{\dagger} \begin{pmatrix} Y_{-N} \\ \vdots \\ Y_k \\ \vdots \\ Y_N \end{pmatrix}. \tag{5.98}$$

For the simulations in this report, we used the pseudo inverse method for the estimator which uses channel smoothing.

5.6.4 Combining estimators

The iterative estimator using channel smoothing is very similar to the iterative estimator from Section 5.5.4, with the exception that a least squares based channel smoothing filter is applied on every channel estimate. This algorithm is illustrated in Figure 5.2.

Note further that simulations seem to indicate that using the "1 step" estimators for receiver and transmitter imbalance in the first iteration seems to give a slightly better performance than immediately using the estimators presented in this section. Of course, from the second iteration on, the estimators from this section should be used.

Note that the estimators presented in this section never restrict the data symbols to BPSK symbols. The estimators presented in this section can therefore in principle use any type of data symbols. Keep in mind though, that the first estimate of the data symbol is still made without any estimate for receiver or transmitter imbalance. Therefore, if the data symbol is BPSK rate 1/2 coded, the probability of a decoding error is much smaller then wen the symbol is 64 QAM rate 3/4 coded. In the latter case, a decoding error is much more likely, and this will have negative impact on the IQ imbalance estimates.

5.6.5 Convergence

As in the case of the algorithm that does not use channel smoothing, convergence of the combination of the estimators cannot be proven, and there are known combinations of channel, IQ imbalance and data for which the algorithm does not converge to the correct values.

However, if there is some way for the receiver to detect that the estimate will not converge, it is possible to skip this data symbol and move on to the next symbol. The next symbol will probably have different data symbols and different noise, and it is possible that the algorithm will converge on this symbol. Once the receiver has obtained good enough estimates, it could decode the first symbol again.

This however, is not implemented in our algorithm, since simulations indicate that the probability that the algorithm does not converge is very low.

5.6.6 Stop criteria

Simulations indicate that this algorithm typically takes twice as many steps to converge to the correct value as compared to the iterative algorithm that does not use channel smoothing. Therefore, a stop criterion could be $2\lceil \mathrm{SNR}/10 \rceil$.

Note however, that, as in the case for the iterative solution in Section 5.5, we have used a stop criteria of 20 iterations on SIGNAL field for the simulation results in this report, just to be sure that the performance of the estimator is not limited by this stop criteria.

5.7 Summary

In this chapter, we have derived several estimators for IQ imbalance:

- Two estimators which find the exact value for receiver imbalance in one step; those estimators are presented in Sections 5.3.3 and 5.5.5. The former estimator is preferred, since it requires less computations and less restrictions on the receiver imbalance. Those estimators assume that transmitter imbalance is absent. Both estimators exploit the orthogonal relationship between pilot and data symbols, and therefore require the data symbols to be BPSK symbols.

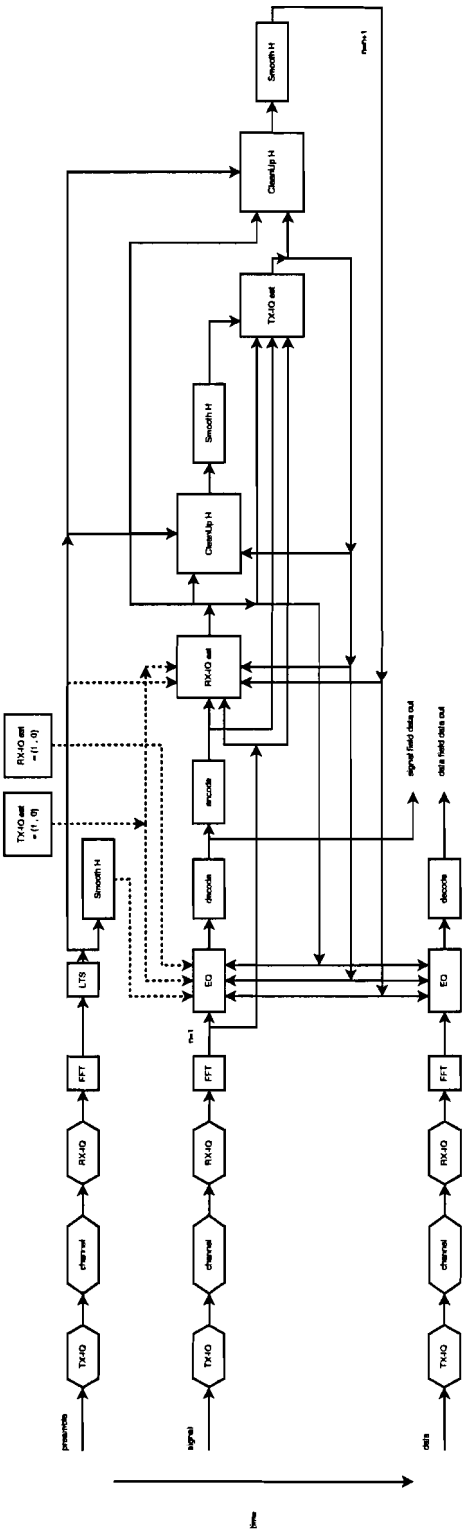

Figure 5.2: Schematic overview of iterative RX and TX imbalance estimator
Dashed lines represent initial values which are only used in the first iteration.

- An estimator which finds the exact value for transmitter imbalance in one step; this estimator is presented in Section 5.5.3. This estimator assumes that receiver imbalance is absent. This estimator too, exploits the orthogonal relationship between pilot and data symbols and thus requires that the data symbols are BPSK symbols.
- One iterative estimator which estimates both receiver and transmitter imbalance, as presented in Section 5.5. The estimator exploits orthogonality between pilot and data symbols, and thus only BPSK data symbols are allowed.
- One iterative estimator which estimates both receiver and transmitter imbalance by using a smoothed channel estimate, presented in Section 5.6.

Note that all estimators assume that noise is absent. In the next chapter, we will use simulations to evaluate the performance of those estimators.

Chapter 6

Simulation results and comparison

In the previous chapter, we have derived several algorithms which estimate the receiver and transmitter imbalance parameters. We have seen that there are solutions that give the exact result if there is only transmitter or receiver imbalance and if the system is free of noise. If there is imbalance in both the transmitter and receiver, two iterative estimators were proposed, for which convergence could not be analytically proven.

In this chapter, we will use simulations to show the convergence behavior of the iterative solutions. Furthermore, the behavior of the "1 step" estimators and the iterative estimators will be evaluated by simulations for systems which are impaired with additive white Gaussian noise. Finally, we will show the performance of systems with IQ imbalance in terms of bit error rate (BER) and packet error rate (PER), applying a compensation based on the proposed algorithms.

The simulation parameters were the same as those for Section 4.6. In short, the channel model used for the simulations in this chapter is a Rayleigh fading channel with an exponentially decaying power delay profile. The channel impulse response had an rms delay spread of 50 ns. Furthermore, channel equalization was done using a zero forcing approach.

The bit error rate and packet error rate simulations were done with correct SIGNAL information. In the simulations, the received SIGNAL field was decoded, and the estimates for IQ imbalance were based on that result. However, the DATA symbols were always decoded with the correct signal rate and length parameters. This was done to avoid excessive bit errors in case the SIGNAL field was not correctly decoded.

6.1 Convergence of dependent iterative estimators

This section will analyze the convergence of the dependent iterative estimator, as proposed in Section 5.5. We will therefore analyze the distribution of the squared absolute error (SAE) of the estimates, i.e., the distribution of $|\varepsilon|^2$ where ε is the error in the estimate of either channel, receiver imbalance or transmitter imbalance.

Figure 6.1 shows the mean squared errors of the estimate of receiver, transmitter and channel per iteration for a signal to noise ratio of 100 dB. The IQ imbalance for this dataset was $\varepsilon_{TX} = -10\%$ and $\phi_{TX} = -5°$ for the transmitter and $\varepsilon_{RX} = 10\%$ and $\phi_{RX} = -5°$ for the receiver. As can be seen in this plot, the average error for the channel estimate linearly increases with every step, which means that, on average, it is not converging to the correct value.

However, this is caused by a few realizations of channel, data and IQ imbalance, since, as we shall see in Figure 6.3, for 90% of the cases, the squared error is below $3 \cdot 10^{-8}$. Figure 6.2 shows the median squared errors of the RX and TX imbalance estimates and the channel estimate, which is much more typical than

the mean squared error. This plot shows that the absolute squared error typically reduces more than a factor of 26 with every iteration, until it reaches a noise floor. In this simulation, the signal to noise ratio was 100 dB and the noise floor is in the order of 10^{-10}. FIXME: link naar stop criteria.

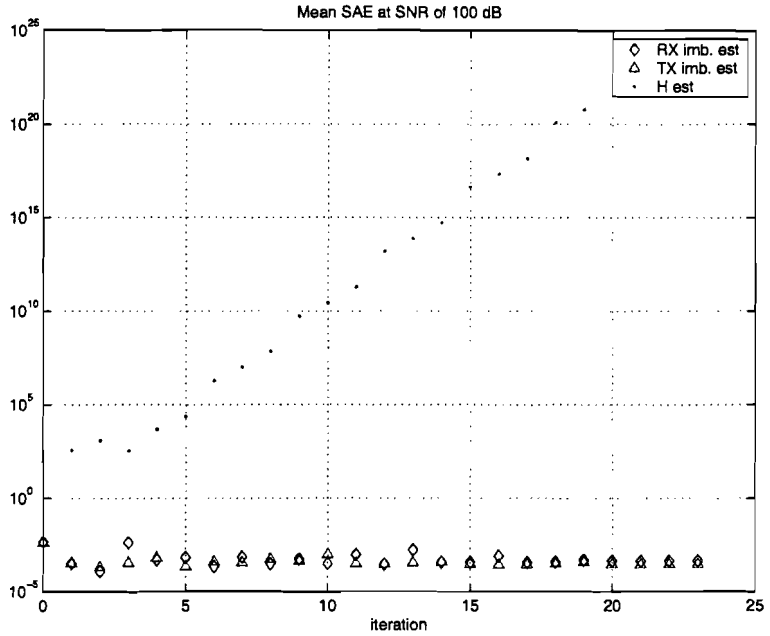

Figure 6.1: Mean squared error of dependent iterative algorithm

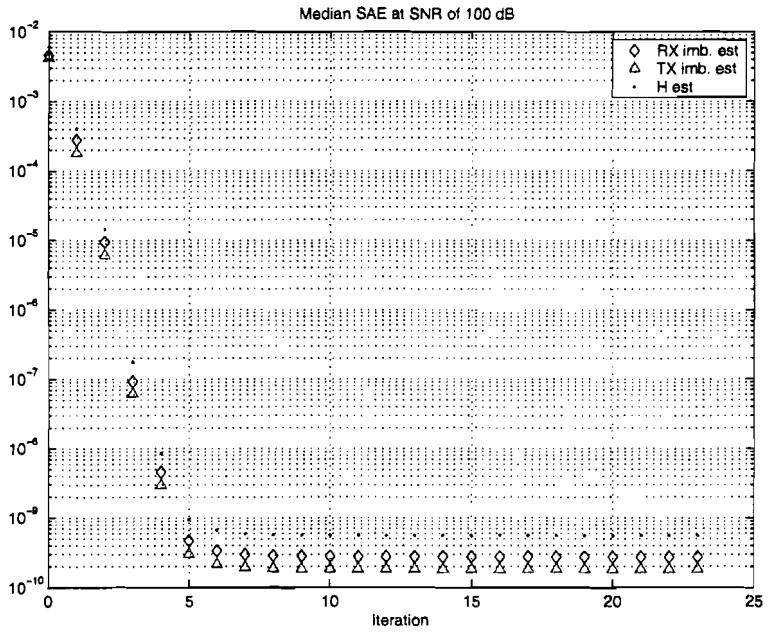

Figure 6.2: Median squared error of dependent iterative algorithm

Figure 6.3 shows the CDF of the errors of the estimated values of the iterative dependent estimator after 20 iterations for an SNR of 100 dB. In this plot it can be seen that in 10% of the cases, the squared error for the

transmitter and receiver imbalance estimates is less than $2 \cdot 10^{-11}$. However, there are virtually no cases where the error in the channel estimate is less than $2 \cdot 10^{-11}$ as the CDF for the channel estimate starts to rise around $6 \cdot 10^{-11}$, which is close to $1/\text{SNR}$. This indicates that it is possible for certain realizations of channel, data and IQ imbalance, to obtain very good estimates of transmitter and receiver imbalances, and to remove the effect of those imbalances from the channel estimate. With that, the dominant error in the channel estimate is just the noise in the channel estimate.

However, there are also quite a lot of situations where this algorithm does not converge to the correct value. Therefore, it is interesting to evaluate the performance of the independent iterative estimator.

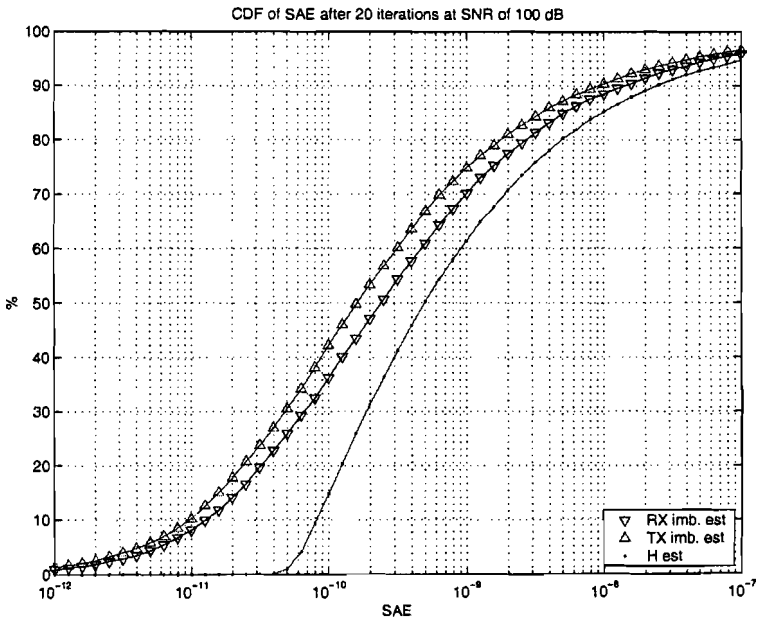

Figure 6.3: CDF of squared error of dependent iterative algorithm

6.2 Convergence of independent iterative estimators

In Section 5.6, we proposed an iterative estimation algorithm based on channel smoothing. In this section, we will analyze the convergence of this estimator. Note that, as indicated in Section 5.6, we used the "1 step" estimators in the first iteration, and the receiver and transmitter imbalance estimators from Section 5.6 in the second and later iterations.

Figure 6.4 shows the mean squared error of the independent iterative algorithm when channel smoothing is used. The IQ imbalance for this dataset was -10% and $-5°$ for the transmitter and 10% and $-5°$ for the receiver. Similar to the case for the dependent iterative algorithm, the independent iterative algorithm with channel smoothing can converge to the wrong value. However, this is very rare, as is demonstrated by figures 6.5 and 6.6, which respectively show the median squared error and the cumulative distribution function of the squared error after 20 iterations.

Figure 6.5 shows that typically, for an SNR of 100 dB, the absolute squared error is in the order of $1 \cdot 10^{-30}$ after 20 iterations. Since the machine precision was $1 \cdot 10^{-16}$, this is very close to the squared machine precision. It can therefore be assumed that the median absolute squared error will continue to fall even after 20 iterations if the computation is done with higher accuracy. This figure also shows that one needs 7 iterations to reduce the error from $1 \cdot 10^{-5}$ to $1 \cdot 10^{-15}$, or, in other words: the absolute squared error

typically reduces about a factor 5 with every iteration. This means that the dependent iterative estimator typically converges twice as fast as the independent iterative estimator.

Figure 6.6 shows that there is a chance of almost 99.99% that the absolute squared error of one of the estimated values after 20 iterations is less than or equal to $1 \cdot 10^{-30}$. Note that this value is not very reliable, as the dataset consisted of just 9166 simulations. This figure indicates that in this dataset, there was only one appearance of a combination of data, channel, noise and IQ imbalance which caused a squared error larger than $1 \cdot 10^{-30}$. More simulations need to be done to obtain higher reliability. However, it can be concluded that for the vast majority of realizations, this estimator finds the correct values for IQ imbalance and channel estimate for extremely high signal to noise ratios.

Since this estimator performs much better than the dependent iterative estimator, in the remainder of this chapter, we will only regard the independent iterative estimator.

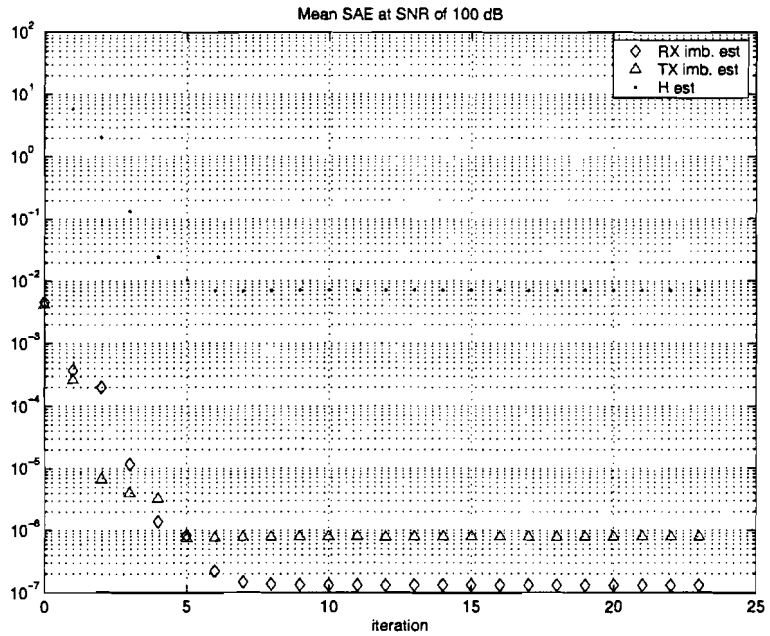

Figure 6.4: Mean squared absolute error of independent iterative algorithm

6.3 Influence of noise on "1 step" estimator for receiver imbalance

Figure 6.8 shows the cumulative distribution function (CDF) for the squared absolute error (SAE) of the "1 step" estimator for receiver imbalance as proposed in Section 5.3.3 for different values of signal to noise ratio. The IQ imbalance parameters for these simulations were $\epsilon_{TX} = 0$, $\phi_{TX} = 0$, $\epsilon_{RX} = 10\%$ and $\phi_{RX} = 5°$.

It can be seen in this figure, that the absolute squared error reduces when SNR increases. Furthermore, the 50% line crosses 45 dB at approximately $6 \cdot 10^{-5}$, 40 dB at $2 \cdot 10^{-4}$, 35 dB at $6 \cdot 10^{-4}$, 30 dB at $2 \cdot 10^{-3}$ and 25 dB at $6 \cdot 10^{-3}$. This means for example, that for a signal to noise ratio of 40 dB, there is a 50% chance that the mean square error of an estimate is less than $2 \cdot 10^{-4}$, which is in the same order as $1/\text{SNR}$. If we look at a fixed probability and if SNR is decreased 10 dB, then the SAE will also decrease a factor 10. Furthermore, if we look at a fixed SAE of $5 \cdot 10^{-4}$, we can gain or lose approximately 17% by increasing or respectively decreasing the signal to noise ratio with 5 dB.

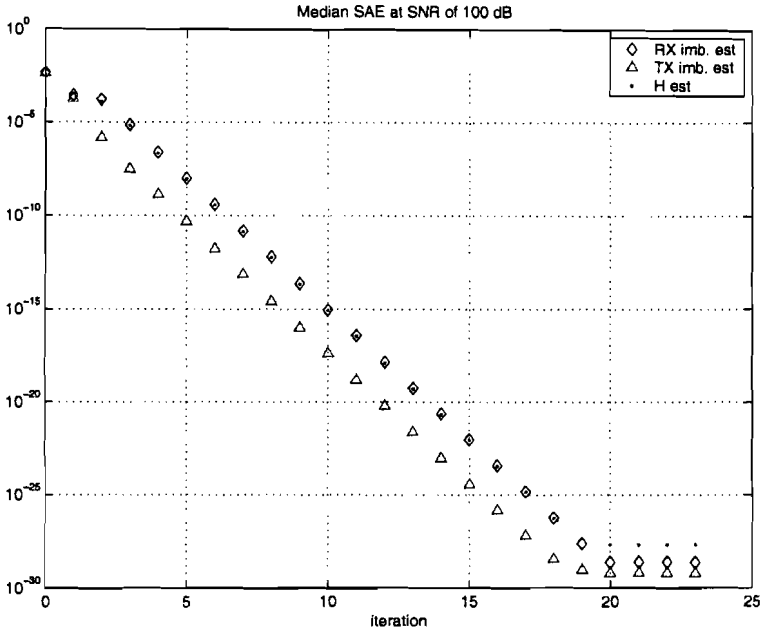

Figure 6.5: Median squared absolute error of independent iterative algorithm

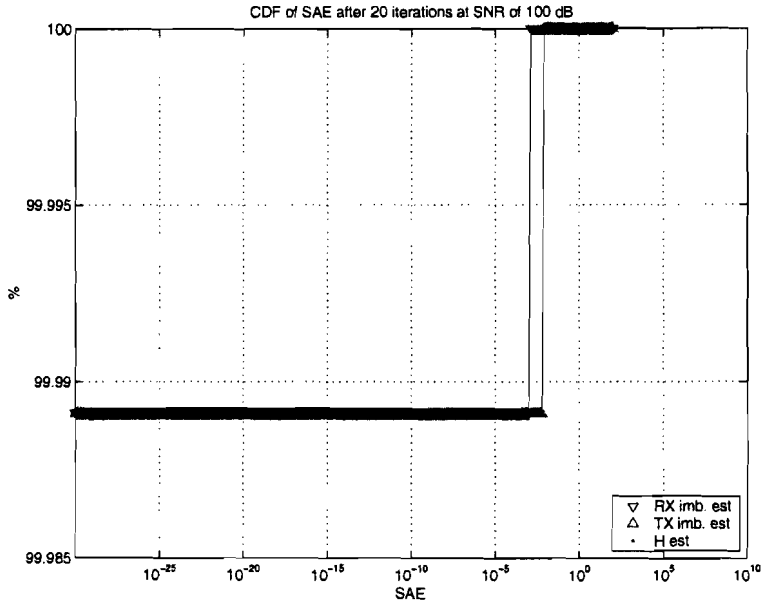

Figure 6.6: CDF of squared absolute error of independent iterative algorithm

Figure 6.7 shows the cumulative distribution function of white Gaussian noise. For 25 dB, the 10% value is at $3 \cdot 10^{-6}$ and the 90% value is at $6 \cdot 10^{-5}$, which is 20 times as large. In contrast, the 10% value for 25 dB in Figure 6.8 is $3 \cdot 10^{-6}$, but the 90% value is at $2 \cdot 10^{-3}$, which is 667 times as large. This factor 667 is much larger than the factor 20 that we found for the original Gaussian distribution. Thus, in this estimator, noise has a strong influence on the estimated value for receiver imbalance.

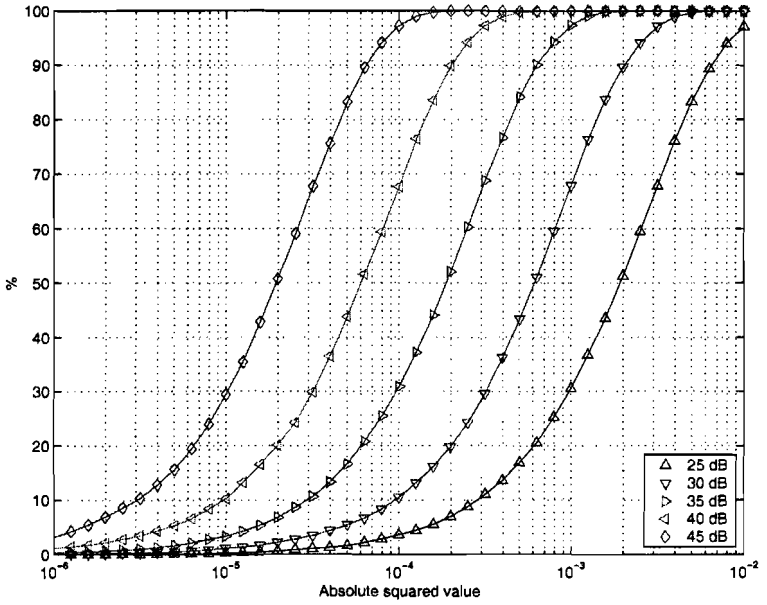

Figure 6.7: CDF of squared absolute value of white Gaussian noise

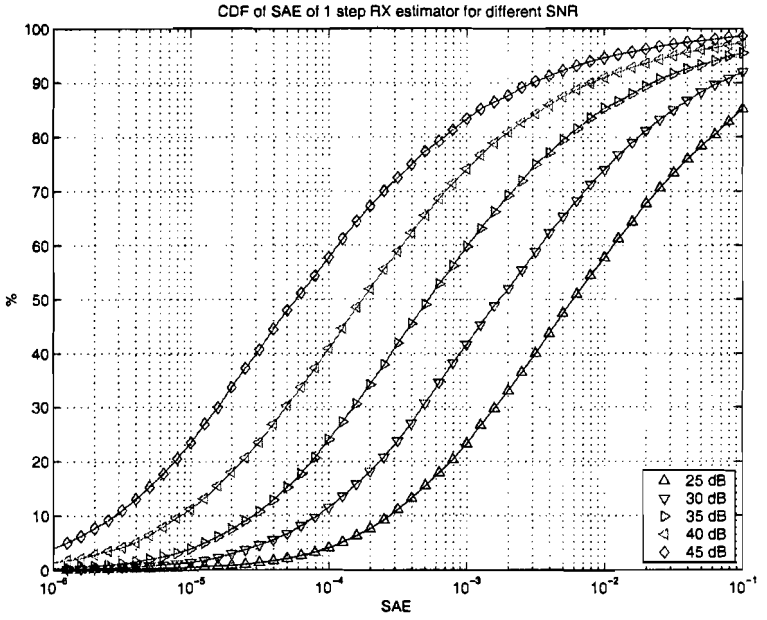

Figure 6.8: CDF of squared absolute error of "1 step" algorithm for RX estimation

A similar plot is shown in Figure 6.9 for the estimator proposed in Section 5.5.5 in equation (5.77), except that in this plot, all points are shifted about a factor 2 to the right side of the plot. Thus, for the same

SNR, this estimator has an MSE which is about twice as large as the previous estimator. Considering that this estimator also needs 3 steps to compute an estimate and requires more computational power, we can conclude that the original "1 step" estimator is to be preferred over the estimator of (5.77).

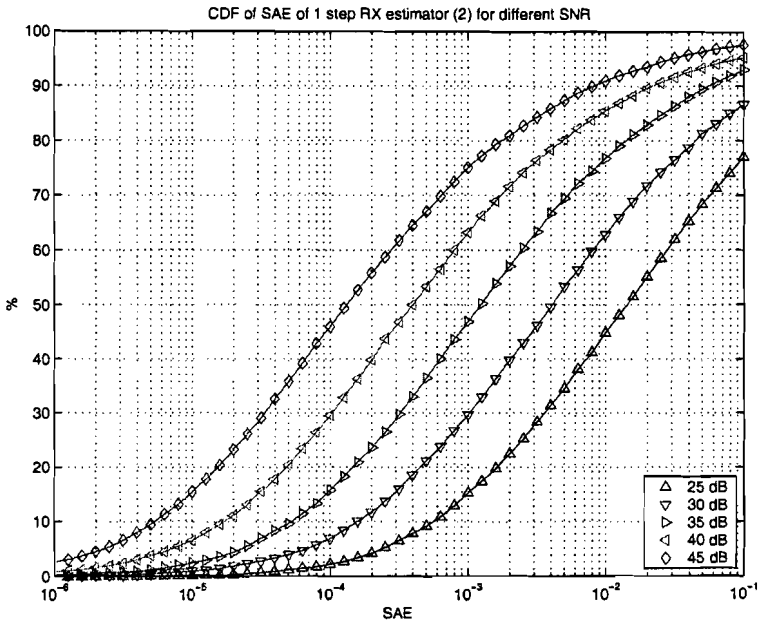

Figure 6.9: CDF of squared error of "1 step" algorithm for RX estimation of equation (5.77)

6.4 Influence of noise on "1 step" estimator for transmitter imbalance

Figure 6.10 shows the CDF curves for the "1 step" estimator for transmitter imbalance. The IQ imbalance parameters for these simulations were $\varepsilon_{TX} = 10$, $\phi_{TX} = 5$, $\varepsilon_{RX} = 0\%$ and $\phi_{RX} = 0°$. This figure shows that the slope of the curves for the transmitter imbalance estimator is steeper than that of the receiver imbalance estimators. If we look at a fixed SAE of $9 \cdot 10^{-6}$, we can gain or lose approximately 27% by increasing or respectively decreasing the signal to noise ratio with 5 dB. Furthermore, the curves in this figure start to rise earlier than the curves in Figure 6.8. For example, according to Figure 6.8, the 10% SAE of the "1 step" estimator for receiver imbalance at 25 dB is approximately $3 \cdot 10^{-4}$, while the corresponding 10% SAE for the transmitter imbalance estimator is approximately $1 \cdot 10^{-5}$, which is 30 times as low. This gap will only widen, since the curves for the transmit estimator are steeper than those for the receiver estimator.

If we compare the ratio between the 10% and 90% values of this estimator with the ratio of the corresponding values of white Gaussian noise in Figure 6.7, we see that in this case, the 90% value is 70 times as large as the 10% value. While this is still larger than the ratio of 20 that we found for the absolute squared value for the noise, it is certainly much better than the factor 667 that we found for the receiver imbalance estimators.

We can conclude from this, that the "1 step" estimator for transmitter imbalance is less sensitive to additive white Gaussian noise than the "1 step" estimator for receiver imbalance.

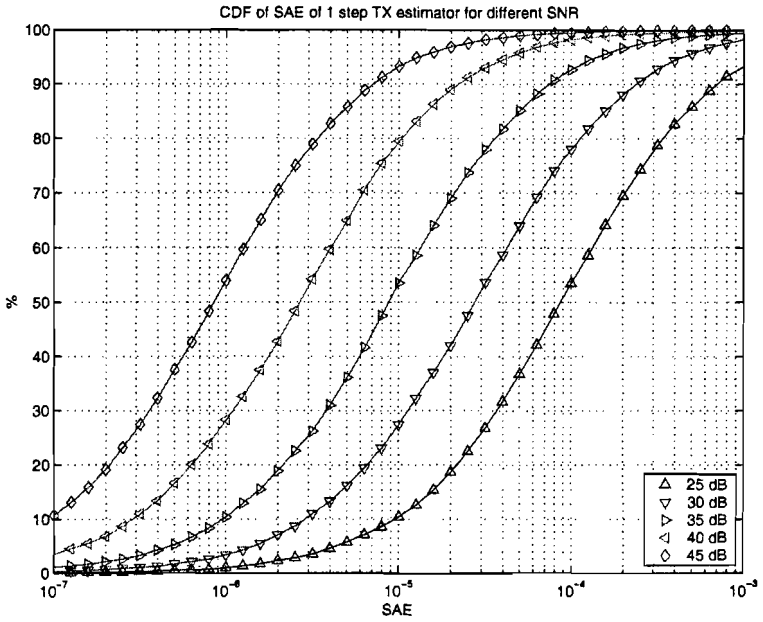

Figure 6.10: CDF of squared absolute error of "1 step" algorithm for TX estimation

6.5 Influence of noise on independent iterative estimator

In figures 6.11 - 6.13, the cumulative distribution functions of the absolute squared error of the receiver, transmitter and channel estimates are plotted for several signal to noise ratios after 20 iterations of the independent estimator are shown. For these simulations, IQ imbalance parameters were $\varepsilon_{TX} = 10$, $\phi_{TX} = 5$, $\varepsilon_{RX} = 10\%$ and $\phi_{RX} = 5°$.

Figure 6.12, which shows the CDF curves for the transmit imbalance estimates, is identical to the plot of the CDF curves for receiver imbalance estimates in figure 6.11.

Figures 6.11 and 6.12 show that for these estimators too, the squared error reduces a factor 10 if signal to noise ratio is increased with 10 dB. Furthermore, the curves are even slightly steeper than the curves for the "1 step" transmit imbalance estimator in figure 6.10. This allows for a gain of 29% if we look at the 50% SAE and increase the SNR by 5 dB.

The 10% SAE for 25 dB is approximately $2 \cdot 10^{-5}$, which is twice as large as for the "1 step" transmitter estimator, but much lower than for the "1 step" receiver estimator. Since the curves for the iterative estimators are steeper than the curves for the "1 step" transmitter estimator, the 90% SAE for 25 dB is less than twice as large. The ratio of 10% and 90% SAE is approximately 40, which is better than the corresponding ratio's for the "1 step" algorithms.

We can conclude from this, that it can be expected that the influence of noise on the independent iterative estimators is comparable to the "1 step" transmitter estimator.

Figure 6.13 shows the CDF of the SAE of the channel estimate. The curves for this figure are even steeper and not symmetric: the 50% line shows we can gain 44% if SNR is increased with 5 dB, but lose almost 50% if SNR is decreased with 5 dB. The ratio of 10% and 90% values is approximately 5, which is 4 times as low as the corresponding ratio for the absolute squared value for noise.

The channel estimate should therefore be quite robust against additive white Gaussian noise, which is at least in part due to the smoothing filter.

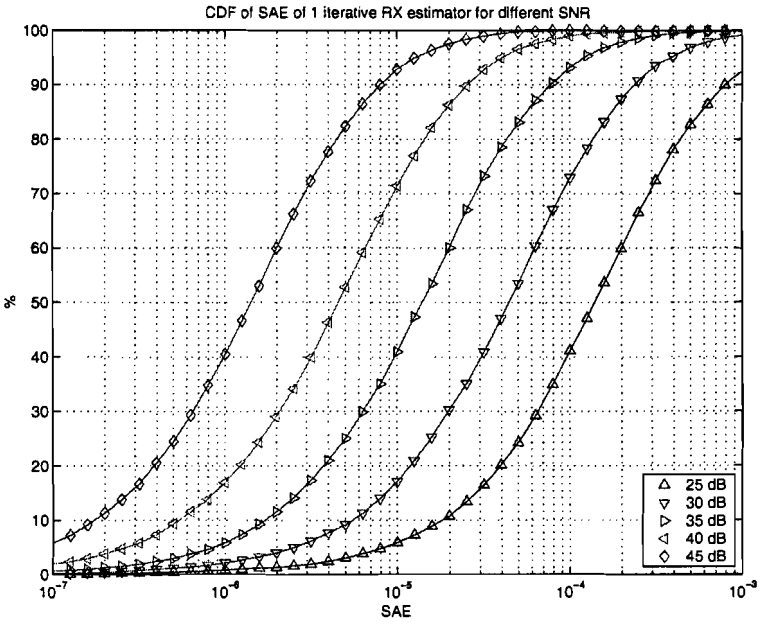

Figure 6.11: CDF of squared error of independent iterative algorithm for receiver imbalance estimation

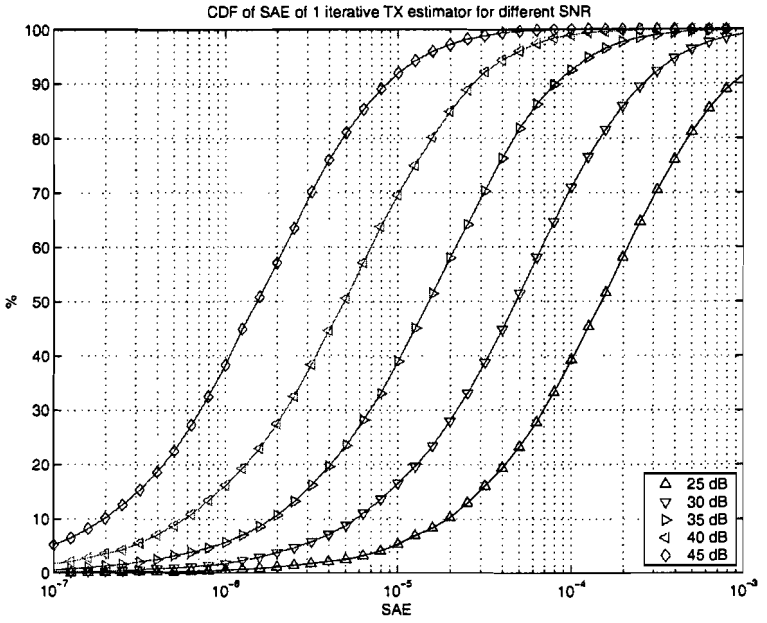

Figure 6.12: CDF of squared error of independent iterative algorithm for transmitter imbalance estimation

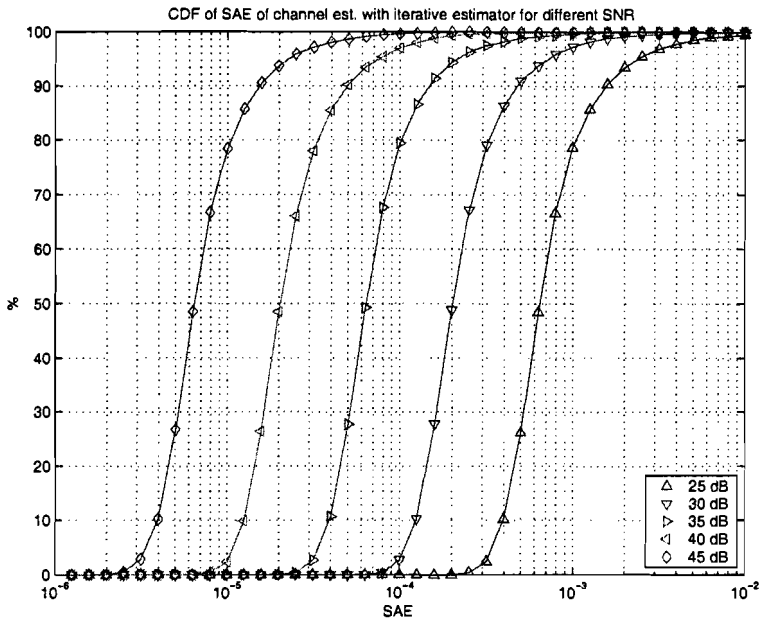

Figure 6.13: CDF of squared error of independent iterative algorithm for channel estimation

6.6 Influence of SIGNAL field structure on independent iterative estimator

Figures 6.14 - 6.16 show the CDF of the squared error of the estimates for receiver imbalance, transmitter imbalance and channel of the independent iterative estimator. Those figures each show two plots for the absolute squared error after 20 iterations at signal to noise ratio of 20 dB: one plot for a SIGNAL field which has 4 orthogonal subcarrier pairs, and one plot for a SIGNAL field which has 20 pairs, conform to the minimum respectively maximum of the IEEE 802.11a specification as shown in Section 2.2 and in Appendix B. Again, IQ imbalance parameters for these simulations were $\varepsilon_{TX} = 10$, $\phi_{TX} = 5$, $\varepsilon_{RX} = 10\%$ and $\phi_{RX} = 5°$.

The CDF for the receiver imbalance is almost identical to the CDF for transmitter imbalance. From figure 6.14, we can see that the CDF for 20 pairs is identical to the CDF for 4 pairs, but shifted to the right. The gap between the two curves is about a factor 4. This means for example, that at 20 dB SNR, there is a chance of 50% that the absolute squared error is less than or equal to $3 \cdot 10^{-4}$ if there are 20 orthogonal pairs, while the 50% squared error for 4 orthogonal pairs is about $1.2 \cdot 10^{-3}$.

The gaps in figure 6.11 show that an increase of 10 dB in signal to noise ratio results in a squared error which is 10 times as low. This indicates that 20 orthogonal pairs at 20 dB SNR give a similar absolute squared error performance for the IQ imbalance estimators as 4 orthogonal pairs at 26 dB SNR.

Note however, that the gap for the absolute squared error of the channel estimate depends on the probability at which one is interested. Indeed, as can be seen in figure 6.16, the gap at 10% is very small, while the gap at 90% is more than a factor 2.5. This is caused by the fact that the noise forces the probability of very small squared errors of channel estimates towards 0. In other words: if the estimates for the transmitter and receiver imbalance parameters are very accurate, the squared error in the channel estimate will most probably be small, but the additive noise will put a lower bound to this error.

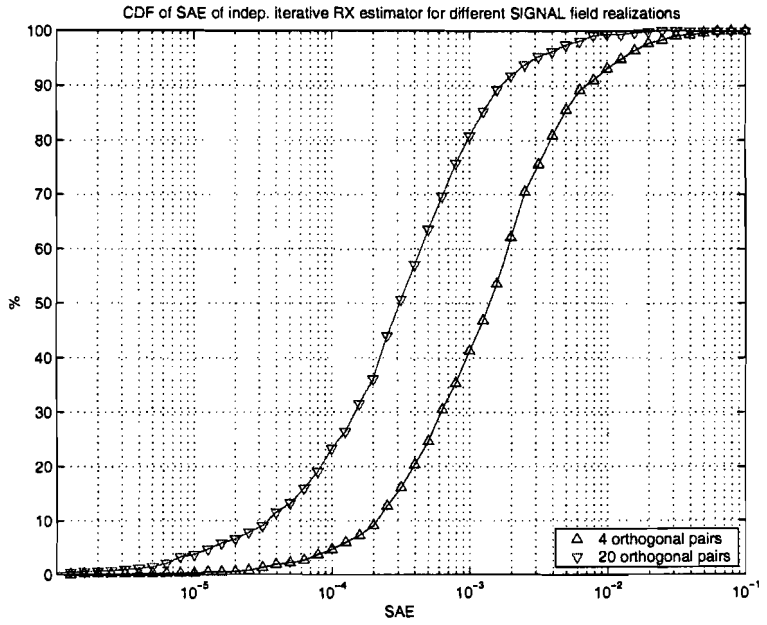

Figure 6.14: CDF of squared error of independent iterative algorithm for receiver imbalance estimation at 20 dB SNR

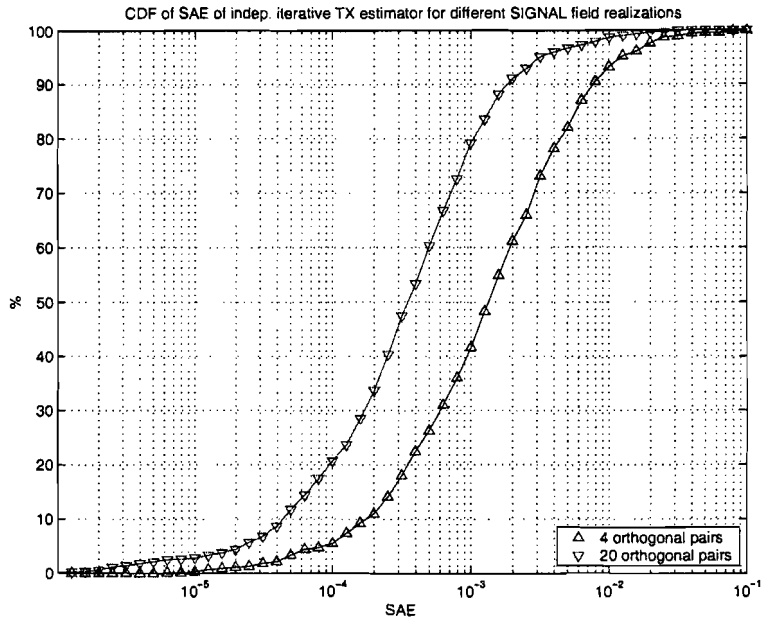

Figure 6.15: CDF of squared error of independent iterative algorithm for transmitter imbalance estimation at 20 dB SNR

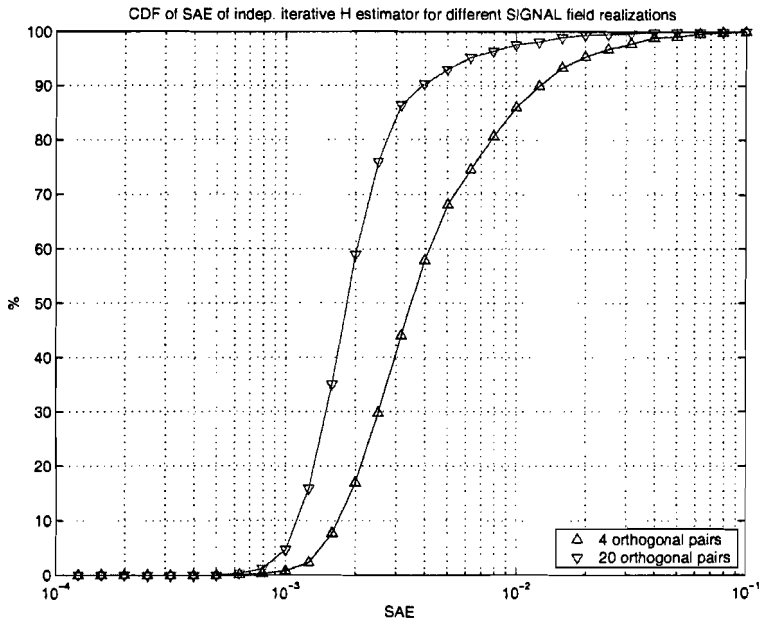

Figure 6.16: CDF of squared error of independent iterative algorithm for channel estimation at 20 dB SNR

6.7 BER performance of "1 step" estimator for receiver imbalance

Figure 6.17 shows the bit error rate for a 64 QAM rate 3/4 system with 10% and 5° imbalance in the receiver, when the "1 step" method for receiver imbalance estimation is used, as proposed in Section 5.3.3.

The blue line marked with '*' symbols shows the performance of a system without IQ imbalance and without compensation algorithm. For such a system, the average bit error rate becomes lower if signal to noise ratio increases. The green line is marked with '+' symbols and shows the performance of a system with IQ imbalance but without compensation. We can see here that the bit error rate hardly becomes any lower if signal to noise ratio is increased, since the IQ imbalance is too severe.

The red line is marked with triangles and shows the performance of a system with IQ imbalance and with the "1 step" receiver estimation method, while the cyan line, which is marked with circles, shows the performance of a system without IQ imbalance, but with the "1 step" receiver estimation method. These two lines clearly show that the "1 step" algorithm for receiver imbalance hardly improves the bit error rate performance, since it is very sensitive to white Gaussian noise. Even worse: in case there is no IQ imbalance in the receiver, the bit error rate degrades to close to the bit error rate performance of a system with IQ imbalance and the "1 step" receiver algorithm.

While Figure 6.18 shows the that the packet error rate performance of a system with the "1 step" estimator algorithm is slightly better than the bit error rate performance, it still leaves much room for improvement.

6.8 BER performance of "1 step" estimator for transmitter imbalance

Figure 6.19 shows the bit error rate for a 64 QAM rate 3/4 system with 10% and 5° imbalance in the transmitter, when the "1 step" method for transmitter imbalance estimation is used.

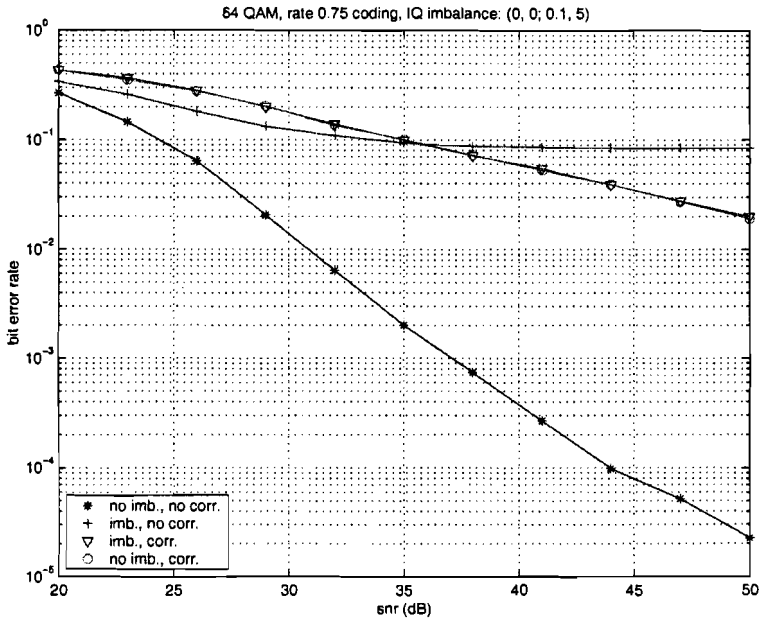

Figure 6.17: Bit Error Rate for 64 QAM rate 3/4 with 10% and 5° imbalance in receiver and "1 step" correction method

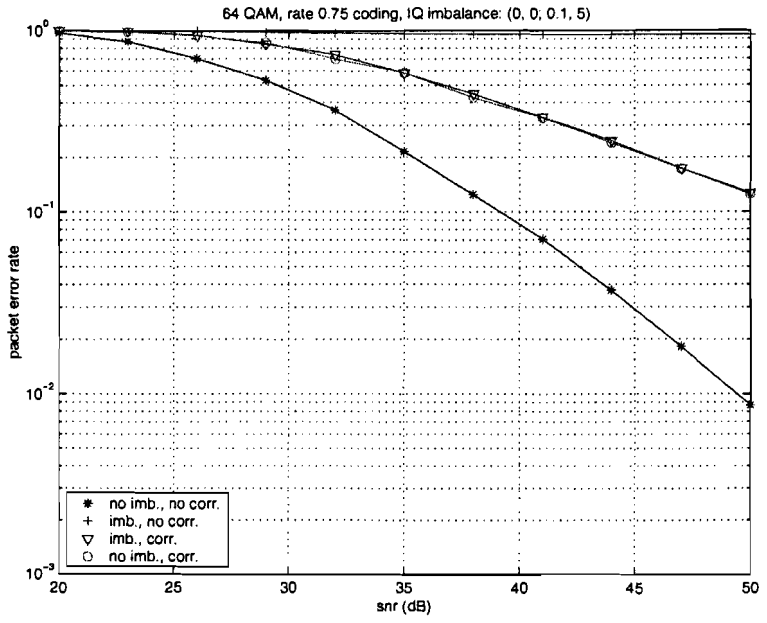

Figure 6.18: Packet Error Rate for 64 QAM rate 3/4 with 10% and 5° imbalance in receiver and "1 step" correction method

This plot clearly shows that a system where the transmitter has IQ imbalance, but where the receiver is free of any IQ imbalance, it is possible to obtain a bit error rate performance which is comparable to the bit error rate performance of a system where neither the transmitter nor the receiver has IQ imbalance.

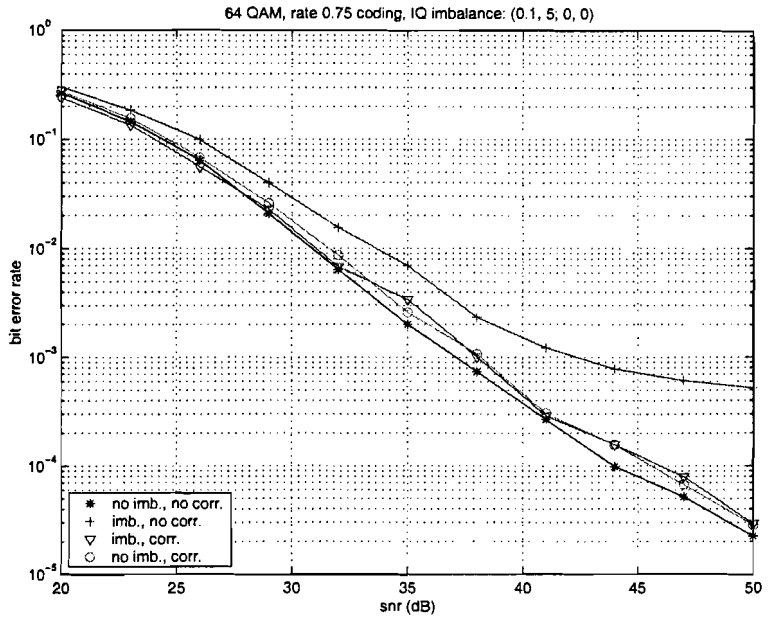

Figure 6.19: Bit Error Rate for 64 QAM rate 3/4 with 10% and 5° imbalance in transmitter and "1 step" correction method

6.9 BER performance of "1 step" estimator for TX and RX imbalance

Figure 6.20 shows the bit error rate for a 64 QAM rate 3/4 system with 10% and 5° imbalance in both the transmitter and receiver, when the "1 step" methods for transmitter and receiver imbalance estimation are used.

As could be expected for a system which uses the "1 step" algorithm for receiver imbalance estimation, the bit error rate performance is not even close to the performance of a system without IQ imbalance, since the "1 step" algorithm for receiver imbalance estimation is far too sensitive to noise.

6.10 BER performance of iterative estimator for TX and RX imbalance

Figure 6.21 shows the bit error rate for a 64 QAM rate 3/4 system with 10% and 5° imbalance in both the transmitter and receiver, when the independent iterative estimators for transmitter and receiver imbalances were used for 20 iterations on the SIGNAL field.

We can see from the line marked with '+' signs, that the IQ imbalance in transmitter and receiver put a floor of about $6 \cdot 10^{-2}$ to the bit error rate performance in case the receiver does not compensate for the imbalances. The plot with '*' symbols shows the performance of a system without IQ imbalance. Such a system obviously does not have a floor in performance. As can be seen by the plot with triangles in

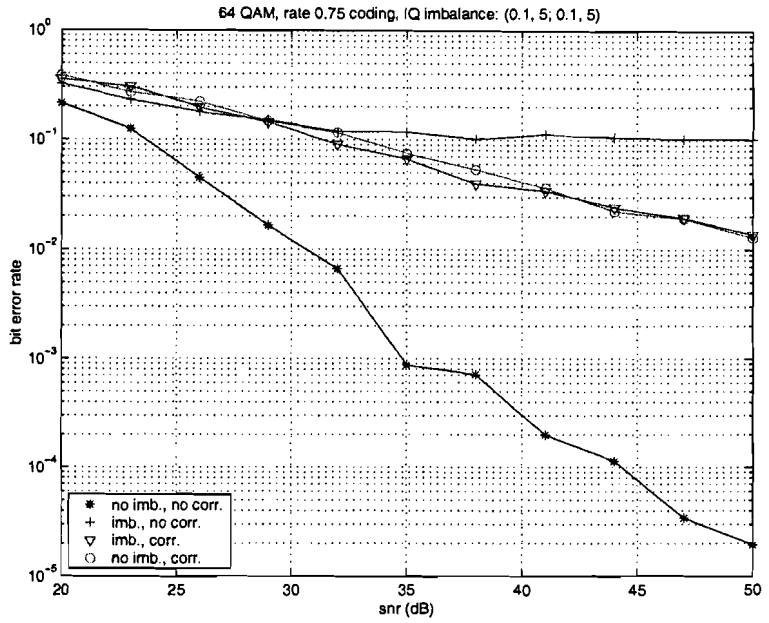

Figure 6.20: Bit Error Rate for 64 QAM rate 3/4 with 10% and 5° imbalance in transmitter and receiver and "1 step" correction methods

this figure, a system with IQ imbalance but which uses the combination of "1 step estimators" and the independent iterative estimators achieves the same performance as a system without IQ imbalance. Finally, the plot with circles shows the performance of a system without IQ imbalance but with the estimators. It shows that a system without IQ imbalance but with the estimation and compensation algorithm does not perform worse than a system without the algorithm.

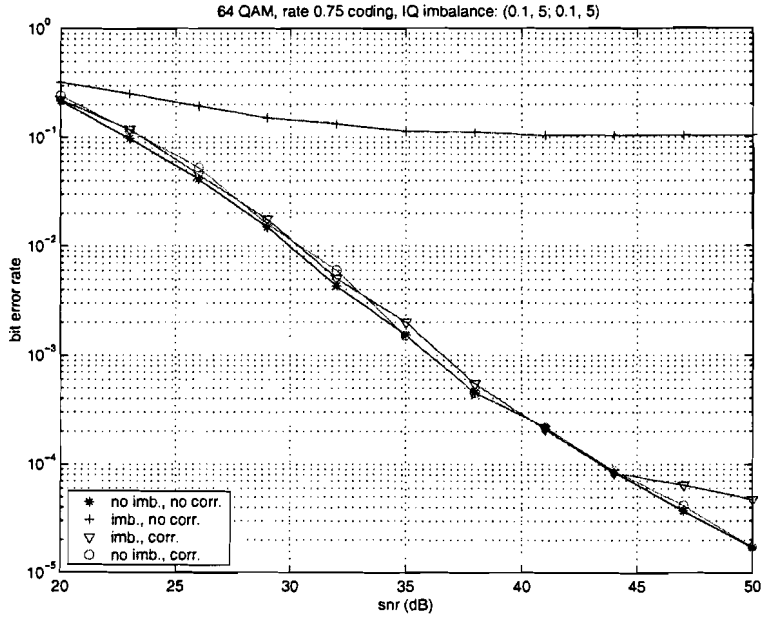

Figure 6.21: Bit Error Rate for 64 QAM rate 3/4 with 10% and 5° imbalance in transmitter and receiver independent iterative correction methods

Figure 6.22 shows the corresponding packet error rate performances. Again, a system with IQ imbalance but without correction algorithm is severely limited in performance, but a system which does use the correction algorithm performs comparable to an ideal system.

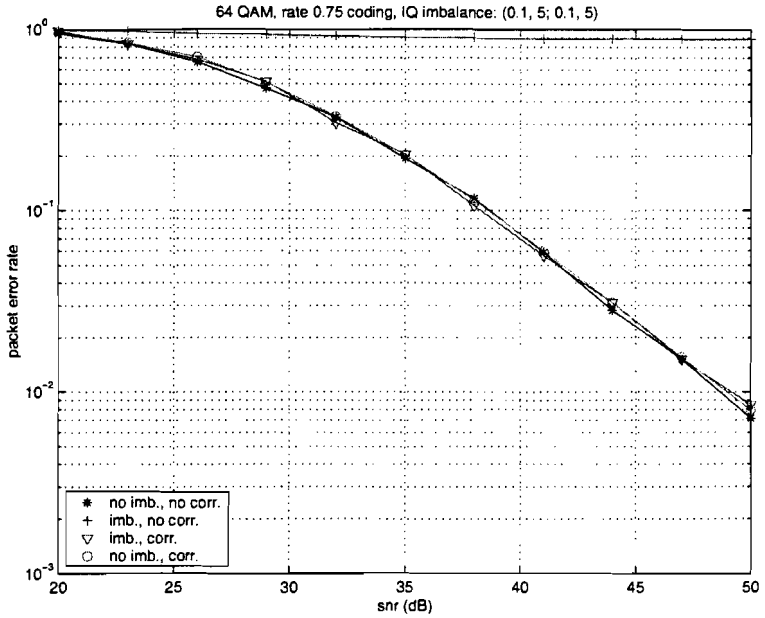

Figure 6.22: Packet Error Rate for 64 QAM rate 3/4 with 10% and 5° imbalance in transmitter and receiver and independent iterative correction methods

6.11 Comparison

In general, it is very hard to compare the performance of the estimators presented in this report with the performance of other algorithms, since the available results for those algorithms are generally for different modulation types or channel models and/or for different values for the IQ imbalance parameters, and were made with different design goals. Nevertheless, in this section, we will try to compare the algorithms in this report with other algorithms.

The algorithm by Tubbax [12] is specifically for IQ imbalance in the receiver only, although he also presents an algorithm for the joint problem of receiver imbalance and frequency offset. The algorithm specifically for receiver imbalance is for IEEE 802.11a based systems and uses the channel smoothness criterion. This algorithm does not find the exact parameters for IQ imbalance in one step. However, according to [12], the iteration can be stopped after one and a half loop. Furthermore, the algorithm is fairly complex and involves a square root operation.

The "one step" receiver algorithm in this report does find the exact value of receiver imbalance without iterating. However, this algorithm is very sensitive to noise and hence, it is of limited use. The independent iterative algorithm however, performs very well.

Lin and Tsui propose an algorithm in [21] and [22] in which they exploit orthogonality between symbol pairs in the pilot field and symbol pairs in the SIGNAL field. However, their algorithm is limited to receiver imbalance only, and does not find the exact values of the IQ imbalance parameters in one step. This algorithm typically needs 20 to 30 iterations to converge to the correct value.

The independent iterative algorithm was given 20 iterations for the simulations in this report, but this can probably be reduced to 5 to 7 iterations for common values of SNR without sacrificing performance.

The proposed solution by Brötje in [13] is for receiver imbalance only and does not find the exact solution in one step. Furthermore, the BER performance of the solution which is compatible with the IEEE 802.11a is not very good. The BER performance of the solution with a modified preamble is very good. However, this violates the IEEE 802.11a specification.

The solutions by Schenk do find the exact solution for receiver imbalance if there is no noise and no transmitter imbalance and for transmitter imbalance if there is no noise and no receiver imbalance. Furthermore, the BER performance of the receiver imbalance is better than the BER performance of the "1 step" algorithm for receiver imbalance, which indicates that his solution is more robust against noise.

His solution for the problem of both transmitter and receiver however, does not perform as good as the independent iterative estimator. This is most probably due to the fact that in his solution, only one estimate for IQ imbalance is made per packet.

In his solution, the current estimates for IQ imbalance parameters are used as initial values for the following packet, but this cannot be done for the channel estimate, as, in general, the channel cannot be assumed constant between two packets. Therefore, in the following packet, a completely new channel estimate has to be made. Furthermore, the usage of the current transmitter imbalance as initial value for the next packet is questionable, since in a multi-user environment such as a wireless LAN environment, it cannot be guaranteed that the next packet is from the same transmitter.

The independent iterative estimator does not have these problems, since it iterates multiple times over one symbol. It can therefore converge faster than the method by Schenk, and also overcomes the multi-user environment problem.

We have to note here that the computational complexity of the method of Schenk is much less than the computational complexity of the independent iterative algorithm. However, it is in most cases not necessary to use the independent iterative algorithm. If the independent iterative algorithm is used only in the first received packet, the receiver can obtain a very reliable estimate of receiver and transmitter imbalance. Once the receiver imbalance is known, the receiver can use the "1 step" algorithm to estimate transmitter imbalance in future packets, since receiver imbalance is time invariant.

6.12 Summary

In this chapter, we numerically evaluated the performance of the estimators presented in Chapter 5. We have shown that convergence of the dependent iterative estimator cannot be guaranteed, but that the independent iterative estimator typically performs very well.

Furthermore, simulations indicate that the "1 step" estimators for receiver imbalance are very sensitive to noise. However, the "1 step" estimator for transmitter imbalance is much more robust, and the performance of a system with transmitter imbalance is comparable to the performance of an ideal system if the "1 step" algorithm for transmitter imbalance is applied.

Finally, we showed that the independent iterative estimator performs very well. A system where both transmitter and receiver experience IQ imbalance can have the same BER performance as an ideal system if the independent iterative algorithm is used.

In the last section of this chapter, we compared the proposed algorithms with existing algorithms. Although such a comparison is very difficult, and perhaps sometimes even unfair due to different design goals, we can conclude that the performance of the independent iterative estimator is certainly one of the best.

Chapter 7

Conclusions and recommendations

In last chapter of this report, we will give a summary of the results and of the conclusions and we will list several topics for further research.

7.1 Conclusions

Chapter 3 showed that IQ imbalance is a typical problem for zero-IF transceivers.

Chapter 4 derived models for frequency dependent and frequency independent IQ imbalance in transmitter and receiver. It was shown in this chapter that in a fading channel environment, IQ imbalance in the receiver has a more severe impact on bit error rate and packet error rate performance than IQ imbalance in the transmitter.

Chapter 5 derived several estimators for IQ imbalance. Two "1 step" estimators for receiver imbalance and one "1 step" estimator for transmitter imbalance were proposed. Those algorithms used the orthogonality between symbol pairs in the long training sequence (P_k, P_{-k}) and in the SIGNAL field (X_k, X_{-k}). With these symbol pairs, it is possible to find the exact value of receiver respectively transmitter imbalance in case there is no noise and the transmitter respectively receiver is free of IQ imbalance.

We also proposed two iterative estimators which estimate both transmit and receive imbalance. The dependent iterative algorithm estimated only b_{RX} and b_{TX} and derived a_{RX} and b_{TX} from those estimates.

The independent iterative algorithm uses a channel smoothing algorithm to improve the channel estimate. This algorithm estimated both a_{RX} and b_{RX} as well as a_{TX}, a^*_{TX}, b_{TX} and b^*_{TX}. From all those estimates, only b_{RX} and b^*_{TX} were used, and with those values, a_{RX} and b_{TX} and a_{TX} we calculated. The independent iterative algorithm can also operate on non-BPSK symbols.

Chapter 6 showed simulation results for the "1 step" the estimators and the iterative estimators. It showed the final error in the estimated values and the BER and PER for these estimators, as well as the convergence of the iterative estimators. From these results, we concluded that the "1 step" estimators for receiver imbalance are very sensitive to noise.

However, the simulations also showed that the "1 step" algorithm for transmitter imbalance works very well. The bit error rate performance of a system with only TX imbalance is comparable to the BER performance of an ideal system if the algorithm is applied.

In case there was no noise, the convergence of the dependent iterative estimator was not very satisfying, but the convergence of the independent iterative estimator was very well. The BER performance of a system with both TX and RX imbalance is comparable to the BER performance of an ideal system if the independent iterative algorithm is applied.

Furthermore, Chapter 6 showed that both the "1 step" estimators for receiver imbalance are very sensitive to noise, while the "1 step" estimator for transmitter imbalance and the independent iterative estimator were quite robust.

Therefore, if only transmitter imbalance needs to be estimated, the "1 step" estimator for transmitter imbalance can be used. If only receiver imbalance is needed, or if an estimate for both receiver and transmitter imbalance is needed, the independent iterative estimator is preferred. As was shown in Chapter 6, this gives near optimum results.

However, further study of the independent iterative estimator needs to be done before it can be implemented in an actual product. In particular, a better understanding of the propagation of errors in the estimated values is necessary, to understand why for example the estimated value for b_{RX} is much better than the estimated value for a_{RX}. Additionally, the iterative estimator is computationally very expensive, so it can be very advantageous to try to reduce the number of computations, or to find a way to spread out the computations over the duration of the packet.

Note also, that, as suggested in Chapter 6, it is perhaps not necessary to use the independent iterative estimator for every packet that is received. IQ imbalance is fairly constant over long time intervals, so once the receiver has a good estimate of the receiver imbalance, it can use the "1 step" algorithm to estimate IQ imbalance in the transmitter for the following packets, without updating the estimate for receiver imbalance. The estimate for transmitter imbalance should be updated with every packet that is received, and the receiver cannot assume that IQ imbalance in the next packet is almost the same as IQ imbalance in the current packet, since in a multi user environment, the next packet can come from a different transmitter. (Optionally, the receiver could compare the SNR of the current packet with the SNR of the packet that was used to estimate receiver imbalance. If the SNR of the current packet is much higher, it could be beneficial to use the iterative estimator to estimate both transmitter and receiver imbalances again.)

7.2 Future work

Besides further study on the independent iterative estimator to understand the propagation of estimation errors and to reduce computational costs, several other areas could be interesting enough to warrant further investigation. Those areas are listed below, in no specific order.

7.2.1 Confined IQ imbalance

The presented estimators could in theory return any number for the estimate of transmit or receive imbalance, including numbers which are highly unlikely, like an estimate for b close to the unit circle scaled by a factor $\frac{1}{2}$ or even far outside that circle. It is possible to restrict the estimated value to this circle, or even to a smaller area if one has knowledge of the maximum imbalance that could be expected for a certain device. The question rises of course what to do if the estimator returns a value for the estimate of b outside the allowed region. Should the receiver in that case ignore that estimate and use the previous estimate (if available)? Or should it set the estimate of b to 0? Would it help to start the iterative estimation over on the next OFDM symbol?

7.2.2 Frequency selective IQ imbalance

It would be interesting to evaluate the impact of a mismatch in low pass filters on bit error rate and packet error rate, and to develop methods to estimate this imbalance. A very simple solution could perhaps be to use one of the proposed algorithms on every subcarrier and to not average the estimates at all. However, it is very likely that this type of IQ imbalance is very flat around the center frequency, but becomes more

selective towards the edges of the spectrum. The challenge would then be to find a good filter which exploits this characteristic.

Furthermore, it would be challenging to find a solution which could separate between frequency independent mismatch in the mixers and phase shifter and frequency dependent mismatch in the filters. This could even be more interesting when the local oscillator and phase shifter is shared between the transmit and receive chain on a chip, or between multiple receive chains on a chip.

7.2.3 MIMO

Multi input, multi output (MIMO) is the technique of adding more transmitter and receiver chains to a terminal in order to increase reliability and/or data rate. While it can be expected that there is virtually no correlation in filter or mixer mismatch between two transmitters or receivers, it is perhaps possible to share the local oscillator and phase shifter between all transmit and receive branches. This could result in a correlation of phase mismatch between those branches.

Another challenge in MIMO systems could be RF interference from neighboring RF chains, for example, as described in Woo [25].

7.2.4 SIGNAL field coding

The dependent estimators exploit the fact that IQ imbalance can be estimated on these subcarrier pairs where the product of pilot tones and data symbols is -1, i.e. $P_k P_{-k} X_k X_{-k} = -1$. Simulations show that the independent iterative estimator is also sensitive to the structure of the SIGNAL field.

The estimators use data symbols from the SIGNAL field, and therefore, to optimize estimation, one has to optimize the SIGNAL field. It is important to have an accurate estimate of IQ imbalance for long packets which use the highest constellation order, i.e., packets with about 1500 bytes payload and 64 QAM rate 3/4 coding. Therefore, for those packets, the corresponding SIGNAL field should have as much orthogonal subcarrier pairs as possible.

However, for 802.11a, a 64 QAM rate 3/4 with 1512 bytes payload (56 OFDM DATA fields), there are just 8 subcarrier pairs out of the possible 24 pairs.

Comparing the number of subcarrier pairs for all possible transmission modes for IEEE 802.11a and all packet lengths from 1 to 1550 bytes reveals that there are always at least 4 and maximum 20 subcarrier pairs with orthogonal symbols.

Further investigation reveals that this maximum of 20 is only achieved for BPSK and QPSK modi, while the minimum is obtained almost exclusively by 16 and 64 QAM modi (see Appendix B for details).

It would be interesting to find a SIGNAL field coding scheme which obtains many orthogonal pairs for high rate packets. Bear in mind though, that this obviously would be incompatible with the IEEE 802.11a specification.

7.2.5 Time varying IQ imbalance

The IQ imbalance parameters can change slightly over time. It is therefore interesting to find an algorithm which can accurately track this variation and still does not require a lot of computations. Questions that arise here are amongst others, how the time variation should be modeled.

7.2.6 Stopping criteria

While the stop criteria mentioned in section 5.5.6 seem to work rather well, more simulations are needed to evaluate the performance, and perhaps there are other stop criteria which are more appealing.

7.2.7 Sensitivity of algorithms to other RF imperfections

If one of the presented algorithms is to be implemented in a real world system, it is likely that IQ imbalance is just one of several imperfections that could occur and could limit the performance of the system. Therefore, it is interesting to see how other imperfections affect the presented algorithms and, if possible, find an algorithm which corrects for several types of imperfections at once. Some examples of these imperfections are carrier frequency offset, phase noise, non-linearity, DC-offset due to self-mixing and even-order distortion.

7.2.8 Adapt algorithms to more specific transceiver implementations

Just as in the case for MIMO systems, it is perhaps possible to share the local oscillator and phase shifter between several units, in this case between the transmitter and receiver. In that case, if IQ imbalance in the receiver is known, the receiver can compute the phase imbalance. With that imbalance, the transceiver can reduce the imbalance in the transmitter part by correcting the signal it is transmitting for phase imbalance.

Another option could be to implement a switch between the transmitter and receiver to create a calibration loop, as illustrated by figure 7.1. This figure shows a schematic of a transmitter above the dotted line and a schematic of a receiver below the dotted line. If they are both implemented on one chip, it is perhaps possible to add switch s1 which could route the signal from the transmitter to the receiver. During normal operation, s1 would route the signal from the receiving antenna and LNA to the mixers of the receive module. However, in calibration mode, s1 can route the signal from the transmitter just before the power amplifier to the mixers of the receiver. In that case, the DSP should be able to estimate the IQ imbalance in both the receiver and local transmitter. This method is especially interesting, since the LNA is bypassed, and thus the signal to noise ratio should be very high, allowing for very accurate estimates.

Note that this solution is similar to calibration loops suggested by Bourdoux [26] and Liu [27], however, the calibration loops in those solutions are more complex and not specifically suited for IQ imbalance estimation.

Problems that could arise in such a system are that in such a system, the channel between local transmitter and receiver in calibration mode is probably frequency flat, which is a problem for our estimators. Furthermore, adding a switch would increase costs, although such a switch could perhaps be cheaper than a usual antenna switch, as the dynamic range of the signals is smaller. Additionally, it is perhaps possible to use a very cheap switch which exhibits some frequency selective behavior. This overcomes the problem that the channel is frequency flat, and thus with such a switch, it is possible for the algorithm to separate between transmitter and receiver imbalance, and estimate them both very accurately.

Additionally, during the calibration phase, the transmitter does amplify and transmit the data that is used for calibration. This is easy to overcome though, by just setting the power amplifier to a minimum level, or even to shut it off completely. Alternatively, one could try to find a calibration sequence that adheres to the IEEE 802.11a specification.

Finally, adding a switch could perhaps have other benefits as well, for example to calibrate other parameters of the system.

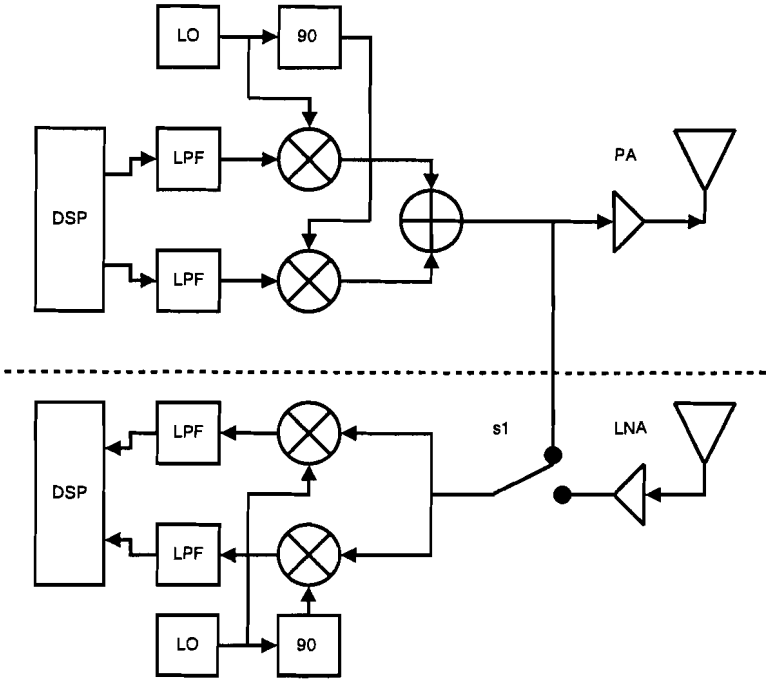

Figure 7.1: Calibration loop for transceiver. Note that the transceiver in this figure has two antennas: one for the transmit chain and one for the receive chain. However, in practice, both chains often share the same antenna with an antenna switch. This antenna switch was left out in this figure for reasons of simplicity.

7.2.9 Maximize signal to interference and noise ratio

In our simulator, we used a zero forcing approach to equalize the signal. While this is a very simple method which eliminates all inter symbol interference (ISI) at the decision instants, it is well known to cause noise enhancement. A different method is to use an MMSE approach, which minimizes the total power of ISI and noise at the decision instants.

It could therefore be interesting to find a compensation algorithm which minimizes the total power of ISI, interference due to transmitter and receiver imbalance and noise at the decision instants.

Acknowledgements

The project described in this document could not have been completed without the help of others. Therefore, I want to thank them here, at the end of my thesis.

First of all, I want to thank Dr. Job Oostveen for being my supervisor on this project. His help, his advice and the discussions that we had, shaped this project into it's current form. I also want to thank Dr. ir. Frans Willems, who always raised questions that I never thought of and gave different perspectives to the problems at hand. I also want express my gratitude to MSc. Ho Chin Keon, with whom I had very nice and fruitful discussions.

Furthermore, I owe a lot to Ir. Tim Schenk of the Eindhoven University of Technology. He always had time for me to explain things and to discuss ideas. He inspired me to go further than what I originally had in mind. Without his help, this project would not have come so far.

I want to thank Prof. dr. ir. Jan Bergmans and Dr. ir. Frans Willems for arranging the possibility to do this project in a company.

I also want to thank Philips Research in Eindhoven and especially Dr. ir. Jean-Paul Linnarz for giving me the opportunity to do this project and for their sponsorship.

Finally, I want to thank my family and friends for their patience and support, and for giving me the (sometimes much needed) distraction from this project.

Admar Schoonen Eindhoven, January 2006

Appendix A

Channel smoothing filter

In this appendix, we will give a summary for a leased squared based method on how to estimate the channel coefficients when the channel impulse response is limited to fewer samples than the number of subcarriers on which the channel estimate is based. Additionally, this method will also estimate the channel coefficients on subcarriers where no pilot symbols were available. This appendix summarizes a Philips internal document by Ghosh [23]. A similar algorithm is proposed by Van de Beek in [24].

The initial channel estimate is obtained by dividing the received signal on subcarrier k by the corresponding pilot symbol:

$$\hat{H}_k = R_k/P_k \qquad k = 0, 1, \ldots, N-1 \tag{A.1}$$

where N is the number of subcarriers, R_k is the received signal on subcarrier k in the long training symbol and P_k is the associated pilot symbol.

This approach treats each channel coefficient independent. However, if the channel impulse response is limited to N_h samples, with $N_h < N$, the channel frequency response has only N_h degrees of freedom and the remaining $N - N_h$ coefficients are determined by those N_h coefficients.

If we write the channel impulse response in vector notation response as

$$\underline{h} = \begin{bmatrix} h_0 \\ h_1 \\ \vdots \\ h_{N_h} \end{bmatrix}, \tag{A.2}$$

we can write for the for the channel frequency response

$$H_k = \sum_{n=0}^{N_h-1} h_n e^{j2\pi nk/N} \qquad k = 0, 1, \ldots, N-1. \tag{A.3}$$

In matrix notation, we can write this as

$$\underline{H} = F\underline{h} \tag{A.4}$$

where F is a $N \times N_h$ truncated Fourier matrix.

Assume that there the pilot symbols were available on only N_c subcarriers. For the other $N - N_c$ subcarriers, no initial channel estimate is available, and thus $\hat{H}_k = 0$. We can now reorganize the channel frequency response $\underline{H}$ in

$$\begin{bmatrix} \underline{H}_1 \\ \underline{H}_2 \end{bmatrix} = \begin{bmatrix} F_1 \\ F_2 \end{bmatrix} \underline{h}, \tag{A.5}$$

where $\underline{H}_1$ is the partition of $\underline{H}$ for the subcarriers where pilot symbols were available and $\underline{H}_2$ is the partition of $\underline{H}$ for the subcarriers where no pilot symbols were available. F_1 and F_2 are the corresponding partitions of the Fourier matrix F. F_1 is a $N_c \times N_h$ matrix and F_2 is a $N - N_c \times N_h$ matrix.

We can now find the least squares estimate for the channel impulse response by

$$\hat{\underline{h}}_{LS} = (F^H F)^{-1} F^H \hat{\underline{H}}. \tag{A.6}$$

If we define $G = (F^H F)^{-1} F^H$, we can reorganize G in $G = [G_1\ G_2]$, where G_1 contains the columns of G where pilot symbols are available and G_2 the columns of G where no pilots are available.

For the estimate of the channel impulse response, we can now write

$$\hat{\underline{h}}_{LS} = G_1 \hat{\underline{H}}_1 + G_2 \hat{\underline{H}}_2. \tag{A.7}$$

Unfortunately, $\hat{\underline{H}}_2$ is not available. However, from equation (A.5) we know that $\underline{H}_2 = F_2 \underline{h}$ and therefore $\hat{\underline{H}}_2 = F_2 \hat{\underline{h}}_{LS}$.

Substituting this in equation (A.7) yields

$$[I - G_2 F_2] \hat{\underline{h}}_{LS} = G_1 \hat{\underline{H}}_1. \tag{A.8}$$

Let us now define $M = [I - G_2 F_2]$. If M has full rank, the channel impulse response can be estimated with

$$\hat{\underline{h}}_{LS} = M^{-1} G_1 \hat{\underline{H}}_1 \tag{A.9}$$

and the full channel frequency response with

$$\hat{\underline{H}}_{LS} = F \hat{\underline{h}}_{LS} \tag{A.10}$$

$$= F M^{-1} G_1 \hat{\underline{H}}_1. \tag{A.11}$$

Note that matrices F, M and G_1 and thus $F M^{-1} G_1$ can be pre-computed since none of them depend on the channel coefficients. Note further, that for an IEEE 802.11a system where $N_c = 52$ and $N_h = 16$, M is of full rank, and therefore, the method described in this appendix can be used for channel estimation.

Appendix B

Orthogonal subcarrier pairs for different SIGNAL field parameters

Table B.1: SIGNAL field parameters that obtain the minimum of 4 orthogonal subcarrier pairs

Number of octets	N_{BPSC}	Coding rate
246	4	3/4
246	6	3/4
253	4	1/2
253	6	2/3
523	6	3/4
756	6	3/4
838	2	3/4
1141	4	3/4
1141	6	3/4
1277	4	3/4
1277	6	3/4
1496	4	3/4
1496	6	3/4
1549	4	1/2

Table B.2: SIGNAL field parameters that obtain the maximum of 20 orthogonal subcarrier pairs

Number of octets	N_{BPSC}	Coding rate
589	2	1/2
610	1	3/4
626	2	1/2
719	2	1/2
991	1	1/2
991	2	1/2
1368	2	3/4

References

[1] *IEEE 802.11a standard*, ISO/IEC 802-11:1999/Amd 1:2000(E).

[2] *IEEE 802.11g standard*, Further Higher-Speed Physical Layer Extension in the 2.4 GHz Band, 2003.

[3] A. Paulraj, R. Nabar, and D. Gore, *Introduction to Space-Time Wireless Communications*, Cambridge University Press, 2003.

[4] T. S. Rappaport, *Wireless Communications, principles and practice*, Prentice Hall, 2 edition, 2002.

[5] H. Harno, "Channel estimation of MIMO OFDM systems", Master's thesis, University of Twente, 2005.

[6] R. van Nee and R. Prasad, *OFDM for Wireless Multimedia Communications*, Arthech House Publishers, 2000.

[7] J. G. Proakis, *Digital Communications*, McGraw-Hill, 4 edition, 2001.

[8] II L. W. Couch, *Digital and Analog Communication Systems*, Prentice Hall, 6 edition, 2001.

[9] B. Razavi, "Design considerations for direct-conversion receivers", in *IEEE Transactions on Circuits and Systems II: Analog and Digital Signal Processing*, June 1997, pp. 428–435.

[10] S. Mirabbasi and K. Martin, "Classical and modern receiver architectures", in *IEEE Communications Magazine, Vol. 38, Issue 11*, Nov. 2000, pp. 132–139.

[11] M. Buchholz, A. Schuchert, and R. Haholzner, "Effects of tuner IQ imbalance on multicarrier-modulation systems", in *Proc. IEEE Conference on Devices, Circuits and Systems*, 2000, pp. T65/1–T65/6.

[12] J. Tubbax, *A digital approach to low-cost low-power broadband radios*, PhD thesis, K. U. Leuven, 2004.

[13] L. Brötje, S. Vogeler, K. D. Kammeyer, R. Rückriem, and S. Fechtel, "Estimation and correction of transmitter-caused I/Q imbalance in OFDM systems", in *Proc of the 7th International OFDM-Workshop*, 2002, pp. 178–182.

[14] T.C.W. Schenk, P.F.M. Smulders, and E.R. Fledderus, "Estimation and compensation of TX and RX IQ imbalance in OFDM based MIMO systems", in *Accepted for IEEE Radio and Wireless Symposium (RWS 2006)*, Jan. 2006.

[15] M. Valkama, M. Renfors, and V. Koivunen, "Advanced methods for I/Q imbalance compensation in communication receivers", *IEEE Trans. on Signal Proc.*, vol. 49, pp. 2335–2344, Oct. 2001.

[16] R. van Nee, G. Awater, M. Morikura, H. Takanashi, M. Webster, and K. W. Halford, "New high-rate wireless LAN standards", *IEEE Communications Magazine*, Dec. 1999.

[17] J. W. M. Bergmans, *Digital baseband transmission and recording*, Kluwer Academic Publishers Group, 1996.

[18] G. Fettweis, M. Löhning, D. Petrovic, M. Windisch, P. Zillmann, and E. Zimmermann, "Dirty RF", in *Proc of the 11th Wireless World Research Forum*, 2004.

[19] M. Windisch and G. Fettweis., "Standard-independent I/Q imbalance compensation in OFDM direct-conversion receivers", in *Proc. 9th International OFDM Workshop*, Sept. 2004.

[20] H. Shafieea and S. Fouladifard, "Calibration of IQ imbalance in OFDM transceivers", in *Proc of the IEEE International Conference on Communications*, May 2003.

[21] J. Lin and E. Tsui, "Joint adaptive transmitter/receiver IQ imbalance correction for OFDM systems", in *Proc of the 15th IEEE Internation Symposium on Personal, Indoor and Mobile Radio Communications PIMRC*, 2004.

[22] J. Lin and E. Tsui, "Adaptive IQ imbalance correction for OFDM systems with frequency and timing offsets", in *Proc of the Global Telecommunications Conference GLOBECOM*, Dec. 2004.

[23] M. Ghosh, "Channel estimation in OFDM with partial training", Philips internal document.

[24] J. van de Beek, O. Edfors, M. Sandell, S. K. Wilson, and P. O. Borjesson, "On channel estimation in OFDM systems", in *IEEE 45th Vehicular Technology Conference*, Jul. 1995, vol. 2, pp. 815 – 819.

[25] Sanghyun Woo, Dongjun Lee, Kiho Kim, Yungsik Hur, Chang-Ho Lee, and Joy Laskar, "Combined effects of RF impairments in the future IEEE 802.11n WLAN systems", in *IEEE 61st Vehicular Technology Conference*, Jun. 2005, vol. 2, pp. 1346 – 1349.

[26] A. Bourdoux, B. Côme, and N. Khaled, "Non-reciprocal transceivers in OFDM/SDMA systems: Impact and mitigation", in *Proc of Radio and Wireless Conference RAWCON*, Aug. 2003.

[27] J. Liu, A. Bourdoux, J. Craninckx, P. Wambacq, B. Côme, S. Donnay, and A. Barel, "OFDM-MIMO WLAN AP front-end gain and phase mismatch calibration", in *IEEE Radio and Wireless Conference*, Sept. 2004.

Literature study on In-phase / Quadrature-phase (IQ) imbalance for Orthogonal Frequency Division Multiplexing (OFDM) wireless LAN systems

A.M.J.M. Schoonen

Company:	Philips Research, Nat. Lab
Name:	A.M.J.M. Schoonen
ID number:	s462529
Address:	Marconilaan 30 B 5621 AA Eindhoven
Telephone:	06-44064472
E-mail:	a.m.j.m.schoonen@student.tue.nl
University:	Eindhoven University of Technology
Department:	Electrical Engineering
Division:	Measurement and Control Systems (MBS)
Chair:	Signal Processing Systems (SPS)
Supervisors:	Dr. Ir. J. Oostveen (Philips), Dr. Ir. F.M.J. Willems (TU/e, Philips)
Professor:	Prof. Dr. Ir. J.M.W. Bergmans (TU/e)
Document created in:	February 2005 - January 2006

Contents

Chapter 1

Assignment

1.1 Graduation project

1.1.1 Motivation

The need for wireless communication at higher bit rates and lower cost is increasingly putting more stress on the analogue part of the communication systems. This is especially the case for Wireless Local Area Networks (WLANs), where standards are defining very high bit rates and where the analogue part is one of the largest manufacturing costs.

1.1.2 Problem definition

Current designs for wireless communication systems usually use two (in theory) identical analogue circuits in both the transmitter and the receiver, which allows saving half of the bandwidth in the transmitted or received signal without having to use very specific and expensive filters. Those circuits are called the in-phase (I) and quadrature (Q) branches. If however, those two circuits are not exactly identical, there is a so called IQ imbalance, and the signal will be distorted.

1.1.3 Objective

The main objective is to develop a method which reduces the effects of IQ imbalance. The goals are to allow larger differences between the branches (which could result in lower manufacturing costs) and / or to allow the use of larger signal constellations (which could result in higher bit rates).

Due to the increase in computational power and decreasing costs of digital signal processors (DPSs) and digital logic, a method which reduces the effects of IQ imbalance on the sampled (digital) signal only by doing operations that can be implemented in software or digital logic, is preferred over a method which requires extra analogue hardware.

1.2 Literature research

The initial literature study is focused on transmitter and receiver architectures and Orthogonal Frequency Division Modulation (OFDM), a very popular modulation scheme used in e.g. IEEE 802.11a WLAN.

Additionally, literature on the effects of IQ imbalance on the signal in both time and frequency domain have been studied, as well as compensation methods for those effects. For those compensation methods, methods which did not require any additional hardware were preferred.

As DSPs for wireless communication systems form a relative new area, the search for literature on compensation algorithms was limited to 1990 and later. However, when a search for more general documents on e.g. OFDM modulation or transceiver architectures was needed, the search was not limited to any time in history.

The search for literature was mostly focused on articles , but also included text books, internal reports and dissertations.

As most of the research on wireless communications is done in North America, Europe and Asia, it was expected that most of the relevant literature came from those areas, but the search queries were deliberately not limited to any specific geographical area. All searches were limited to documents written in English, since my knowledge of other languages besides Dutch is too limited to understand technical writing, and since in general, there are not many Dutch documents on these topics (compared to the vast amount of English documents).

Chapter 2

Title and table of contents of final report

This chapter gives an overview of the title and contents of the graduation report.

2.1 Title

The title of the graduation report is "IQ imbalance in OFDM Wireless LAN systems".

2.2 Table of contents

The table of contents is as follows:

1. Introduction
2. IEEE 802.11a Wireless LAN packet structure
3. Zero-IF transceivers
4. IQ imbalance modeling
5. Estimation and compensation algorithms
6. Simulation results and comparison
7. Conclusions and recommendations
8. Appendices
9. References

Chapter 3

List of search terms

The following English search terms were used to search literature. Combinations of those terms were used to create search expressions. The expressions were applied to the sources mentioned in chapter 4.

1. Wireless transmitter architecture
2. Wireless receiver architecture
3. Transceiver architecture
4. Direct conversion
5. Zero IF
6. IQ imbalance
7. IQ mismatch
8. Filter mismatch
9. Estimation
10. Compensation
11. RF imperfection
12. Dirty RF
13. WLAN
14. OFDM

Chapter 4

List of sources and number of references

The sources that were used for this literature search are listed in Table 4.1. The search terms listed in Chapter 3 are combined to form search expressions which were used on the online search engines of the corresponding sources.

Table 4.1: List of sources used for the literature search

Source	Search in	No. Hits
TU/e VUBIS online library catalogue	All words	1
Philips NatLab online library: Catalogue (books, reports)	Title, Abstract	1
Science Citation Index: Using regular expressions	Title, Full text	8
Science Citation Index: Citation Method	Title, Full text	6
INSPEC	Subject/Keyword	36
IEEE - IEE Electronic Library	All fields (meta data)	39
Google Scholar	Full text	117

Notes:

- Google Scholar gave so many hits that it is impossible to view all of them to sort out all less relevant documents. Therefore, the searches on Google Scholar were each time limited to the first 30 or 40 hits.
- Google Scholar was usually used as a 'last resort', just to check if it would come up with any different and interesting documents. Google was also used if access to the full text document was not available. In some cases, Google could return a link to the homepage of the author, which had the document available.
- Many duplicates were found, especially between INSPEC and the IEEE - IEE Electronic Library.

4.1 Alternative literature sources

Very early in the beginning of this project, one of the supervisors gave me the PhD dissertation of Jan Tubbax of K.U. Leuven, titled "A digital approach to low-cost low-power broadband radios" [1], which gives a good overview of IQ imbalance and a detailed solution to this problem. Furthermore, during the

project, my supervisor gave me an unpublished document by Ghosh [2] on advanced channel estimation. I also obtained a copy of the master's thesis of Harno [3], who was finishing his thesis while I was working there.

Chapter 5

Criteria for selection of literature

In the first part of the assignment, it was of most importance to understand the concept of wireless transceivers, especially of Zero IF transceivers. Relevant keywords were: "transmitter architecture", "receiver architecture", "transceiver architecture", "zero IF" and "direct conversion"

Once a good understanding of Zero IF transceivers was obtained, it was important to understand the influence of IQ imbalance on OFDM systems (using Zero IF transceivers). Relevant keywords in this case were: "IQ imbalance", "IQ mismatch", "OFDM", "RF imperfection". Note that keywords such as "Zero IF" and "direct conversion" were not very useful in this case, since IQ imbalance is a typical problem for Zero IF transceivers. Thus, adding or removing "Zero IF" or "direct conversion" to the search expression did not result in very different search results. Note also that most of the documents found with these search results were very short on discussing the actual effects of IQ imbalance and instead focused on a new proposal for estimating and/or compensating IQ imbalance.

To get an overview of the current methods for estimation and compensation of IQ imbalance, the same expressions were used as listed in the previous paragraph. This time, it was very helpful that those search expressions revealed so many different proposals on estimating and compensating IQ imbalance. Since at this time, the focus of this project was narrowed down to IEEE 802.11a wireless LAN systems, documents on estimation and compensation of IQ imbalance in OFDM wireless LAN systems were preferred.

Online available full text articles were preferred above printed documents in the library or articles that had to be ordered, since it is much easier to search in an electronic document and since electronic documents do not have any delivery period at all.

As mentioned in Section 1.2, when searching for documents on OFDM or transceiver architectures, no restriction on publication date was used. However, when a search query for IQ imbalance was formulated, the search was restricted to those documents which were published in 1990 or later. Furthermore, only English documents were searched, as Dutch is the only other language which I understand well enough to read technical documents, but only very few technical documents on IQ imbalance are written in Dutch.

Chapter 6

The snowball method

The snowball method was applied on Lin [4], as this document gives a short introduction to the problem and proposes a very elegant solution. It contains references to both extensive introductions on the topic as well as to other solutions. The resulting diagram of the snowball method is shown in Figure 6.1.

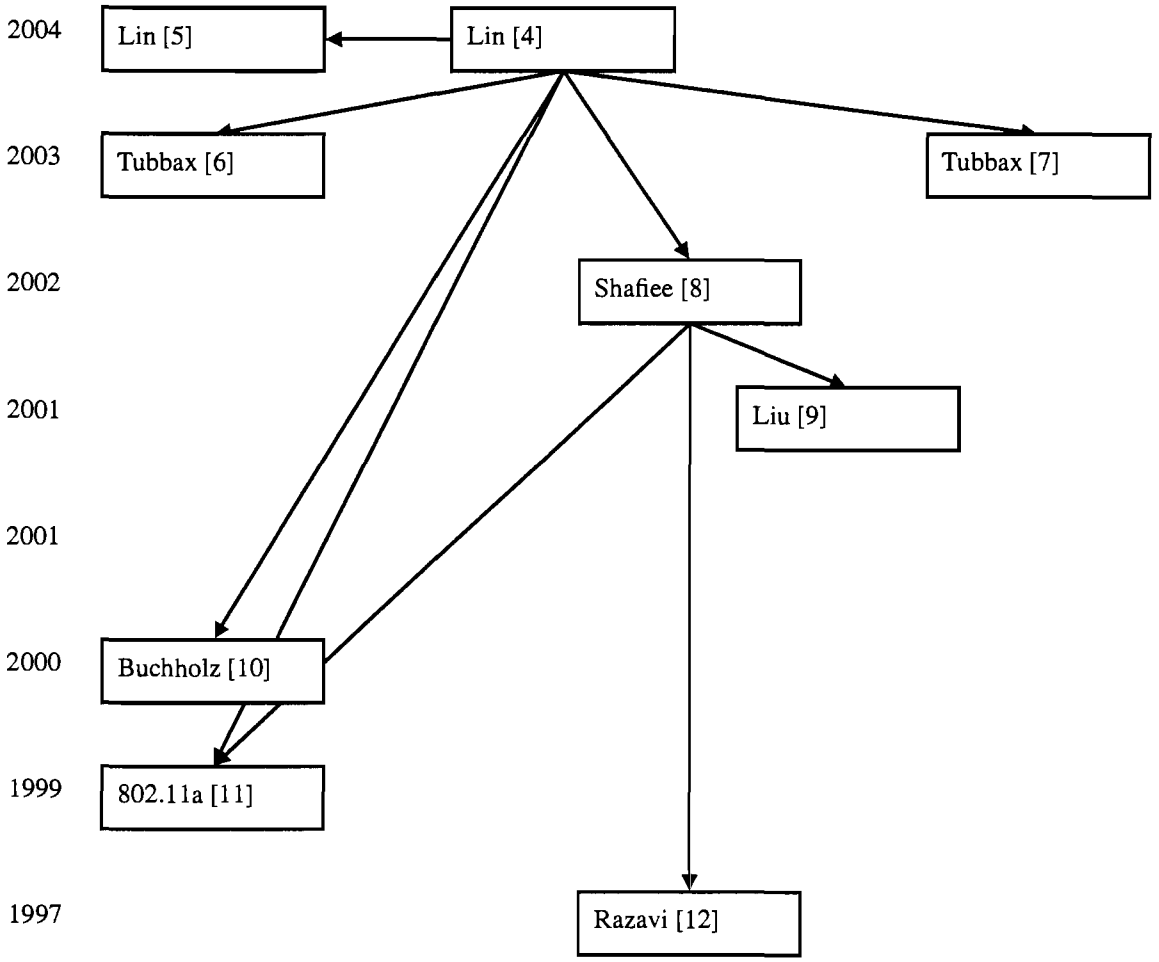

Figure 6.1: Snowball diagram for a selected paper

Chapter 7

The citation method

The Science Citation Index in the Web of Science was searched for referring literature from 1986 until now. The paper by Tubbax [6] was chosen as it provides a good background and a novel solution to the problem.

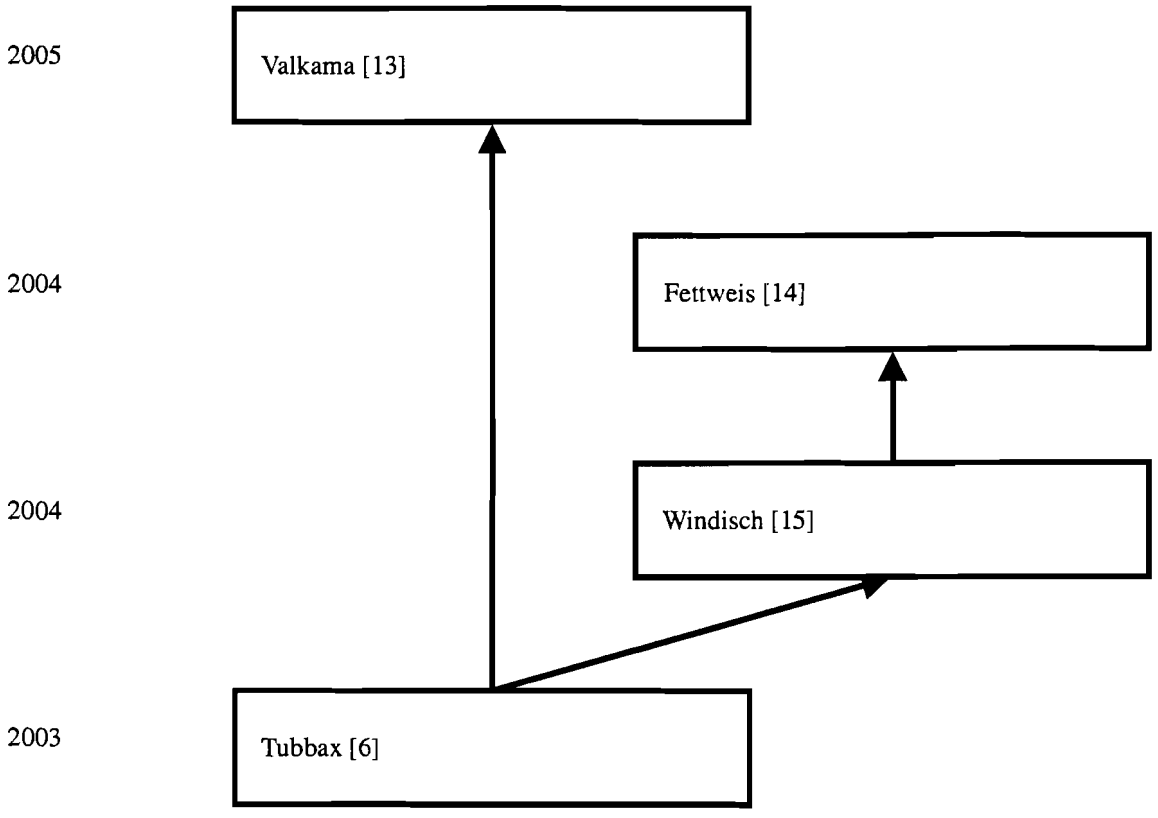

Figure 7.1: Citation method for a selected paper

Chapter 8

Relation of found literature with respect to the graduation report

The relation between the final report and the found literature is presented in Table 8.1.

Table 8.1: Found literature related to chapters of the report

Chapter	Reference
1. Introduction	[11], [16], [17]
2. IEEE 802.11a Wireless LAN packet structure	[11], [18], [3], [19], [20]
3. Zero-IF transceivers	[21], [12], [22]
4. IQ imbalance modeling	[18], [10], [1], [23], [24], [25], [26], [27]
5. Estimation and compensation algorithms	[1], [23], [24], [25], [14], [15], [8], [5], [4], [2], [28]
6. Simulation results and comparison	[1], [23], [5], [4]
7. Conclusion and recommendations	[29], [30], [31]

This information can be sorted by chapter and year of publication, as shown in Table 8.2.

Table 8.2: Literature in the report sorted by chapters and year of publication

Ch.	**'95**	**'96**	**'97**	**'99**	**'00**	**'01**	**'02**	**'03**	**'04**	**'05**	**'06**	**un-publ.**
1					[11] [11]			[16] [17]				
2					[11] [19]	[20]	[18]			[3]		
3			[12]		[22]	[21]						
4		[27]		[26]	[10]	[25]	[18], [23]		[1]		[24]	
5	[28]					[25]	[23]	[8]	[1], [14] [15], [5] [4]		[24]	[2]
6							[23]		[1], [5] [4]			
7								[30]	[31]	[29]		

Chapter 9

Conclusions and recommendations

The assignment of this graduation project is to analyze the effect of IQ imbalance in a OFDM wireless LAN system and to find methods to reduce the negative effects of this imbalance. Those methods should require as little additional hardware as possible, and preferably no additional hardware at all.

IQ imbalance is typically a problem in transmitters and receivers which are highly integrated and which use very large signal constellations. Such systems are very new and state of the art, and as such, IQ imbalance has gained much interest in the last 10 years, and hardly any literature on this topic is from 1996 or earlier.

Although the current IEEE 802.11a standard does not explicitly describe the maximum amount of IQ imbalance that is allowed, or how such a maximum can be achieved, most of the relevant literature can be found by searching in the IEEE - IEE Electronic Library via the IEEE Xplore online search engine. The INSPEC online bibliographic database can be used to find additional conference proceedings.

Due to some excellent papers on this topic, most notably by Razavi [12] and Valkama [25], the citation method can reveal many documents.

A list of literature relevant to this topic found through the search methods described in this report can be found in the list of references at the end of this document.

Important authors on the topic of IQ imbalance are:

- Valkama, M. *Tietoliikennetekniikka Institute, Tampere University of Technology (TUT), Tampere, Finland.*
- Razavi, B. *Department of Electrical Engineering, University of California, Los Angeles (UCLA), Los Angeles, USA*
- Tubbax, J. *Department of Electrical Engineering, Katholieke Universiteit Leuven (KUL), Leuven, Belgium*
- Lin, J. *Communications-Technology Lab, Corporate Technology Group Intel, Santa Clara, USA*

Important institutes are:

- The Institute of Electrical and Electronics Engineers (IEEE)

References

[1] J. Tubbax, *A digital approach to low-cost low-power broadband radios*, PhD thesis, K. U. Leuven, Apr. 2004.

[2] M. Ghosh, "Channel estimation in OFDM with partial training", Philips internal document, unpublished.

[3] H. Harno, "Channel estimation of MIMO OFDM systems", Master's thesis, University of Twente, May 2005.

[4] J. Lin and E. Tsui, "Adaptive IQ imbalance correction for OFDM systems with frequency and timing offsets", in *Proc. of the Global Telecommunications Conf. (GLOBECOM)*, Dec. 2004, vol. 6, pp. 4004–4010.

[5] J. Lin and E. Tsui, "Joint adaptive transmitter/receiver IQ imbalance correction for OFDM systems", in *Proc. of the 15th IEEE Internation Symposium on Personal, Indoor and Mobile Radio Communications PIMRC*, Sep. 2004, vol. 2, pp. 1511–1516.

[6] J. Tubbax, B. Come, L. V. d. Perre, L. Deneire, S. Donnay, and M. Engels, "Compensation of IQ imbalance in OFDM systems", in *Proc. of IEEE Int. Conf. on Communications (ICC)*, May 2003, vol. 5, pp. 3403–3407.

[7] J. Tubbax, B. Come, L. V. d. Perre, S. Donnay, M. Engels, M. Moonen, and H. D. Man, "Joint compensation of IQ imbalance and frequency offset in OFDM systems", in *Proc. of Radio and Wireless Conference (RAWCON)*, Aug. 2003, pp. 39–42.

[8] H. Shafieea and S. Fouladifard, "Calibration of IQ imbalance in OFDM transceivers", in *Proc. of the IEEE International Conference on Communications (ICC)*, May 2003, vol. 3, pp. 2081–2085.

[9] Tien-Yow Liu, Stuart Golden, and Naiel Askar, "A spectral correction algorithm for I-Q channel imbalance problem", in *Proc. of IEEE Global Telecommunications Conf. (GLOBECOM)*, Nov. 2001, vol. 1, pp. 334–338.

[10] M. Buchholz, A. Schuchert, and R. Haholzner, "Effects of tuner IQ imbalance on multicarrier-modulation systems", in *Proc. IEEE Int. Caracas Conference on Devices, Circuits and Systems*, Mar. 2000, pp. T65/1–T65/6.

[11] The Institute of Electrical and Electronics Engineers (IEEE), *Wireless LAN Medium Access Control (MAC) and Physical Layer (PHY) specifications: High-speed Physical Layer in the 5 GHz Band*, ISO/IEC 802-11:1999/Amd 1:2000(E), Jun. 1999, IEEE 802.11a standard.

[12] B. Razavi, "Design considerations for direct-conversion receivers", in *IEEE Transactions on Circuits and Systems II: Analog and Digital Signal Processing*, Jun. 1997, vol. 6, pp. 428–435.

[13] M. Valkama, M. Renfors, and V. Koivunen, "Blind i/q imbalance compensation in OFDM receivers based on adaptive I/Q signal decorrelation", in *IEEE International Symposium on Circuits and Systems*, May 2005, vol. 3, pp. 2611–2614.

[14] G. Fettweis, M. Löhning, D. Petrovic, M. Windisch, P. Zillmann, and E. Zimmermann, "Dirty RF", in *Proc. of the 11th Wireless World Research Forum (WWRF11)*, Jun. 2004.

[15] M. Windisch and G. Fettweis., "Standard-independent I/Q imbalance compensation in OFDM direct-conversion receivers", in *Proc. 9th International OFDM Workshop*, Sept. 2004.

[16] The Institute of Electrical and Electronics Engineers (IEEE), *Wireless LAN Medium Access Control (MAC) and Physical Layer (PHY) specifications: Amendment 4: Further Higher Data Rate Extension in the 2.4 GHz Band*, Jun. 2003, IEEE 802.11g standard.

[17] A. Paulraj, R. Nabar, and D. Gore, *Introduction to Space-Time Wireless Communications*, Cambridge University Press, May 2003.

[18] T. S. Rappaport, *Wireless Communications, principles and practice*, Prentice Hall PTR, 2 edition, Dec. 2002.

[19] R. van Nee and R. Prasad, *OFDM for Wireless Multimedia Communications*, Arthech House Publishers, Jan. 2000.

[20] J. G. Proakis, *Digital Communications*, McGraw-Hill, 4 edition, Aug. 2001.

[21] L. W. Couch II, *Digital and Analog Communication Systems*, Prentice Hall, 6 edition, 2001.

[22] S. Mirabbasi and K. Martin, "Classical and modern receiver architectures", in *IEEE Communications Magazine, Issue 11*, Nov. 2000, vol. 38, pp. 132–139.

[23] L. Brötje, S. Vogeler, K. D. Kammeyer, R. Rückriem, and S. Fechtel, "Estimation and correction of transmitter-caused I/Q imbalance in OFDM systems", in *Proc. of the 7th International OFDM-Workshop*, Sep. 2002, pp. 178–182.

[24] T. C. W. Schenk, P. F. M. Smulders, and E. R. Fledderus, "Estimation and compensation of TX and RX IQ imbalance in OFDM based MIMO systems", in *Accepted for IEEE Radio and Wireless Symposium (RWS 2006)*, Jan. 2006.

[25] M. Valkama, M. Renfors, and V. Koivunen, "Advanced methods for I/Q imbalance compensation in communication receivers", *IEEE Trans. on Signal Proc.*, vol. 49, pp. 2335–2344, Oct. 2001.

[26] R. van Nee, G. Awater, M. Morikura, H. Takanashi, M. Webster, and K. W. Halford, "New high-rate wireless LAN standards", *IEEE Communications Magazine*, vol. 37, pp. 82–88, Dec. 1999.

[27] J. W. M. Bergmans, *Digital baseband transmission and recording*, Kluwer Academic Publishers Group, Oct. 1996.

[28] J. van de Beek, O. Edfors, M. Sandell, S. K. Wilson, and P. O. Borjesson, "On channel estimation in OFDM systems", in *IEEE 45th Vehicular Technology Conference (VTC)*, Jul. 1995, vol. 2, pp. 815 – 819.

[29] Sanghyun Woo, Dongjun Lee, Kiho Kim, Yungsik Hur, Chang-Ho Lee, and Joy Laskar, "Combined effects of RF impairments in the future IEEE 802.11n WLAN systems", in *IEEE 61st Vehicular Technology Conference (VTC)*, May/Jun. 2005, vol. 2, pp. 1346 – 1349.

[30] A. Bourdoux, B. Côme, and N. Khaled, "Non-reciprocal transceivers in OFDM/SDMA systems: Impact and mitigation", in *Proc. of IEEE Radio and Wireless Conference (RAWCON)*, Aug. 2003, pp. 183–186.

[31] J. Liu, A. Bourdoux, J. Craninckx, P. Wambacq, B. Côme, S. Donnay, and A. Barel, "OFDM-MIMO WLAN AP front-end gain and phase mismatch calibration", in *Proc. of IEEE Radio and Wireless Conference (RAWCON)*, Sept. 2004, pp. 151–154.